Universidade de Aveiro Departamento de Química
Ano 2013

Telma Patrícia Cova Martins

Estudo da HAP usando uma abordagem proteómica

Study of PAH using a proteomic approach

Universidade de Aveiro Departamento de Química
Ano 2013

Telma Patrícia Cova Martins

Estudo da HAP usando uma abordagem proteómica

Study of PAH using a proteomic approach

Tese apresentada à Universidade de Aveiro para cumprimento dos requisitos necessários à obtenção do grau de Mestre em Bioquímica, ramo Bioquímica Clínica, realizada sob a orientação científica da Doutora Rita Maria Pinho Ferreira, Professora Auxiliar Convidada, e do Doutor Rui Miguel Pinheiro Vitorino, Investigador Auxiliar, ambos do Departamento de Química da Universidade de Aveiro.

Este trabalho foi financiado pela FCT, União Europeia, QREN, FEDER e COMPETE (PEst-C/QUI/UI0062/2013 e PTDC/DES/114122/2009)

o júri

presidente

Prof. Doutor Pedro Miguel Dimas Neves Domingues
professor auxiliar do Departamento de Química da Universidade de Aveiro

Prof. Doutora Rita Maria Pinho Ferreira
professora auxiliar convidada do Departamento de Química da Universidade de Aveiro

Prof. Doutor Rui Miguel Pinheiro Vitorino
investigador auxiliar do Departamento de Química da Universidade de Aveiro

Prof. Doutor Daniel Moreira Gonçalves
professor assistente da Escola Superior de Educação do Instituto Jean Piaget de Gaia

agradecimentos

Aos meus orientadores, Doutora Rita Ferreira e Doutor Rui Vitorino, pela orientação científica, pela partilha de conhecimentos, pelo incentivo e pela constante disponibilidade.

A todas as pessoas que fazem parte do Departamento de Química, em especial aos colegas de laboratório pela simpatia, acolhimento e partilha de experiências.

À Virgínia, à Ana e à Rita pelo apoio incansável, pela infinita disponibilidade e paciência e pela boa disposição.

Aos meus amigos por todos os desabafos acerca das minhas aventuras laboratoriais, quando muitas vezes nem sabiam do que estava a falar.

Ao Nuno pela eterna paciência, apoio e incentivo em todos os momentos.

Aos meus pais, pais do Nuno e restante família por acreditarem e me apoiarem sempre.

palavras-chave

hipertensão arterial pulmonar, insuficiência cardíaca crónica, caquexia cardíaca, biomarcadores, proteómica, biofluidos.

resumo

A hipertensão arterial pulmonar é uma doença com mau prognóstico que coloca em risco a vida dos pacientes, e cuja severidade e sintomas estão fortemente relacionados com a função do ventrículo direito. A caquexia cardíaca é uma complicação da insuficiência cardíaca crónica que resulta de um desequilíbrio entre as vias catabólica e anabólica. Este desequilíbrio é consequência de uma série de processos imunológicos, metabólicos e neuro-hormonais. Apesar de vários biomarcadores terem sido propostos no contexto da insuficiência cardíaca, a maioria é usada apenas para indicação de prognóstico. A aplicação da proteómica à análise de fluidos biológicos para estudo da insuficiência cardíaca e caquexia associada poderá ser útil na identificação de um painel complementar de biomarcadores com melhor desempenho e poder de diagnóstico. De modo a caracterizar o efeito da hipertensão arterial pulmonar nos perfis proteico e proteolítico da urina dos pacientes, recorreu-se a tecnologias como SDS-PAGE nanoLC-MS/MS e zimografia. Os dados da análise por nanoLC-MS/MS foram submetidos à base de dados *UniProt*, sendo depois analisados com base em ferramentas bioinformáticas. Foi identificado um total de 277 proteínas, sendo que 51 delas eram comuns a todos os indivíduos. Várias proteínas exclusivas foram identificadas tanto nos pacientes com hipertensão arterial pulmonar, como nos indivíduos saudáveis. A WNK4 foi a única proteína comum aos 2 pacientes. Em suma, os resultados evidenciam uma elevada actividade proteolítica na urina de pacientes com hipertensão arterial pulmonar, enfatizando a inflamação e caquexia associadas à doença, e permitiram também sugerir a WNK4 como um novo potencial biomarcador para o diagnóstico da hipertensão arterial pulmonar.

keywords pulmonary arterial hypertension, chronic heart failure, cardiac cachexia, biomarkers, proteomics, biofluids.

abstract Pulmonary arterial hypertension is a life-threatening disease associated with poor prognosis, whose severity of symptoms and survival are strongly related with right ventricular function. Cardiac cachexia is a serious complication of chronic heart failure that results from an imbalance of catabolic and anabolic pathways. This imbalance is caused by a series of immunological, metabolic and neurohormonal processes. Although several biomarkers have been proposed in the context of heart failure, most of them present only potential prognostic value. The application of biofluids' proteomics to the study of heart failure and related cachexia may help to identify a panel of complementary biomarkers with better performance and diagnostic power. In order to characterize the effect of pulmonary arterial hypertension on the urinary protein and proteolytic profiles, SDS-PAGE nanoLC-MS/MS and zymography were performed. Data from nanoLC-MS/MS was submitted to UniProt database and then were analyzed using bioinformatics tools. A total of 277 proteins were identified and 51 of them are common between all the individuals. Several exclusive proteins were identified in both pulmonary arterial hypertension patients and healthy subjects and WNK4 was the only common protein between pulmonary arterial hypertension patients. Taken together, data highlight a high proteolytic activity in the urine of pulmonary arterial hypertension patients, emphasizing the disease-related inflammation and cachexia and also allow to suggest WNK4 as a new potential biomarker for the diagnosis of pulmonary arterial hypertension.

Table of Contents

List of Figures

List of Tables

List of Abbreviations

1DE	One-dimensional electrophoresis
2DE	Two-dimensional electrophoresis
4E-BP1	Eukaryotic translation initiation factor 4E binding protein
ACE	Angiotensin-converting enzyme
ACN	Acetonitrile
ANP	Atrial natriuretic peptide
APC	Antigen presenting cell
BLAST	Basic local alignment search tool
BMD	Bone mineral density
BMI	Body mass index
BNP	Brain natriuretic peptide
BSA	Bovine serum albumin
CC	Cardiac cachexia
CE	Capillary electrophoresis
CHF	Chronic heart failure
CID	Collision-induced dissociation
cNOS	Constitutive nitric oxide synthase
CPVL	Carboxypeptidase vitellogenic-like
CT	Computed tomography
DHEA	Dehydroepiandrosterone
EDTA	Ethylenediamine tetraacetic acid
eIF-4E	Inhibitor of the eukaryotic translation initiation factor 4E
ESI	Electrospray ionization
ESR	Erythrocyte sedimentation rate
FBxl2	F-box and leucine rich repeat protein 2
FBxo3	F-box only protein 3
FOXO	Forkhead box O
GC	Glucocorticoids
GC-MS	Gas chromatography-mass spectrometry
GFR	Glomerular filtration rate
GH	Growth hormone

HF	Heart failure
Hpα1	Haptoglobin alpha 1 chain
Hpα2	Haptoglobin alpha 2 chain
HSP27	Heat-shock protein 27
HSPs	Heat-shock proteins
HUPO	Human proteome organization
ICAT	Isotope-coded affinity tags
IEF	Isoelectric focusing
IgA	Immunoglobulin A
IGF-1	Insulin-like growth factor 1
IGFBP-3	Insulin-like growth factor binding protein 3
IGFBPs	Insulin-like growth factor binding proteins
IgG_1	Immunoglobulin G_1
IL-1	Interleukin 1
IL-10	Interleukin 10
IL-1β	Interleukin 1 beta
IL-6	Interleukin 6
iPAH	Idiopathic pulmonary arterial hypertension
ITIH4	Inter-alpha-trypsin inhibitor heavy chain H4
iTRAQ	Isobaric tags for relative and absolute quantification
LC	Liquid chromatography
LC-MS	Liquid chromatography mass spectrometry
LPS	Lipopolysaccharide
LVR	Left ventricular remodeling
m/z	Mass to charge ratio
MALDI-TOF-MS	Matrix-assisted laser desorption ionization time of flight mass spectrometry
MDLC	Multidimensional liquid chromatography
MHC	Major histocompatibility complex
MMP-2	Matrix metalloproteinase 2
MMP-9	Matrix metalloproteinase 9
MMPs	Matrix metalloproteinases
MPO	Myeloperoxidase
MRI	Magnetic resonance imaging
MS	Mass spectrometry

MS-MS	Tandem mass spectrometry
mTOR	Mammalian target of rapamycin
MW	Molecular weight
NGAL	Neutrophil gelatinase-associated lipocalin
NMR	Nuclear magnetic resonance
NOS	Nitric oxide synthase
NPS	Natriuretic peptide system
NT-proBNP	N-terminal pro-brain natriuretic peptide
OD	Optical density
p70S6K1	p70 ribosomal protein S6 kinase 1
PAH	Pulmonary arterial hypertension
PET	Positron emission tomography
p*I*	Isoelectric point
PI3K	Phosphatidylinositol 3-kinase
PNS	Parasympathetic nervous system
Ppa	Pulmonary artery pressure
PRA	Plasma renin activity
Pro-MMP-2	Pro-matrix metalloproteinase 2
Pro-MMP-9	Pro-matrix metalloproteinase 9
PVR	Pulmonary vascular resistance
RAAS	Renin-angiotensin-aldosterone system
RC-DC	Reagent compatible-detergent compatible
ROMK	Renal outer medullary of K^+ channel
SAP	Serum amyloid P component
SCX	Strong cation exchange
SDS-PAGE	Sodium dodecylsulfate polyacrylamide gel electrophoresis
SELDI-TOF	Surface-enhanced laser desorption/ionization time of flight
Ser	Serine
SNP	Single nucleotide polymorphism
SNS	Sympathetic nervous system
SOM	Self-organizing map
SPECT	Single-photon emission computed tomography
sTNFR	Soluble form of tumor necrosis factor receptor
TGF-β1	Transforming growth factor beta 1
TIMP-1	Tissue inhibitor of metalloproteinase-1

TIMPs	Tissue inhibitors of metalloproteinases
TNFRs	Tumor necrosis factor receptors
TNF-α	Tumor necrosis factor alpha
TRAF	TNF receptor-associated factor
UPP	Ubiquitin-proteasome pathway
WAX	Weak anion exchange
WNK4	With-no-lysine kinase 4

I. Introduction

Pulmonary arterial hypertension (PAH) is a life-threatening disease associated with poor prognosis(1) and with a range of underlying etiologies characterized by pathological changes in the pulmonary arteries. These changes lead to a progressive increase in pulmonary vascular resistance (PVR) and pulmonary artery pressure (Ppa)(2). PAH is usually defined by a mean Ppa ≥ 25 mmHg(3) and patients present exercise intolerance with marked fatigue and dyspnea, limiting their daily life activity(1). Severe pulmonary hypertension increases right ventricular afterload and eventually leads to the clinical syndrome of right heart failure(4). The severity of symptoms and survival are strongly associated with right ventricular function, and right heart failure is the main cause of death in patients with PAH(2).

Chronic heart failure (CHF) is a systemic state, which begins with an abnormality of the heart, but involves the dysfunction of most body organs and systems(5-11), including cardiovascular, musculoskeletal, renal, neuroendocrine, immune, haemostatic and inflammatory ones(6). CHF resulting from impaired right ventricular function may lead, at advanced states, to cardiac cachexia (CC)(10). CC is a serious complication of CHF which is characterized by significant body wasting, particularly of skeletal musculature(12). The progressive muscle wasting impairs the tolerance to exercise, leading to early fatigue and dyspnea(13).

Despite the advances in the diagnosis and management of PAH resulting in significant improvements in outcomes for patients, the non-specific nature of its symptoms, and the low level of suspicion among clinicians make the prompt and accurate diagnosis of this disease remain a challenge(14). This prompted the search for disease biomarkers that allow diagnosis and a better stratification of the disease(15, 16). In this context, biofluids' proteomics appear as an interesting approach to search for disease-related differentially expressed proteins(17, 18).

II. Review of the Literature

1. Cardiac Cachexia: a serious complication of CHF

It has long been recognized that significant weight loss (>7,5%) and body wasting are important features of advanced CHF(19, 20). The presence of general weight loss in patients with heart failure (HF) has somewhat misleadingly been termed CC(19). It is important to differentiate cachexia from malnutrition and anorexia(21). In contrast to cachexia, malnutrition and anorexia are reversible once food is supplied(21, 22). According to Anker and Coats(19), when weight loss higher than 7,5% of the previous normal weight is observed in patients with CHF of at least six months duration and without signs of other primary cachectic states (like cancer, thyroid disease, or severe liver disease), cachexia must be diagnosed. The previous normal weight would be the average body weight prior to the onset of heart disease. When weight loss is higher than 66% of ideal body weight patients usually die from cachexia.

There are several possible approaches to evaluate a cachectic state and the methods used include: body composition analysis with fat and lean tissue estimation along with anthropometric measurements (e.g.: skinfold thickness and arm muscle circumference); calculations of the ideal percentage of mass matched for sex, age, and height; scores including serum albumin concentrations, cell-mediated immunity changes, weight/height index or body mass index (BMI), and the history of weight loss(19). Additionally, characterization of lean tissue is made possible by studying urinary creatinine excretion rates, skeletal muscle protein turnover, bioelectrical impedance, and total body potassium content, or via skeletal muscle size measurement by magnetic resonance imaging (MRI), computed tomography (CT) or body densitometry(19, 23).

CHF-related muscle wasting is not due to a single factor, but rather it is influenced by many factors, interacting in a complex system with metabolic, immune and neurohormonal consequences(12). Moreover, weight loss in CC results not only from the loss of lean tissue, but also from reductions in the fat mass and in bone mineral density (BMD)(21). Loss of adipose tissue in patients with cachexia seems to be mediated by increased lipolysis or reduced lipogenesis(24). Anker *et al*.(25) reported that in cachectic patients, increased levels of catecholamines and cortisol could be the cause for increased lipolysis and might also contribute to the increased resting metabolic rate that has been described in CHF patients.

1.1. Pathophysiology of CC

Little is known about the HF-related mechanisms that result in CC(19, 23). In 1964, Pittman and Cohen (Reviewed in 23) analyzed extensively the pathogenesis of the CC syndrome and pointed cellular hypoxia as a leading pathogenic factor, causing less efficient intermediary metabolism, therefore producing increased catabolism and reduced anabolism. Nowadays it is known that this catabolic/anabolic imbalance is caused by a series of immunological, metabolic, and neurohormonal processes(26). Most of these processes were found to be activated early in the development of CHF. Many of these pathways are initially activated to protect the heart and the circulation from damage and to compensate for impaired myocardial function(21).

1.1.1. Immune activation in CHF

Many studies have referred the association of CHF with increased circulating levels of pro-inflammatory cytokines, namely tumor necrosis factor alpha (TNF-α), interleukin-1 (IL-1) and interleukin-6 (IL-6)(27-31). Importantly, the rise of these inflammatory mediators seems to be combined with inadequately raised or even decreased levels of anti-inflammatory mediators such as interleukin-10 (IL-10) and transforming growth factor beta 1 (TGF-β1)(32). The origin of immune activation is still uncertain(6). Some hypotheses about the main stimulus for the immune activation in CHF were raised(33). One assumes that the heart itself is the main source of inflammatory cytokines(8, 33), since the failing myocardium is capable of producing TNF-α(34). Although some authors(6) refer that myocardial production of cytokines is a localized phenomenon, Tsutamoto *et al*.(35) have found increased levels of TNF-α in the coronary sinus when compared to the aortic root, supporting that the elevated plasma TNF-α is partly derived from the failing heart. Not only cardiomyocytes, but also other cells within the failing heart such as endothelial cells and fibroblasts may contribute to the myocardial inflammation in CHF. Moreover, several extramyocardial tissues and cells – circulating leukocytes, blood platelets, endothelial cells, liver, lungs and tissue macrophages – also seem to contribute to the systemic inflammation that characterize this disorder(11). Nevertheless, the direct stimuli triggering their activation are unknown(6).

The second hypothesis postulates that extramyocardial cytokine production due to tissue hypoxia may be the primary stimulus for increased TNF-α production in patients with CHF(8). The last hypothesis is that the bowel wall edema and ischemia, which occur in CHF as a result of venous congestion, are responsible for bacterial translocation, leading to

endotoxin (lipopolysaccharide, LPS) release and subsequent activation of the circulating immune cells(6, 8). Indeed, endotoxin is one of the strongest inducers of TNF-α and other pro-inflammatory mediators. Very small amounts of this substance are capable of inducing TNF-α secretion(5). Raised concentrations of endotoxin were found in patients with CHF, which can be normalized by intensified diuretic treatment(36). Jankowska *et al*.(6) also proposes two other theories. According to these authors, immune activation seen in CHF is a consequence of the long-term neurohormonal overactivation and exaggerated stimulation of the sympathetic nervous system(SNS), as well as the initial mechanism triggering inflammatory processes in CHF is secondary to the central suppression of parasympathetic nervous system(PNS).

1.1.1.1. Cytokines-related signaling pathways underlying muscle wasting

The regulation of skeletal muscle wasting has been attributed to several transcription factors and intracellular signaling pathways. These pathways may be anabolic or catabolic and there is significant cross-talk between individual cascades(37). Muscle wasting results from a chronic imbalance in the activation of these pathways and the activation of TNF-α is one of the candidates that have been suggested as a final common pathway in all forms of cachexia(21, 37). TNF-α activates proteasome-dependent protein breakdown in striated muscle and other tissues, thus maintaining the wasting process(21). The major catabolic pathways involve cytokine-induced activation of NF-κB signaling (Figure 1) that upregulates the transcription of members of the proteolytic ubiquitin-proteasome pathway (UPP). This upregulation can also be assured by forkhead box O (FOXO) transcription factors. TNF-α induces the cytosolic release of NF-κB from its inhibitory IκB proteins, allowing the translocation of NF-κB into the nucleus and subsequent transcription of proteolytic pathway components(37). Proteins degraded by this mechanism are first conjugated to multiple molecules of ubiquitin to be degraded in 26S proteasome complex in an ATP-dependent process(38). However, the proteasome is not able to degrade intact myofibrils(22), so actin and myosin need to dissociate from myofibrils before they can be ubiquitinated and degraded(38).

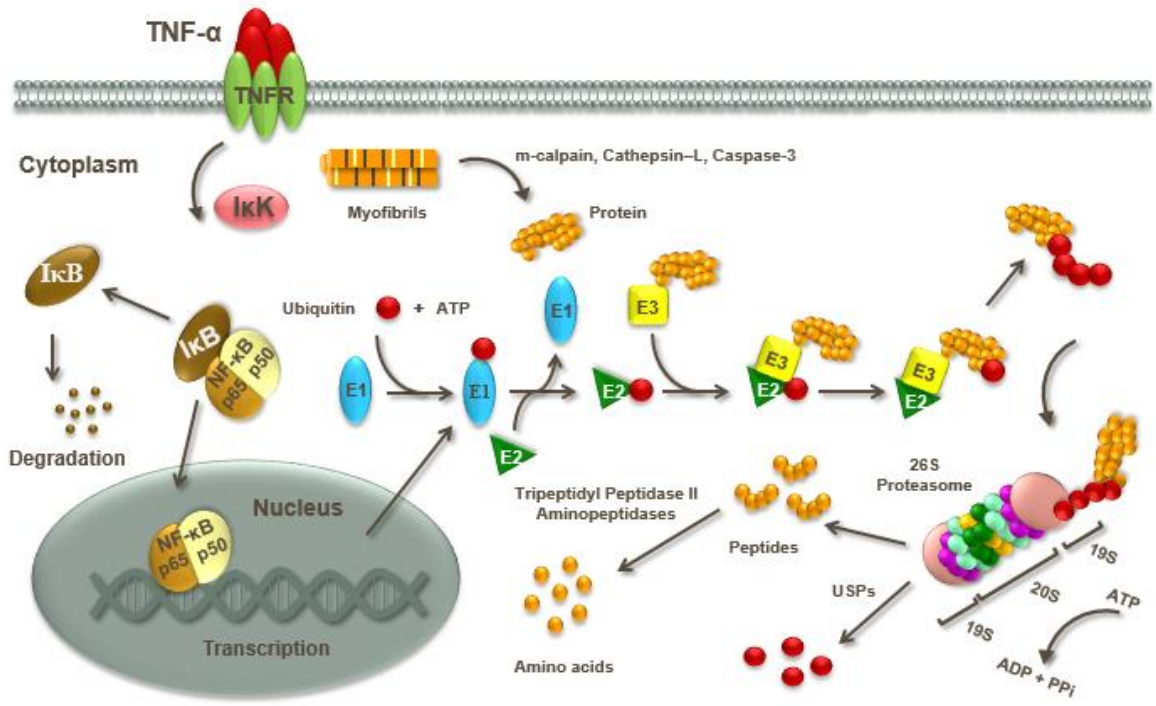

Figure 1 – TNF-induced activation of NF-κB signaling.

Thus, there are other proteolytic enzymes that act upstream UPP, namely m-calpain, cathepsin-L and/or caspase-3(37). Protein ubiquitination is regulated by at least three different enzymes: ubiquitin activating enzyme, E1; ubiquitin conjugating enzyme, E2; and ubiquitin ligase, E3(38). Initially, ubiquitin is activated by E1, in an energy-dependent step; it is then transferred by E2 to E3, that finally catalyzes the binding of ubiquitin chains to different substrate proteins(39). In addition to the activity of enzymes involved in the ubiquitination and deubiquitination of proteins, certain features of a protein can make it susceptible to degradation(38). According to the N-end rule, the *in vivo* half-life of a protein is related to the identity of its N-terminal residue(40). Ubiquitination of proteins in the N-end rule pathway is regulated by $E2_{14k}$ and E3α. Initially, the role of this pathway was questioned, since most proteins do not have a destabilizing N-terminal under normal conditions(38). However, Solomon *et al*.(41) reported that the enhanced muscle proteolysis in disease states is due to this mechanism. The involvement of N-rule pathway in muscle cachexia is also reinforced by an increased gene expression of $E2_{14K}$ and E3α(38). After unfolding, the proteins are transferred to the catalytic core of the complex, 20S proteasome, where they are hydrolyzed in an energy-dependent process(42). Finally, short oligopeptides are released by the proteasome, being rapidly degraded by cytosolic peptidases (tripeptidyl

peptidase II and aminopeptidases) into free amino acids(37, 42). Glucocorticoids (GC) an myostatin can also activate the UUP, whereas insulin and insulin-like growth factor (IGF) exert an inhibitory effect on this pathway(22, 43).

The effects of TNF-α can also be observed on endothelial cells, rearranging the cytoskeleton and increasing albumin and water permeability. In addition, it can induce surface procoagulant activity, enhance expression of antigens and IL-1 release and reduce constitutive nitric oxide synthase (NOS) mRNA in vascular endothelial cells(33). A long-term detrimental effect of increased levels of TNF-α is the inverse correlation with peripheral blood flow in patients with CHF during stable disease and at times of decompensation(21, 33). TNF-α exerts its effects via TNF receptors (TNFRs), which are expressed by almost all nucleated cells(5). Most deleterious and cytotoxic effects mediated by TNF-α involve TNFR-1, whereas TNFR-2 appears to have a more protective role in the heart(44). The soluble forms (sTNFR-1 and 2) of the extracellular domain fragments of the TNFRs can be detected and, at physiological levels, seems to stabilize the TNF-α molecule, prolonging its detrimental actions. However, increased concentrations of these soluble receptors inhibit TNF-α activity, suggesting that they may have an important role as regulators of its activity in CHF(8, 9). Indeed, sTNFRs are elevated in cachectic and non-cachectic patients with CHF(25). sTNFRs levels are also shown to vary over time to a lesser degree than TNF-α and IL-6(45).

IL-1 has important negative inotropic effects(8, 9), reducing the myocardial contractility by stimulating NOS(46). It is also involved in myocardial apoptosis, hypertrophy and arrhythmogenesis(5). Along with TNF-α, IL-1 can inhibit cardiac myocyte β-adrenergic responsiveness(47) and act directly on the brain inhibiting food intake. The action of these cytokines seems to increase the permeability of the blood-brain barrier, promoting their own uptake(21). In addition, TNF-α and IL-1 increase the expression of leptin(48), whereas the latter can induce a significant decrease of hypothalamic neuropeptide Y mRNA levels(49).

IL-6 has also been implicated in the pathogenesis of CHF(8, 9, 50), by potently inducing the acute phase response, whose maintenance requires an excess of essential amino acids. The need for amino acids yields loss of body proteins and, because skeletal muscle accounts for almost half of the body's protein mass, this compartment is intensively affected(21). Levels of IL-6 are increased in patients with CHF(5, 8, 9, 31, 32, 50), which correlate with a worse NYHA functional class, increased length of hospital stay and poorer left ventricular function(8, 9, 50). Since IL-6 is thought to be released in direct response to TNF-α, the existence of a cytokine cascade has been suggested. Cells susceptibility to IL-

6 is not assured by IL-6R itself, but rather by small transmembrane glycoprotein termed gp130. Thus, IL-6 can act even on cells which lack the expression of IL-6R after complex formation with soluble IL-6R. Gp130 and IL-6R are always required for signaling. The soluble form of gp130 inactivates the soluble IL-6/IL-6R complex. However, both concentrations of gp130 and the overall level of bioactivity of IL-6 are increased in CHF(5). Furthermore, IL-6 may be important in the development of osteoporosis, which is known to occur in CHF patients(8, 9).

1.1.2. Neuroendocrine abnormalities

Numerous hormone systems contribute to the wasting process by altering appetite and energy expenditure. The imbalance in these hormone systems, potentially triggered by the effects of pro-inflammatory cytokines, may be responsible for the development of satiety without adequate food intake(21). Most of the secondary changes related to CHF are mainly a response to the impaired cardiac function and include general neurohormonal activation via stimulation of the SNS, the rennin-angiotensin-aldosterone axis and the natriuretic peptide system(NPS)(19, 23, 33). According to the neurohormonal hypothesis(51), heart failure progresses because endogenous neurohormonal systems, which are activated by the heart injury, exert deleterious effects on the circulation. There is a strong relation between neurohormonal activation and mortality; however, different hormones correlate weakly with each other(19, 23).

Chronic autonomic sympathetic/parasympathetic imbalance is a crucial element of CHF pathophysiology, and is accompanied by abnormalities of reflex cardiorespiratory control. Autonomic imbalance, in favor of sympathetic tone, which is accompanied by depleted vagal drive, occurs at an early stage of the disease and precedes other major derangements, including immune and hormonal pathologies(6). Both norepinephrine and epinephrine can cause a catabolic metabolic shift, leading to graded increase in resting energy expenditure in CHF patients with CC(33). Initially, the increase in sympathetic activity is beneficial, since it increases cardiac output and redistributes blood flow from the splanchnic area to the heart and skeletal muscles. Renal vasoconstriction leads to salt and water retention, which may help to improve perfusion of vital organs. However, sustained sympathetic stimulation, as is seen in CHF, activates the renin-angiotensin-aldosterone system (RAAS) and other neurohormones with subsequent salt and water retention, vasoconstriction, edema and increased pre- and after-load(52). Increased aldosterone plasma levels and plasma rennin activity – a stimulator of the production of angiotensin II

and norepinephrine – reflect also a specific association between cachexia and neuroendocrine activation in CHF. (33).

The activation of NPS, caused by the decrease in cardiac output, is responsible for the renal retention of sodium and water observed in CHF patients. Plasma levels of both atrial natriuretic peptide (ANP) and brain natriuretic peptide (BNP) have been found to be increased in patients with various heart diseases. However, the raise in circulatory BNP correlates better than ANP with the severity of CHF. Thus, circulatory BNP has been utilized as a prognostic marker in CHF, as well as a hormone guide in the evaluation of the efficacy of the conventional treatment of this disease state(53).

1.1.2.1. Hormone-related signaling pathways underlying muscle wasting

Many of the hormones that are altered in conditions of wasting have been implicated in the regulation of protein degradation at the cellular level. Cortisol is known to be disproportionately elevated in untreated HF, and may be directly involved in the transcriptional regulation of the proteasome complex in the cell(54). GC contribute to muscle atrophy either by decreasing the rate of protein synthesis or increasing the rate of protein breakdown. GC can limit protein synthesis by three different mechanisms (Figure 2): (i) inhibiting the amino acid transport into the muscle; (ii) inhibiting the stimulatory action of insulin, IGF-1, and amino acids on the phosphorylation of eukaryotic translation initiation factor 4E binding protein (4E-BP1) – an inhibitor of the eukaryotic translation initiation factor 4E (eIF-4E) - and the p70 ribosomal protein S6 kinase 1 (p70S6K1); (iii) inhibiting myogenesis through the downregulation of myogenin, which is a key transcription factor for differentiation of satellite cells into muscle fibers. The inhibition of protein synthesis mainly results from the inhibition of mammalian target of rapamycin (mTOR), leading to a reduction in the initiation phase of mRNA translation with downregulation of protein synthesis(55). In fact, insulin-like growth factor 1 (IGF-1)/phosphatidylinositol 3-kinase (PI3K)/Akt pathway presents chronic deactivation in muscle wasting(37). Akt also regulates gene transcription through inactivation of FOXO, which is associated with E3 expression(42). As Akt is inactive in wasting process, FOXO is not deactivated and remains in nucleus, which leads to the activation of genes involved in cell death, cell cycle inhibition and metabolism(37). In what concerns to muscle proteolysis, GC increase the expression of several components of the UPP either involved in the ubiquitination (ubiquitin; E2; atrogin-1 and MuRF-1) or directly responsible for the protein degradation by proteasome (several subunits of the 20S proteasome)(55). IGF-1 seems to exert a protective effect on the GC-induced wasting, since the activation of UPP by GC is diminished by IGF-1 or IGF-1 variants that bind weakly to

insulin-like growth factor binding proteins (IGFBPs)(54). The GC-induced muscle cell catabolism seems to be mediated by the transcription factors FOXO. GC can also cause muscle atrophy by altering the production of growth factors that control locally the muscle mass development, namely the production of IGF-1 by the muscle(55).

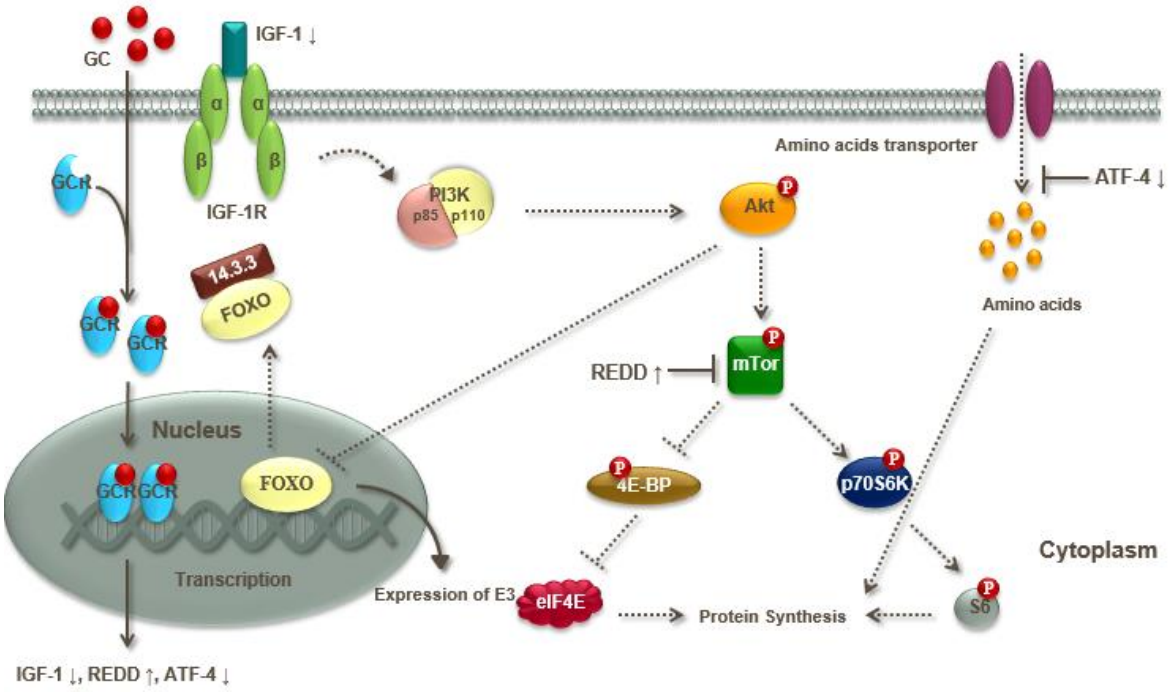

Figure 2 – **GC inhibition of protein synthesis**(Adapted from 55).

The major anabolic hormones modulating protein metabolism in skeletal muscle include insulin, growth hormone (GH) and IGF-1. Since IGF-1 has been shown to stimulate protein synthesis and to reduce protein degradation, changes in the GH/IGF-1 axis may impact the anabolic/catabolic balance in the wasting syndrome(54). Patients with CHF-related systolic or diastolic dysfunction have significantly lower plasma levels of total IGF-1 and insulin-like growth factor binding protein 3 (IGFBP-3), but free IGF-1 is significantly higher than in healthy controls. In the same study, patients on angiotensin-converting enzyme (ACE) inhibitor therapy had normal IGF-1, whereas patients without this treatment had lower IGF-1 levels than controls, suggesting that reduced IGF-1 is related to stimulation of the RAAS(Reviewed in 54). Inflammatory cytokines are well known to have significant interactions with neurohormonal pathways in CHF(8). Beyond the positive correlation between TNF levels and the degree of insulin resistance(8, 9), pro-inflammatory cytokines uncouple the GH/IGF-1 axis through the suppression of the GH receptor, producing, in response, a state of GH resistance, which is characterized by high GH and normal to low

IGF-1. This has been attributed in part to increased serum levels and the local expression of pro-inflammatory cytokines such as interleukin 1 beta (IL-1ß) and TNF-α(10).

2. Therapeutic approaches to CC

There are currently no approved therapies to treat CC-related weight loss(22). Furthermore, as CC is a multifactorial disorder, it is unlikely that any single agent will be completely effective in treating this condition, thus it will be necessary to target different pathways(23). There are several treatment procedures that might be applied to preventing or treating wasting states and some of these have been proven to be beneficial. However, others seem to be less effective although they have theoretical therapeutic appeal(22). Table 1 summarizes some potential therapeutic approaches to CC.

Table 1 - Therapeutic approaches to CC(22).

Drug Therapy	**Prevention of weight loss**	ACE inhibitors β-blockers	
	Pharmacotherapy of CC	Appetite stimulants	Megestrol acetate Medroxyprogesterone acetate Cannabinoids Anabolic steroids β-adrenergic agonists
		Anti-inflammatory substances	TNF-α inhibitory antibodies Inhibition of lipopolysaccharide bioactivity Statins Thalidomide Proteasome inhibitors Other substances (Pentoxifylline)
Non Pharmacological Approaches		Nutrition Exercise	

Despite survival of patients with HF was significantly improved by the introduction of ACE inhibitors and β-blockers therapeutics, the overall prognosis remains fairly poor, and patients usually die of CHF(5, 44). Recent insights into the pathophysiology of this disease provide promising targets for future therapies(44).

2.1. Drug therapy

2.1.1. Prevention of weight loss

The treatment of CHF varies according to disease's severity. The standard therapeutic approach currently involves ACE inhibitors or angiotensin receptor blockers, β-blockers, and diuretics (thiazide or loop diuretics). In patients with advanced disease the administration of aldosterone antagonists is also needed(21). It has been demonstrated that the use of ACE inhibitors and β-blockers potentially delay and eventually prevent the onset of CC(22). Moreover, increasing evidence suggest that ACE inhibitors can improve the endothelial dysfunction, which may prove to be a major reason for their efficacy. This effect may occur due to the blockade of bradykinin with subsequent release of nitric oxide and prostaglandins from endothelial cells(50). Treatment with ACE inhibitors can also reduce circulating levels of ANP and BNP, TNF-α and IL-6, as well as restore depressed levels of circulating IGF-1 in CHF patients(33). Additionally, although high-dose enalapril therapy has been shown to significantly decrease IL-6 bioactivity in patients with CHF(56), ACE inhibitors seem to have only minor influence on inflammation, since a persistent immune activation exists in these patients which may be of importance for the progression of the disease(11, 56).

The β-blockers metoprolol, bisoprolol, carvedilol, and most recently nebivolol have been included in CHF treatment guidelines. The latter was shown to have beneficial effects in elderly patients with CHF. Beyond their effects on survival, β-blockers may inhibit catecholamine-induced lipolysis, decrease resting energy expenditure, and decrease insulin sensitivity, which may reduce the wasting process(22). Packer *et al*.(57) verified that the risk of death decreases 35% when carvedilol is added to conventional therapy. Despite preventing the development of cachexia in CHF, β-blockers and ACE inhibitors can not reverse CC(33). Unlike those patients with left-sided HF, where β-blockers and ACE inhibitors are indicated, patients with PAH and right HF are managed only with supportive therapies such as diuretics and digoxin(58).

2.1.2. Pharmacotherapy of CC

Some therapeutic approaches are currently pursued in order to reverse weight loss in patients with cachexia. CC has not specifically been targeted and it is noteworthy that none of the following treatments are currently approved for the treatment of cachexia in CHF or any other chronic illness (with the exception for AIDS-related cachexia)(21). The therapeutic concepts comprise interventions with appetite stimulants, and anti-inflammatory substances(22).

Appetite stimulants such as megestrol acetate and medroxyprogesterone acetate have been reported to improve appetite, caloric intake and nutritional status(59). The precise mechanism by which weight gain is mediated is unknown(22), but studies suggest the role of neuropeptide Y(60), the inhibition of pro-inflammatory cytokines(61), and the modulation of calcium channels in the ventromedial hypothalamus(62). Cannabinoids are also known to stimulate appetite(22). The mechanism by which cannabinoids exert their effects is not clarified, but it was suggested that they may act via endorphin receptors, or by inhibiting prostaglandin synthesis(59). Other studies also suggest that cannabinoids may inhibit cytokine production and/or secretion(63, 64). Anabolic steroids are another possible therapeutic approach to treat CC(21), since they increase muscle mass. However, some side effects, such as alteration of kidney function and the potential to induce prostate hyperplasia, may limit their potential(23, 33). β-adrenergic agonists, especially β_2-adrenergic agonists, are also known to exert favorable effects on muscle mass, providing a potential means of anabolic therapy(22). The relevance of these molecules is related to their effects on protein metabolism in skeletal muscle, promoting protein deposition. Newer drugs, in particular formoterol, have recently received some attention because they present relatively low toxicity and are able to reverse the muscle-wasting process(59).

Several substances from different drug classes have shown to suppress inflammation, especially the production or the action of pro-inflammatory cytokines. Among these substances are TNF-α antibodies like etanercept or infliximab(22). Etanercept is a TNFR-2 fusion protein, which binds to TNF-α and functionally inactivates this cytokine(5), whereas infliximab, a chimeric immunoglobulin G_1 (IgG_1) monoclonal antibody, binds both soluble and membrane-bound TNF-α. However, it appears that inhibition of single mediators is not beneficial, thus broader approaches – immunomodulatory therapies, statins inhibition of inflammatory triggers, and potentially the immunoadsorption of inflammatory mediators – might be necessary. The inhibition of LPS, which is thought to be a potential candidate that triggers inflammatory activation in CHF, may serve as a therapeutic aim. This inhibition can

be accomplished either by micelle formation around LPS or by inhibition of its signaling cascade(22). Some statins may improve endothelial function by inducing constitutive nitric oxide synthase (cNOS) gene transcription, as well as reduce vascular production of ROS and decrease the production of TNF-α and IL-6 form macrophages(5). Other anti-inflammatory substances that can be used in the pharmacotherapy of CC are thalidomide, proteasome inhibitors and pentoxifylline(22).

2.2. Non pharmacological approaches

Patients with CHF are predisposed to reduced appetite and reduced food intake due possibly to: (i) changes in taste and smell, (ii) dietary advice on salt and calorie intake, (iii) social isolation, (iv) derangements in bowel perfusion, (v) and an altered intestinal barrier. These alterations may lead to micro and macronutrients deficiencies(22). Thus, the nutritional status in cachectic patients must be improved in order to regain energy reserves, which results in a gain in skeletal muscle tissue and a subsequent improvement of exercise capacity(23). There are no controlled studies of nutritional strategies in CC with exception for preoperative and postoperative nutritional support. Moreover, nutritional treatment studies in CHF have not been able to quantify nutrient and caloric intake and often comprise small numbers of patients without cachexia being assessed(33).

Patients with advanced CHF or CC must restrict the sodium intake (2g per day) as well as avoid food and lifestyle factors that trigger the acute phase response such as an increased intake of carbohydrates or saturated fats, alcohol, and smoking. These restrictions can be accompanied by food that counteracts inflammatory responses, namely fish oil supplements, olives, walnuts, flaxseed oil, any fruits or vegetables, garlic, ginger turmeric, sunflower seeds, eggs, herring, or nuts(22). Although intensive nutritional support can increase the body's oxidative demands, it has been shown that this is safe in cachectic CHF patients and can lead to an increase in the amount of lean tissue(23).

Exercise rehabilitation training can reverse the muscular metabolic abnormalities and atrophy seen in cachectic patients, as well as the impaired peripheral blood flow, thus improving the exercise capacity and anaerobic threshold(19, 23). Low intensity exercise practice can diminish cardiovascular events and increase the oxidative capacity of the skeletal muscle in patients with mild CHF, by changing oxygen uptake and mitochondrial density. Besides, exercise training potentially reduces the expression of cytokines in the muscle and increases anti-apoptotic factors like IGF-1(12). Despite of being considered a

hallmark of CHF, exercise intolerance studies assessing skeletal muscle function are relatively rare(20).

3. Monitoring CHF-related CC: biomarkers with clinical impact

Some biomarkers, mainly associated to hormonal, inflammatory and oxidative stress changes, have been proposed in the context of CC (Table 2). However, they present only potential prognostic value(65). The biomarkers of cardinal significance in HF which are now applied in routine clinical practice are the B-type natriuretic peptides(66). Plasma concentrations of natriuretic peptides are useful biomarkers in the diagnosis of HF and in the management of patients with established CHF(67). Together with imaging, only the BNP/N-terminal pro-BNP (NT-proBNP) assay is recommended by international guidelines for diagnostic evaluation and risk stratification of patients with HF(68). Therefore, BNP is one of the best prognostic indicators in all stages of HF, predicting outcome in hospitalized and outpatients(69). BNP measurement is also used for guidance in HF therapy, for example adjusting the dose of ACE inhibitors, β-blockers, and diuretics(70). Several other parameters are consider for the diagnostic evaluation and management, including the complete blood count, serum electrolytes, serum creatinine, estimated glomerular filtration rate (GFR), glucose, liver function tests, and urinalysis. Moreover, troponin I or T should be measured in suspect of HF. Mild increases in cardiac troponins are frequently seen in severe HF or during episodes of decompensated HF. An elevated troponin is a strong prognostic marker in HF, especially when associated with elevated natriuretic peptides(67). Biomarkers of matrix remodeling and inflammation have emerged as potential preclinical indicators to identify individuals at risk of developing clinical HF(71).

Table 2 - Candidate biomarkers proposed for CC.

	Biomarker	Levels	Complications	Biofluid	References
Hormonal markers	B-type natriuretic peptides	↑	CC, increased severity	Plasma	(72-75)
	A-type natriuretic peptides	↑	CC, increased severity	Plasma	(72-74, 76)
	Plasma renin activity (PRA)	↑	CC, advanced HF	Plasma	(73, 77)

Hormonal markers	Angiotensin II	↑	CC, poor prognosis	Plasma	(30, 72, 78)
	Aldosterone	↑	CC, advanced HF	Plasma/ Serum	(72, 73, 77, 79)
	Norepinephrine	↑	CC, increased severity	Plasma	(25, 30, 72, 73, 76, 77, 80)
	Epinephrine	↑	CC, increased severity	Plasma	(25, 30, 72, 77)
	GH	↑	CC	Serum	(72, 77, 81)
	IGF-1	= ↓	CC	Serum	(72) (77, 81)
	Ghrelin	↑	CC	Plasma	(72)
	Cortisol	↑	CC, increased mortality	Plasma/ Serum	(25, 72, 77, 79)
	Dehydroepiandrosterone (DHEA) / DHEA sulfate	↓	CC, increased severity	Plasma	(72, 74, 75, 77)
Inflammatory markers	TNF-α	↑	CC, poor prognosis	Plasma/ Serum	(25, 27, 28, 30, 31, 72, 82)
	sTNFRs	↑	CC, increased severity	Plasma	(25, 32, 83)
	IL-1β	↑	CC		(25)
	Erythrocyte sedimentation rate (ESR)	↑	CC, poor prognosis	Whole blood	(25, 84, 85)
Oxidative stress markers	Uric acid	↑	CC, poor prognosis	Serum	(86, 87)

Available biomarkers, however, present limitations. Biomarkers' concentrations are broadly distributed, thus making it hard to differentiate between individuals with or without disease, as concentrations can overlap, disguising possible disease-dependent variations. Moreover, the information provided is often not entirely new, since most current biomarkers are involved in pathways associated with atherosclerotic cardiovascular disease, such as those implied in inflammation and cholesterol biosynthesis(88). Because individual biomarkers may have limited sensitivity and specificity(15), multimarker strategies will likely identify biomarker combinations that will allow to monitor various stages during the evolution of heart failure(71). So the prognostic power can be improved by combining two or more circulating biomarkers reflecting different aspects of HF pathophysiology and independently associated with clinical outcome(66). These limitations emphasize the importance of identifying uncorrelated biomarkers associated with new disease pathways. Emerging technologies (Table 3) allow the systematic unbiased characterization of genes, RNA, proteins and metabolites associated with disease conditions(88). For the purpose of this study we will focus on proteomics' strategies.

Table 3 - Available techniques for biomarker development(89).

Technology	Method	Objective	Tissue
Genomics	SNP genotyping	Identify susceptibility or disease modifying gene	Nucleated cells, diseased tissue
	Positional cloning/microsatellites	Fine mapping/sequencing of disease loci	
	Expression analysis	Identification of differential expression of genes and signaling pathways	
Proteomics	2DE, MS, LC-MS, GC-MS, MS-MS, MALDI-TOF MS	Identification of low-abundance proteins, their subcellular location, posttranslational modification, interactions among proteins	Urine, blood, saliva, tissues
Metabolomics	NMR spectroscopy, MS, infrared spectroscopy	Small molecule identification and characterization	Nucleated cells, urine, blood, saliva, tissues
Pharmacogenetics	SNP genotyping	Relate genetic makeup to drug response	Nucleated cells

Integratomics	SNP genotyping, positional cloning/microsatellites, expression analysis, 2DE, MS, LC-MS, GC-MS, MS-MS, MALDI-TOF MS, NMR spectroscopy, infrared spectroscopy	Use of high-throughput technology to produce an integrated picture at the DNA, RNA, protein, tissue, and pharmacological levels	Nucleated cells, urine, blood, saliva, tissues
Bioinformatics	BLAST, hierarchical clustering, SOM	Link microarray data to biological pathways	Data from various techniques
Molecular imaging	CT, MRI, PET, SPECT, biophotonic imaging	Noninvasively identify and quantify the causative molecular constituents of diseased tissues in time and space	Patients

2DE – two-dimensional electrophoresis; BLAST – basic local alignment search tool; GC-MS – gas chromatography mass spectrometry; LC-MS – liquid chromatography mass spectrometry; MALDI-TOF MS – matrix assisted laser desorption ionization time of flight mass spectrometry; MS – mass spectrometry; MS-MS – tandem mass spectrometry; NMR – nuclear magnetic resonance; PET – positron emission tomography; SNP – single nucleotide polymorphism; SOM – self-organizing map; SPECT – single-photon emission computed tomography.

Proteomics-based approaches are increasingly being used to address biomedical questions, since they examine the expressed proteins of tissue or cell type, complementing genomic initiatives(90). Since phenotype is influenced by the interaction between pathways that are regulated in a coordinated way or that overlap, proteomics technologies present some advantages when compared to genomics. Neither these effects, nor the biological basis of multigenic processes such as ageing, stress, and some diseases, can be identified solely from examination of the genome(90). The application of proteomics, as a study of more than one protein at a time, may help to identify a panel of complementary biomarkers that will have more robust operating characteristics(15, 91).

3.1. Proteomics for the identification of new biomarkers for CHF

The study of proteome involves the integration of a number of technologies aiming to analyze the complete complement of proteins expressed by a biological system in response to various stimuli and/or under different physiological or pathophysiological conditions(92). Proteome comprises products arising from events such as the processing of mRNA transcripts (e.g., alternative splicing) and post-translational modifications (e.g., phosphorylation, glycosylation, and oxidation)(17).

One of the goals of proteomic analysis in cardiovascular diseases is to compare the protein complements of diseased hearts or sera of patients with cardiovascular pathologies with control individuals. All proteins with altered expression between two or more groups are candidates to be involved in disease pathogenesis and should be further studied. Thus, proteomics provides a platform in which the molecular, cellular, and signaling mechanisms involved in cardiovascular disease and cardiac dysfunction can be delineated(17). The molecular mechanisms underlying proteome change may be investigated by broad-based screening or more focused approaches. In these cases, modified proteins and the nature of each modification are identified, and in some cases, modified amino acid residues may be determined. The potential of this information can be improved by linking all proteome changes directly to functional consequences, what may be called “functional” proteomics(93).

First proteomic-based studies were focused in the construction of protein maps, which include information such as protein type and, in some instances, functional data of proteins identified from myocardial tissue. Later, the study and comparative analysis of myocardial protein profiles from different species constituted an important step in the application of proteomics to cardiovascular diseases(92). Furthermore, Human Proteome Organization (HUPO) efforts allow the development of a human protein reference database, where the proteins detected in biological samples are listed. This initiative also includes the mapping of proteomes in biological compartments such as plasma, urine, brain, liver, and heart(89). Databases of human cardiac proteins are based on information from two-dimensional gel studies and include HSC-2DPAGE, HEART-2DPAGE, and HP-2DPAGE(94) Proteomics has also been used to identify cardiac-specific antigens that produce an antibody response in heart disease and after transplantation(95). Finally, proteomic programs are now broadly applied in the pharmaceutical industry, with a wide use in drug development(96).

The great majority of the proteomic-based studies developed in the context of CHF use animal or human tissue samples. Dohke *et al*.(97) compared protein patterns of left ventricular samples from normal and tachycardia-induced CHF dogs and verified that the phosphorylation of some small heat-shock proteins (HSPs) – alpha B crystallin at serine (Ser)-59 site and of heat-shock protein 27 (HSP27) at both Ser-78 and Ser-82 sites – were increased in CHF. More recently, Petrak and colleagues(98) used rats with HF due to volume overload and proposed annexin A1 and A2 as new potential biomarkers of HF. They also pointed monoamine oxidase A and transglutaminase 2 as highly potential therapeutic targets for treatment of HF. In another study using peripheral blood mononuclear cells to

determine proteome profiles in human HF, Mazzola *et al*.(99) observed differences between CHF subjects and controls. Two proteins were increased in CHF (only one was identified, the translationally controlled tumor protein), whereas four were decreased (nucleoside diphosphate kinase A, 14-3-3 protein zeta/delta, CAP-Z and T-complex protein 1). There were also proteins present only in controls (HSP27 and T-complex protein 1-beta subunit), as well as proteins expressed only in CHF (elongation factor-1 delta, talin 1, NADH-ubiquinone oxidoreductase, PRP19/PSO4). More recently, biofluids has become part of the CHF-related proteomic studies.

Despite great improvements, proteomic analysis remains challenging. Several proteins that have key roles in pathophysiologic conditions are enzymes present in low concentrations, which makes their separation and identification difficult within a complex mixture that includes many high-concentrated proteins. Furthermore, some proteins have low turnover which makes difficult to detect their small concentration changes, especially during short intervention studies. Many proteins may also be altered by modifications without a change in concentration(95).

3.2. Technical considerations in proteomic analysis

Proteomic studies include sample preparation, protein separation and identification. The first and foremost requirement, sample preparation, is crucial to proteome analysis. Regarding this aspect, it is important to maximally and consistently solubilize sample proteins without introducing non-experimental modifications. This implies the need to disrupt numerous protein/protein and protein/non-protein interactions within tissue or biofluid. In order to achieve this, various combinations of detergents and reducing and chaotropic agents are used(92). Proteome analysis can be carried out in a single solubilization step or using a set of subproteomes. Fractionation methods may be used in order to selectively solubilize specific subproteomes. The selectivity of these methods can be achieved exploiting specific characteristics of the proteome, such as their inherent chemical properties (biospecificity, hydrophobicity, charge) or differential cellular compartmentalization(93). Sample prefractionation is one strategy to reduce the sample complexity or to enrich for a group of proteins, especially those present in low concentrations. Many of the techniques that have been utilized to enrich for particular fractions and specific cell types within sample preparation for proteomic analysis include sequential protein extraction, immunoprecipitation, laser capture micro dissection, and fluorescence activated cell sorting. However, these procedures are time consuming and may also leads to loss of proteins(17).

The success of the proteome analysis is determined by the ability to separate complex protein mixtures with a high resolving power and reproducibility(17). Proteomic analysis can be performed according to two main approaches – gel-based and gel-free (Figure 3).

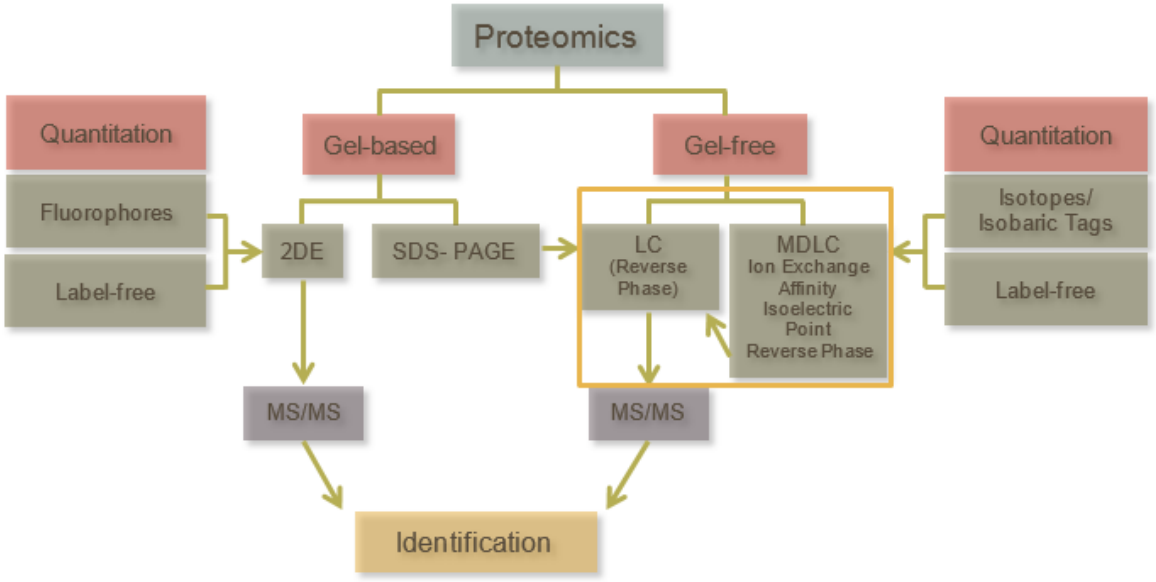

Figure 3 – Strategies used in proteomics.
LC – liquid chromatography; MDLC – multidimensional liquid chromatogrhapy.

When gel-based techniques are used, samples can be labeled with fluorophores (i. e. 2D-DIGE) or separated without labeling (label-free)(100). Gel-based approaches comprise 2DE and one dimensional electrophoresis (1DE) techniques such as sodium dodecylsulfate polyacrylamide gel electrophoresis (SDS-PAGE)(94). 2DE allows the resolution of thousands of proteins simultaneously by combining two different separation strategies(17). In the first dimension, protein separation is carried out by isoelectric focusing (IEF). Proteins are focused by relative charge according to their inherent charge or isoelectric point (p*I*) and are then resolved orthogonally in the second dimension by their relative molecular mass, usually by SDS-PAGE(93). 2DE is followed by in gel digestion and MS/MS analysis of selected proteins. MALDI-TOF/TOF instruments are the most suitable for protein identification in 2DE strategy, allowing the identification of many proteins in one spot if they cannot be separated in the electrophoretic procedure(101). 1DE is a widespread technique, used for many applications: (i) comparison of protein composition of different samples; (ii) analysis of the number and size of polypeptide subunits; (iii) western blotting coupled to immunodetection; (iv) as second dimension in 2DE maps. Taking the advantage of both gel-based protein separation and gel-free peptide separation, SDS-PAGE is, nowadays,

coupled to subsequent analysis by LC before MS analysis. After protein separation on SDS gel, the entire gel lane is excised and divided into slices prior to the proteolytic digestion. Peptide fractions are then subjected to second separation by LC, followed by MS/MS analysis. The main advantages of this procedure are the ability of SDS to solubilize proteins during size-separation and the reduced sample complexity prior to LC, increasing the chance of identifying low abundant proteins. When compared to other fractionation methods (i.e. cation exchange, isoelectric focusing, etc), the 1DE-LC approach showed superior performance and higher proteome coverage(102). Gel-based approaches used individually (not coupled with gel-free techniques) present some technical limitations, failing to visualize all proteins in complex samples. Typically, 2DE gel can only visualize 30-50% of the entire proteome, therefore proteins at extremely low concentrations or proteins that cannot be separated due to their physicochemical properties will not be detected(100). Despite these limitations, gel-based strategy is very efficient in solving biological questions, being a good initial approach in a study(101).

The development of gel-free high throughput technologies (i.e. LC-MS) allows overcoming some of the limitations of 2DE(100). Liquid chromatography LC is a powerful fractionation method that is compatible with virtually any mass spectrometer(103) and that can be used alone or in combination with other protein purification techniques(104). In the LC-MS based strategy (Figure 3), proteins are first cleaved into peptides by proteolytic enzymes. The resulting peptide mixture are then separated by LC and analyzed by MS(100, 101). Because this mixture consists in thousands of peptides, frequently MDLC is needed(101). Based on this need Washburn et al.(105) developed a proteomic approach that combines the high separation efficiency of multidimensional chromatography with the powerful peptide identification capacity of electrospray ionization (ESI) MS/MS. This multidimensional system (called MudPIT) is based on the sequential stacking of strong cation exchange (SCX) beads and reversed phase beads on a biphasic column. MudPIT technology demonstrated an ability to detect and identify proteins, including low-abundant ones(100). In order to obtain maximum sensitivity, research efforts have focused on coupling nano-scale LC at submicroliter flow rates to the highly sensitive micro-scale ESI interface. Detection limits of a few fentomoles of peptide material loaded on the column make this technique compatible with silver-stained, fluorescently labeled, or faintly stained Coomassie gel bands and capable of detecting proteins and peptides present at a low copy number per cell(104). As described for gel-based approaches, samples for gel-free purposes can also be labeled, in this case with isotopes (i.e. isotope-coded affinity tags - ICAT and ^{18}O) or isobaric tags (isobaric tags for relative and absolute quantification - iTRAQ), or the

procedure can be performed without labeling (label free)(102). In a typical LC-MS/MS experiment, the analyte is eluted from a reversed-phase column to separate the peptides by hydrophobicity, and is ionized and transferred with high efficiency into mass spectrometer for analysis(104). Identification of the protein content present in the initial sample is based on peptides fragmentation by MS/MS(101). The sequence of peptides can be determined by interpreting the data resulting from fragmenting the peptides in tandem mass spectrometers. One peptide species out of a mixture is selected in the first mass spectrometer and is then dissociated by collision (collision-induced dissociation, CID) with an inert gas (i.e. argon or nitrogen). The resulting fragments are separated in the second part of the tandem mass spectrometer, producing the MS/MS spectrum(104). The obtained spectra are compared with the theoretical MS/MS spectra generated from databases. Because peptides are more easily separated by LC than proteins, peptide based proteomic analysis is much faster and cheaper than a complete gel-based analysis. LC-MS strategy has also some disadvantages. As proteins are identified based on only few peptides, isoforms of the proteins may not be distinguished and post translational modifications are often missed. Moreover, the number of peptides sequenced by the mass spectrometer in a given time is limited. These peptides will originate the most intense peaks, whereas low abundant peaks will not be sequenced. To overcome this limitation, peaks which are sequenced in a first run can be excluded in a second run, due to the introduction of exclusion lists which enable to get deeper in the proteome(101).

3.3. Proteomic analysis of biofluids

Biofluids are among the easiest types of clinical samples to obtain(106), presenting several advantages such as low invasiveness, minimum cost, and easy sample collection procedure and processing(18). Tissue collection, on the other hand, requires invasive procedures that may include general or local anesthesia(106). Another reason for the preferential use of biofluids arises from a forward thinking vision for development of routine clinical assays(107).

Plasma and serum represents the two most important biofluids in which the search of biomarkers has primarily been focused(108). Plasma protein levels are associated with physio and pathological states, being useful for diagnosis and prognosis. Serum protein composition largely differs from that of plasma. Since preparation and handling of these samples are critical for proteome analysis, its processing should be performed in a standard way as well as establishing whether to use one or another. The complexity of the proteome is another critical issue that must be taking into account(18). Despite the high protein

concentration, the great majority comprises only 22 proteins. Thus, direct analysis of serum or plasma results, frequently, in the repeated identification of proteins such as albumin, transferrin and immunoglobulins(108). Consequently, it is often necessary to deplete these highly-abundant proteins before proteome analysis. Proteomic studies using plasma and serum samples are limited in the context of HF. Hawkridge *et al*.(109) analyzed plasma samples of CHF patients by LC- MS and verified that brain natriuretic peptide 32 (BNP-32) was absent in advanced states of the disease. In another study, Pinet and colleagues(110) searched for plasma biomarkers that would allow predicting left ventricular remodeling (LVR) after a first myocardial infarction. They found two candidate proteins, haptoglobin alpha 1 chain (Hpα1) and hemoglobin. The first one is more elevated in LVR patients, whereas the latter is more elevated in non-LVR ones. Zhang *et al*.(111) used gel-based techniques and also pointed these two proteins as markers for CHF, however, they referred haptoglobin alpha 2 chain (Hpα2) instead of Hpα1. They also reported the elevation of both proteins in CHF patients, in contrast with Pinet *et al*. results which only showed an elevation in Hpα1.

Urine, with less complexity than serum and relatively high thermodynamic stability, is a promising study medium for discovery of novel biomarkers in many diseases (18). Besides, it can be obtained in large quantities allowing repeated sampling from the same individual, which facilitates the development of longitudinal studies. Nevertheless, there are also some drawbacks including: (i) large dynamic range in protein concentrations, mainly due to differences in patient fluid intake; (ii) the inconsistency of the pH may modify the activity of proteases and as a consequence lead to greater variability in the concentration or composition of particular peptide fragments; (iii) biological intra-day variability of the proteome(112). The proteins excreted in urine can come from sediments (48%), exosomes (3%) or can be soluble forms (49%). The soluble proteins in urine result largely from glomerular filtration. Although glomerular filter has low sieving coefficients, high molecular proteins from plasma (e.g. albumin) can pass through this filter in sufficient amounts to reach the lumen of the nephron. Moreover, peptides and small proteins (<10 kDa) such as β_2-microglobulin, immunoglobulin light chains, retinol-binding protein and amino acids pass freely the glomerulus. Some of the soluble proteins in urine are produced as membrane-bound proteins that are proteolytically cleaved from their membrane attachments(113). One of this proteins is uromodulin (Tamm-Horsfall protein), the most abundant urinary protein in healthy conditions, excreted in quantities of 20-70 mg/day(113, 114). Uromodulin is a 68-kDa heavily glycosylated protein, synthesized exclusively in the ascending limb of the loop of Henle, that polymerizes into high molecular weight (MW) filaments in urine(114). Solid

phase components of urine such as epithelial cells and casts constitute a source of urinary proteins and a pool of potential disease biomarkers. Some of these components are small fragments of membrane that are delivered to the urinary space by shedding of microvilli or by apoptosis. These components can be isolated by centrifugation at moderate speed(113).

The last few years many clinical urinary proteome analysis have been reported. Analytical protein MS generally uses a bottom-up approach in which protein identification depends on initial treatment with a protease (usually trypsin) to break proteins into small peptides whose mass to charge ratio (m/z) can be accurately determined by MS. Protein identification is achieved by peptide mass fingerprinting or using peptide fragmentation spectra in a tandem mass spectrometer(113). Several bottom-up approaches had been applied for urinary proteomic analysis. Thongboonkerd *et al*.(115) used 2DE-MS and identified 67 protein forms of 47 unique proteins. Lu *et al*.(116) coupled 2DE with LC-MS/MS for identification of low-abundant proteins via fractionation of the urinary proteome with weak anion exchange (WAX) chromatography. More recently, Abdalla and co-workers(117) used LC-MS/MS to identify promising biomarkers for early detection of hepatocellular carcinoma and Su *et al*.(118) performed iTRAQ and 2DE LC-MS/MS for identification of novel biomarkers for sepsis prognosis. Another popular methodology used in biomarker discovery is the so-called top-down approach in which native proteins and peptides are delivered to the mass spectrometer without prior digestion. Top-down approaches uses capillary electrophoresis (CE)-MS and surface-enhanced laser desorption/ionization time of flight (SELDI-TOF)-MS systems. CE-MS was used by Weissinger and colleagues(119) to establish urinary proteomic patterns of healthy individuals and some selected diseases. This approach was also used to define polypeptide patterns in the urine of patients with immunoglobulin A (IgA) nephropathy(120). SELDI-TOF-MS methodologies had been applied for protein profiling of diverse conditions(121-124). Besides this methodologies are less efficient to absolute identification, it is able to recognize native small peptides. On the other hand, bottom-up approaches are advantageous for protein identification, however quantification is more challenging(113). To the best of our knowledge, there are no known studies that evaluated the effect of CHF on urine protein profile.

III. Aims

Proteomic analysis of biofluids is a promising approach for the discovery of new biomarkers for several diseases. PAH and its complications are associated to a high morbidity and mortality, making urgent the discovery of biomarkers for its diagnosis. Based on these facts, the aims of this work are:

(i) The characterization of the urinary proteome using SDS-PAGE nanoLC-MS/MS;

(ii) The evaluation of the effect of PAH on the urine proteome profile, correlating with the proteolytic activity of this biofluid.

IV. Materials and Methods

1. Characterization of study population

In order to evaluate the effect of cardiac cachexia on the urinary proteome, first morning urine samples were collected from two patients with PAH and five healthy individuals, from both genres and with ages ranging from 35 to 55 years. One of the patients presented PAH associated to scleroderma and the other had idiopathic PAH (iPAH). Both patients presented CC, characterized by an involuntary weight loss higher than 6% of the total body weight.

2. Experimental design

In order to fulfill the proposed objectives, the experimental design represented in Figure 4 was followed.

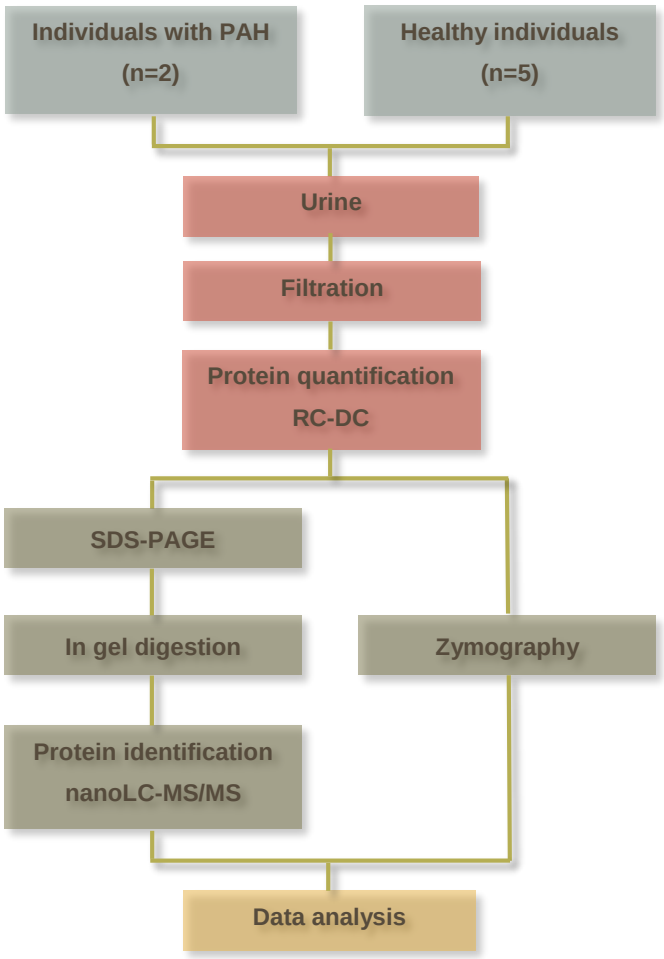

Figure 4 – Experimental design.
(RC-DC – reducing agent compatible-detergent compatible)**.**

3. Sample collection and preparation

After collection, urine samples were submitted to centrifugation for 10 minutes at 1000 x g at 4ºC. In order to concentrate samples, the supernatant was passed through 50-kDa filters and the retentate was ressuspended in 100 µL of a solution of 6M urea, 2M tiourea, 1% CHAPS and 0.5% SDS. The samples were then stored at -80ºC. Total protein content of the retentate fraction was estimated using a RC-DC assay kit (BioRad®), based on Lowry method. The optical densities were read at 750 nm in a microplate spectrophotometer (Thermo Scientific® Multiskan GO) and a calibration curve was obtained with different concentrations of standard solutions of bovine serum albumin (BSA). Finally, samples were stored at – 80ºC until further analysis.

4. Protein separation by SDS-PAGE

Previously filtrated proteins were separated by SDS-PAGE, according to their MW, using 12.5% polyacrylamide gels. A total volume of 20 µL (sample with charge buffer) was added to each electrophoresis well. In one gel this volume contains 20 µg of protein, whereas in the other, samples were normalized to volume and 12 µL of each sample were added. Electrophoresis was performed at a constant voltage of 200 V for approximately 45 minutes. After this, gels were fixed (40% methanol and 10% acetic acid) for 1 hour with agitation. The fixation solution was then removed and gels were incubated overnight, with permanent agitation, in a colloidal Coomassie staining solution (0.12% Coomassie G250 in 20% methanol). Once the Coomassie solution was removed, a destaining solution (25% methanol) was added to remove de excess of stain.

5. Protein identification by nanoLC-MS/MS

First, some gel bands of a healthy individual sample were excised and proteins were submitted to in gel digestion with trypsin. In a second approach, all the gel lanes were cut to get 16 fragments, which were also digested with trypsin. In gel digestion was initiated with 2 washes, first with 25 mM ammonium hidrogenocarbonate and then with ultrapure acetonitrile (ACN). This procedure was repeated 2 times and was followed by another wash with ACN. Washes were performed to wash, destain and dehydrate gel fragments. After this, gel fragments were dried at 37ºC during approximately 45 minutes and trypsin was added. Gel fragments with trypsin were incubated at 37ºC for 1 hour and were then submerged in 25 mM ammonium hidrogenocarbonate to overnight incubation period. Digestion process was quenched by the addition of 10% formic acid. Peptides were extracted from gel fragments by the addition of a solution of 10% formic acid and ultrapure

ACN (1:1) and dried on SpeedVac® Plus SC 210ª (Thermo Savant, USA). Dried peptides were resuspended in 20 µL of a solution of 5% ACN, 95% H_2O and 0,1% trifluoroacetic acid (TFA) and 9 µL were transferred to the nanoLC plate to be injected in the nanoLC column and after chromatographic separation, analyzed by MS/MS.

6. Analysis of the proteolytic activity by zymography

Zymography was performed to analyze the proteolytic activity of the samples, using a 10% polyacrylamide gel with gelatin as substrate. A total volume of 20 µL (sample with charge buffer) was added to each electrophoresis well. Electrophoresis was performed at a constant voltage of 100 V for approximately 1 hour and 15 minutes. Gels were then incubated for 1 hour (2 washes of 30 minutes each) in a renaturing buffer (2.5% Triton X-100) with soft agitation. After Triton, gels were submerged in a development buffer (50 mM Tris pH 7,4, 5 mM NaCl, 10 mM $CaCl_2$, 1 µM $ZnCl_2$, 0.02% Triton X-100) for 30 minutes with agitation, followed by a 4 hour incubation period at 37ºC in the same buffer. Two different development buffers were prepared and ethylenediamine tetraacetic acid (EDTA) was added to one of them (50 mM Tris pH 7,4, 5 mM NaCl, 10 mM $CaCl_2$, 1 µM $ZnCl_2$, 0.02% Triton X-100, 10 mM EDTA). For staining, gels were incubated overnight, with agitation, in a colloidal Coomassie solution. After Comassie removal, several washes with destaining solution (25% methanol) were performed in order to obtain a contrast between the light bands corresponding to the areas with enzymatic activity and the blue background.

7. Data analysis

In order to edit gel images and obtain optical density (OD) curves, gels were analyzed using the software Image Lab® and Quantity One® by BioRad. Data from nanoLC-MS/MS was submitted to UniProt database and then were analyzed using bioinformatics tools, such as PATHER, STRING and Venny.

V. Results

1. Urine protein profiling by SDS-PAGE nanoLC-MS/MS

In order to characterize urinary protein and proteolytic profiles, proteins were separated by SDS-PAGE and zymography respectively, and the obtained profiles are presented in Figure 5.

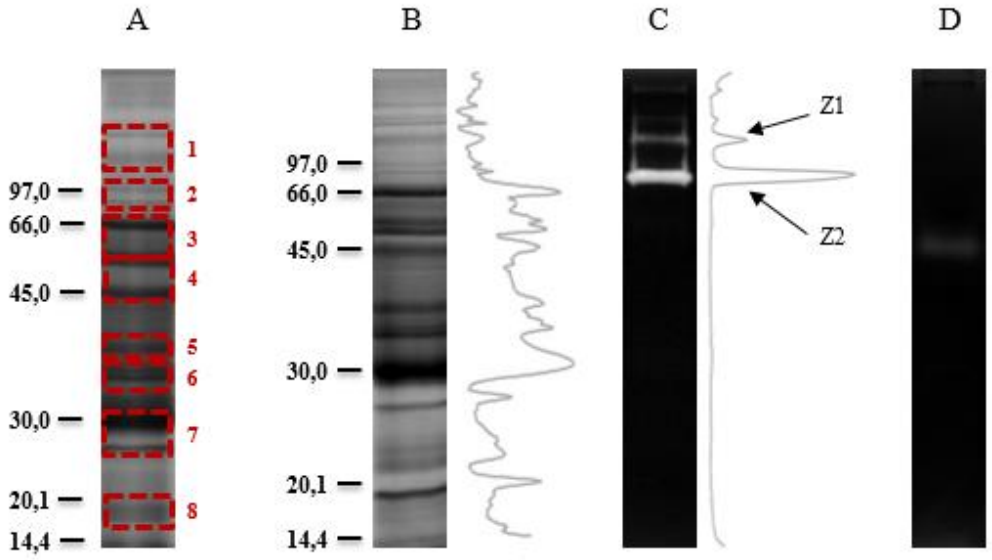

Figure 5 – **Urinary protein profiles of healthy individuals and its optical density curves.** SDS-PAGE gel 12.5 %, corresponding to the separation of 20 µg urinary proteins (A) and 12 µL of urine sample (B). Zymography gel impregnated with gelatin corresponding to 12 µL of sample (C) and after incubation with EDTA (D).

Several bands were observed in SDS-PAGE gel, with the higher intensity ones corresponding to 66 e 30 kDA. Proteolytic profile achieved by copolymerizing SDS-PAGE gel with gelatin (Figure 5C) revealed two bands with a more pronounced activity. According to Caseiro *et al*.(125) the band with approximately 72 kDa (Z2), corresponding to the higher OD peak, is the pro-matrix metalloproteinase 2 (pro-MMP-2). Since the zymo band corresponding to the active form – matrix metalloproteinase 2 (MMP-2) – has a similar MW(126), this hypothesis has to be considered too. The second zymo band (Z1) presents a higher MW and an OD peak with lower intensity than Z2. This band corresponds to the matrix metalloproteinase 9 (MMP-9)(125) or to their latent form pro-matrix metalloproteinase 9 (pro-MMP9)(126). The presence of matrix metalloproteinases (MMPs) was confirmed by the incubation of zymography gels with EDTA, an inhibitor of MMPs activity. The inhibitory effect of EDTA was clearly noticed (Figure 5D).

For further characterization, proteins were excised from SDS-PAGE gel, digested with trypsin and identified by nanoLC-MS/MS. In a first approach we analyzed the entire lanes. Data was submitted to UniProt database and a total of 277 proteins (Appendix 1) were retrieved. A list of all proteins identified in healthy individuals is presented in the appendices section (Appendix 2). The distribution of urinary proteins according to MW (Figure 6) and p*I* (Figure 7) highlights the prevalence of proteins with MW between 10 and 70 kDa, and p*I* in the range from 5 to 7.

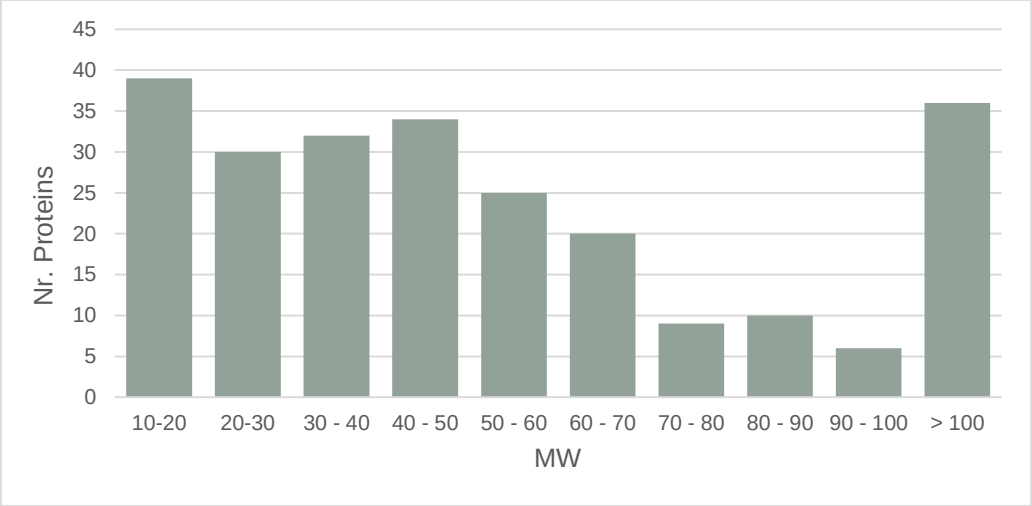

Figure 6 – Distribution of urinary proteins according their MW.

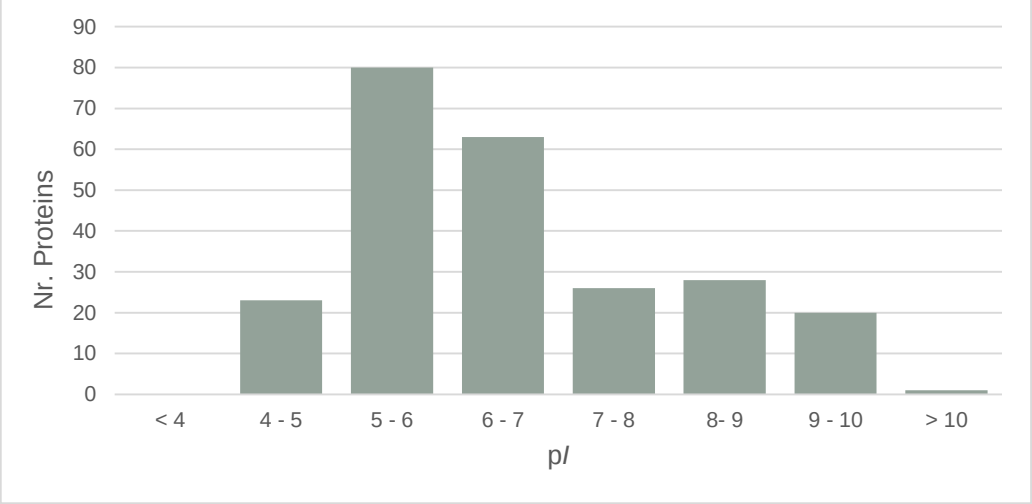

Figure 7 – Distribution of urinary proteins according their p*I*.

Using PANTHER software, data from nanoLC-MS/MS was distributed into clusters according to their molecular function and biological processes in which they are involved (Figure 8). Binding and catalytic activity are the most significant molecular functions of the identified proteins. Concerning biological processes, the majority of urinary proteins participate in cellular and metabolic activities.

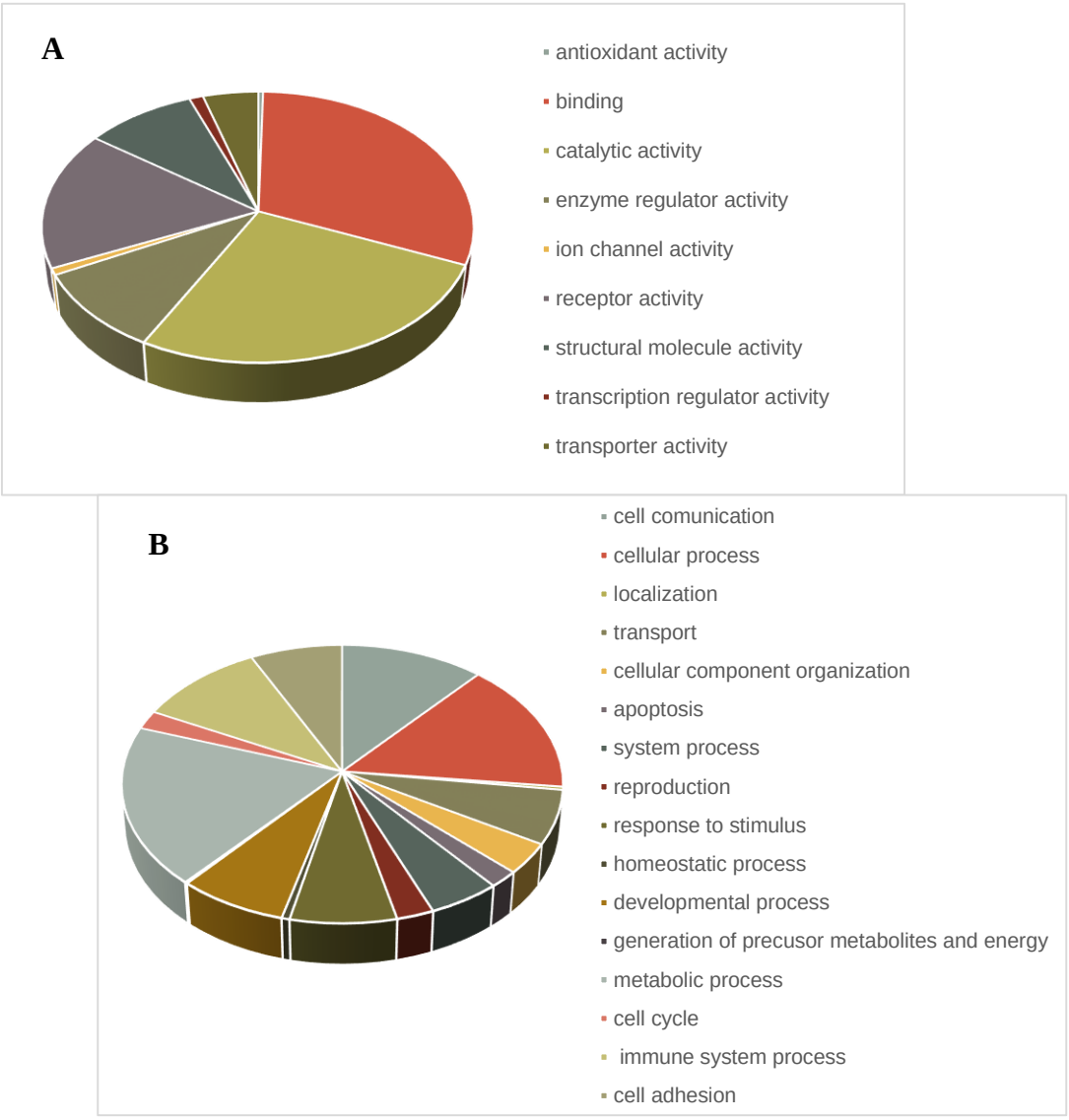

Figure 8 – Proteins' distribution according (A) molecular function and (B) biological process using PANTHER software.

In another approach, eight regions of the SDS-PAGE gel (Figure 5A) were excised and proteins identified by nanoLC-MS/MS. Data was submitted to UniProt database and only the proteins with p<0,005 were considered. Several proteins were identified in more than one band of the gel, suggesting an increased susceptibility to proteolysis. Proteins more susceptible to fragmentation are summarized in Table 4.

Table 4 - Urinary proteins with increased susceptibility to proteolysis.

Band #	Accession #	Protein ID	MW (Da)	p*I*
1/2/3/4/5/6/7/8	Q676U5	A16L1_HUMAN APG16 autophagy 16-like isoform 1; 1500009K01Rik; WD repeat domain 30	58235,59	6,20
2/3/4/5/6/7/8	O95967	FBLN4_HUMAN EGF-containing fibulin-like extracellular matrix protein 2; fibulin 4	49427,39	4,79
1/2/3/4/5/6/8	P20700	LMNB1_HUMAN lamin B1	66367,71	5,11
1/2/3/4/5/6/7	_____	PREDICTED: chromosome 19 open reading frame 14	166405,7	_____
1/2/3/4/7/8	Q15746-8	MYLK_HUMAN myosin light chain kinase isoform 6; myosin light chain kinase	110006,1	_____
1/2/3/4/6/8	Q70J99	UN13D_HUMAN unc-13 homolog D	123204,8	6,19
1/3/4/6/8	P00390	GSHR_HUMAN glutathione reductase	51667,4	7,61
2/3/4/5/8	Q06190	P2R3A_HUMAN alpha isoform of regulatory subunit B'', protein phosphatase 2 isoform	130195	5,09
2/3/4/5/8	Q9UKF6	CPSF3_HUMAN cleavage and polyadenylation specific factor 3, 73kDa	77436,22	5,37
1/3/4/6/8	_____	PREDICTED: similar to CG11994-PA	42542,92	_____
1/2/5/6/8	Q9BYX2	TBD2A_HUMAN TBC1 domain family, member 2	54384,32	6,15
1/2/4/5/7	Q8IXF0	NPAS3_HUMAN basic-helix-loop-helix-PAS protein	96959,3	6,16

Interestingly it was also observed that most of these proteins are phosphorylated. Using PANTHER software it was found that these proteins are essentially associated to metabolic, cellular and development processes.

2. The effect of PAH on the urinary proteome profile

In order to evaluate the effect of PAH on urinary protein profile, a label free SDS-PAGE-nanoLC-MS/MS approach was performed. The list of all proteins identified in individuals with PAH can be seen in the appendices section (Appendix 3). Proteins from desalted urine samples were separated according its molecular weight by SDS-PAGE and the proteolytic profile was determined by zymography. The obtained profiles are represented in Figure 9.

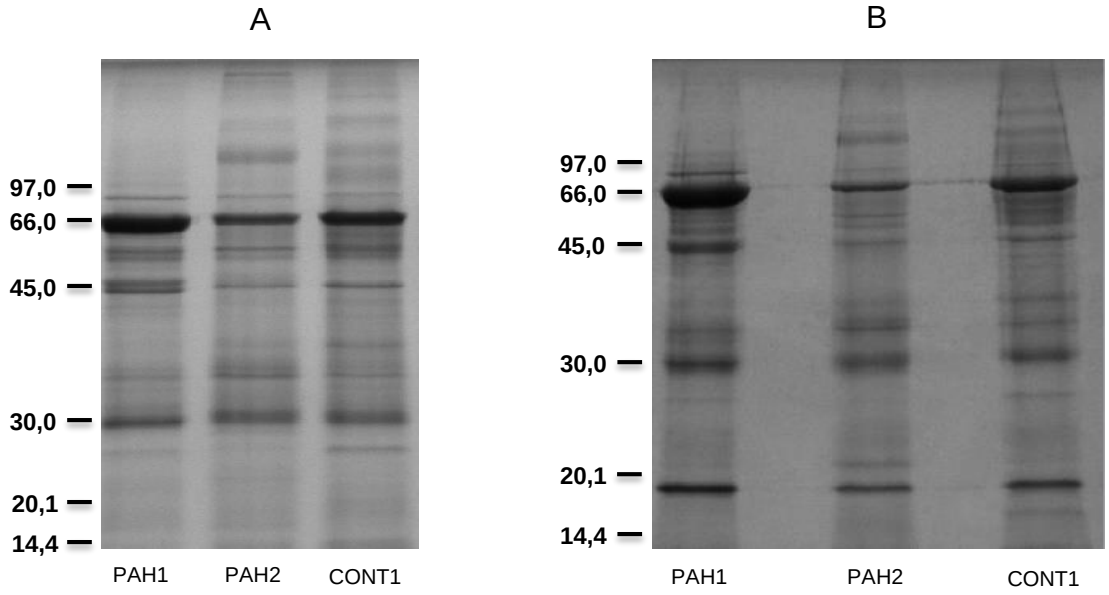

Figure 9 – Urinary protein profiles of patients with PAH. SDS-PAGE gel 12.5%, corresponding to the separation of 20 µg of urinary proteins (A) and 12 µL of urine sample (B).

Similarly to the healthy individuals, the band corresponding to 66 kDa presents higher intensity; however, the one corresponding to 30 kDa is less intense. Furthermore, one of the patients (PAH1) has an extra band of approximately 45 kDa. The band immediately below 30 kDa seems to be less intense in patient PAH1 or even absent in PAH2 and an extra band above 20.1 kDa is present in patient PAH2. Concerning proteolytic activity (Figure 10), there are some differences between patients.

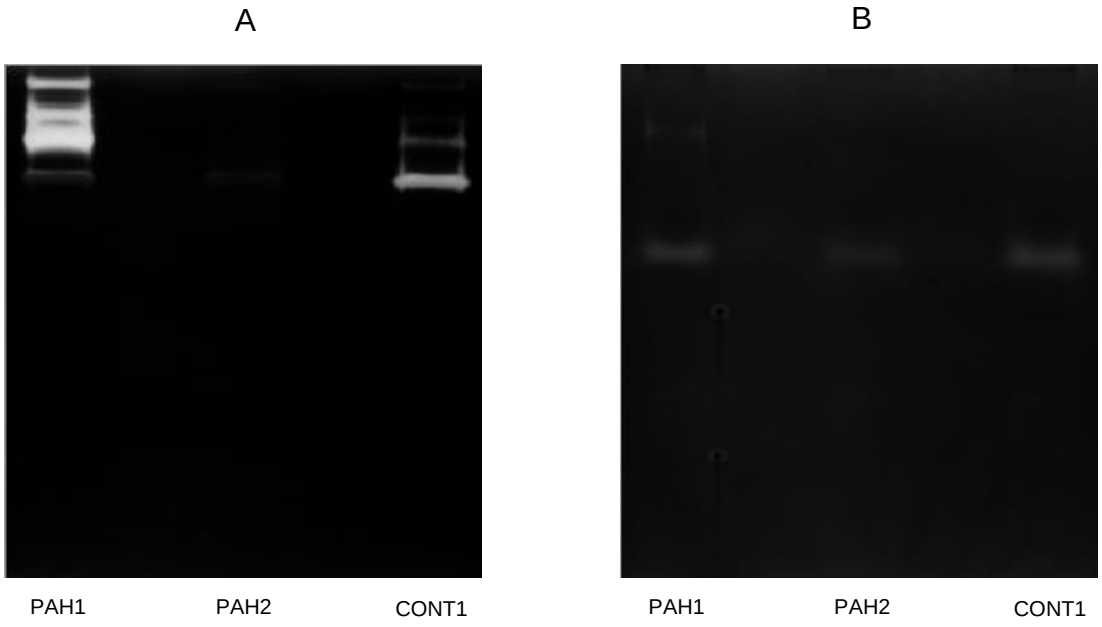

Figure 10 – Urinary protein profiles of patients with PAH. Zymography gel impregnated with gelatin corresponding to 12 µL of sample (A) and after incubation with EDTA (B).

One of the patients (PAH1) presents a higher activity in the region of upper molecular weight, whereas the urine of the other (PAH2) seems to have no significant proteolytic activity. The least intense band of the PAH1 patient, with approximately 72 kDa, is the same zymo band identified for healthy individuals, corresponding to pro-MMP-2, though it has higher intensity in control individuals. The band with higher intensity, also identified in healthy individuals, is MMP-9(125, 127). According to literature, the band immediately above MMP-9, with 92 kDa, is its latent form pro-MMP-9(127) or the complex neutrophil gelatinase-associated lipocalin (NGAL)/MMP-9, and the band with higher molecular weight (125 - 130 kDa) is the complex NGAL/MMP-9(128-132) or a MMP-9 dimer (with approximately 220 kDa)(130, 132). In the zymography gel that was incubated with development buffer containing EDTA, these gelatinolytic bands were missing, confirming the presence of MMPs.

Urinary proteins' distribution by individual was obtained via the bioinformatics tool Venny (Figure 11).

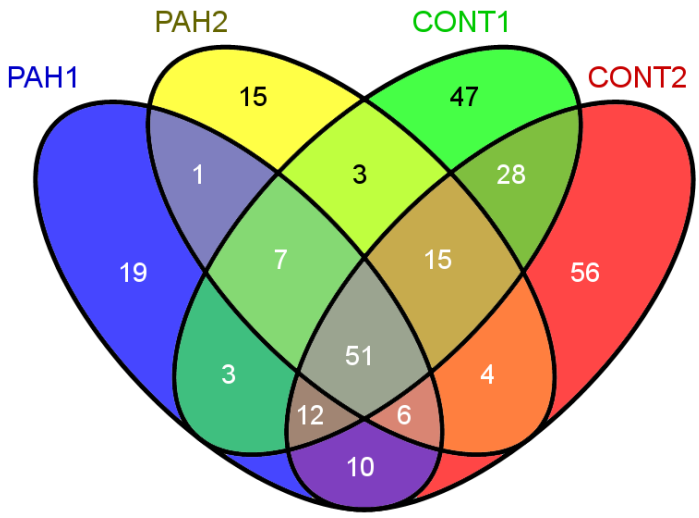

Figure 11 - Venn diagram representing the distribution of urinary proteins identified between individuals. http://bioinfogp.cnb.csic.es/tools/venny/.

The presence of several proteins that are exclusive of an individual highlights interindividual variations of urinary proteome. There were 51 proteins in common between all the individuals (Appendix 4), including albumin, uromodulin and osteopontin. According to PANTHER tool, most of these proteins are associated to binding, receptor and catalytic activities, and are involved in biological processes such as proteolysis, amino acid synthesis, cell adhesion, signal transduction, protein transport and immune response. According to Venn diagram, there are 131 proteins that are exclusive from healthy individuals, but only 28 of them are common between them. The analysis with PANTHER software demonstrated that most of these 28 proteins are involved in binding activities, being catalytic, receptor and enzyme regulator activities other important molecular functions. Regarding PAH patients, 35 exclusive proteins were identified, being essentially related to protein binding, metabolic processes including proteolysis, cell adhesion and communication, immune response and signal transduction.

Only one protein in common between the two patients was identified, the serine/threonine-protein kinase with-no-lisine kinase 4 (WNK4). In order to integrate this protein in the cellular processes potentially modulated by PAH, protein-protein interaction analysis was performed with STRING (Figure 12).

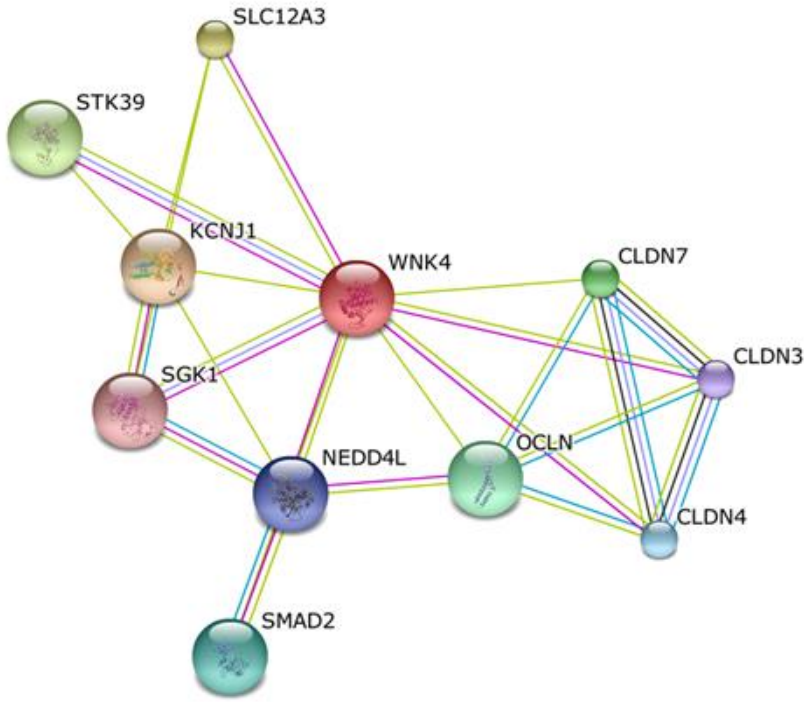

Figure 12 – Protein-protein interactions associated with WNK4.

STRING analysis evidence several protein-protein interactions involving WNK4, including the inhibition of the thiazide-sensitive sodium chloride (NaCl) cotransporter (encoded by SLC12A3) activity by diverting it to the lysosome for degradation, inhibiting the NaCl reabsorption(133). WNK4 also regulates the activity of the renal outer medullary K^+ channel (ROMK), which is encoded by KCNJ1 and is the main molecular determinant of K^+ secretion in the collecting duct(134). Thus, WNK4 appears to be involved in the balance between NaCl reabsorption and K^+ secretion to maintain integrated homeostasis(135). Furthermore, WNK4 interacts with Smad 2(136) from TGF-β-Smad pathway, involved on the pathogenesis of familiar PAH(137, 138).

Label-free quantitative analysis based on the ratio between emPAI values of PAH patients and healthy individuals (Appendix 4), highlight some proteins with different relative excretion profiles. The most prominent differences correspond to Ig kappa chain C region, transferrin and Ig kappa chain V-II region that presented relative overexcretion, and to glutaminyl-peptide cyclotransferase, inter-alpha-trypsin inhibitor heavy chain H4 (ITIH4) and osteopontin with lower relative excretion.

VI. Discussion

Increased protein breakdown is a known feature of wasting conditions as the ones related to heart failure. Proteins released from wasted tissues may be excreted in urine and act as biomarkers of the cachectic process(139). Urine is a promising biofluid for clinical proteomics aiming to identify potential disease biomarkers, because of noninvasiveness and simplicity of specimen collection(140-142) and the possibility of collecting samples repeatedly over long time periods. In healthy people, approximately 30% of urinary proteins are plasma proteins and the other 70% are produced in the kidney(143). Normal total protein concentration in the urine is very low and usually does not exceed 150 mg/day or 10 mg/mL in any single specimen. When concentration is higher than 150 mg/day the designation proteinuria is used, indicating glomerular or reabsorption dysfunction(141).

In the present work, the effect of PAH on the urinary proteome was evaluated and regarding SDS-PAGE profiles (Figure 9), there were some differences in some bands' intensity between subjects. However, to the best of our knowledge, there are no known studies using SDS-PAGE to characterize the urinary protein profile of patients with PAH. The analysis of zymographic profiles also evidenced differences between patients and healthy individuals and even among patients. Gelatin zymography analysis of urine samples mainly highlights the contribution of MMPs to biofluids proteolysis(125) Benisty *et al*.(144) also reported distinct urinary MMPs patterns in individuals with idiopathic iPAH and with other forms of PAH. MMPs have key roles in modulating structural extracellular matrix proteins and are known to be upregulated in remodeled lung vasculature of patients with iPAH and PAH(145). An *in situ* and *in vitro* study of human pulmonary arteries revealed an imbalance between MMPs and tissue inhibitor of metalloproteinase-1 (TIMP-1) and an increase in active MMP-2 in iPAH cells when compared with controls(146). In patient PAH1, the presence of several zymo bands highlight an increase in proteolytic activity, whereas patient PAH2 seems to have no significant activity. There is only one band with lower intensity that corresponds to pro-MMP2.

The distribution of the urinary proteins *per* individual highlighted interindividual variations, since there were several exclusive proteins for each subject. In a total of 277 identified proteins, 51 were present in all individuals. Most of these proteins were expected in the urine and include albumin, immunoglobulins(113), uromodulin(113, 114) and osteopontin(147). From the 131 unique proteins of healthy individuals, only 28 were common between them, most of which involved in proteolysis, with some protease inhibitors identified. These inhibitors include serpins, cystatins, and caspase-14, and their absence in the urine of PAH patients may justify, at least in part, the increased proteolytic activity

observed in one of the patients. Furthermore, a great part of the exclusive proteins of the patient PAH1 were associated to proteolysis and protein modification. Proteins involved in proteolysis include cathepsins (B and C), α2-macroglobulin (an inhibitor of endoproteinases such as MMPs(148)), f-box only protein 3 (FBxo3), ubiquitin-60s ribosomal protein L40 (ubiquitin precursor) and carboxypeptidase vitellogenic-like (CPVL). Cathepsins are known as lysosomal cysteine proteases involved in the bulk degradation of intracellular and endocytosed proteins(149). The involvement of cathepsins in extracellular matrix degradation has been largely referred in several pathophysiological conditions(150-160). The activity of secreted cathepsins in the ECM is facilitated by acidification of the peri- and extracellular space under inflammatory conditions(149). Cathepsin B were associated to the degradation of several components of the ECM such as proteoglycan(150, 151), aggrecan(152-154), collagen (types II, IX, XI(155) IV and X(156, 157)), fibronectin(156, 158), laminin(156), osteocalcin(159) and osteonectin(160). Moreover, muscle atrophy seems to be associated with increased mRNA levels of cathepsins (B and L)(161). FBxo3 is an E3 ligase subunit that stimulates cytokine secretion from human inflammatory cells by destabilizing a TNF receptor-associated factor (TRAF) inhibitor, f-box and leucine rich repeat protein 2 (Fbxl2)(162). TRAF proteins are crucial adaptor proteins that link membrane-bound immune receptors (including TNF receptors and Toll-like receptors) to downstream signaling cascades(163). FBxo3 triggers ubiquitination and degradation of FBxl2, thereby increasing the amount of TRAF proteins. TRAF proteins are critically involved in inflammation, innate and adaptive immune responses, and programmed cell death(162). CPVL is a serine carboxypeptidase of unknown function, first characterized in human macrophages, and that may play a role in the biosynthesis of secretory molecules or could be involved in the processing and/or transport of peptides for loading onto major histocompatibility complex (MHC) class I molecules or in MHC class II-dependent antigen presenting cell (APC) functions, but it is unclear whether it is involved in endocytosis(164). Some of the unique proteins from patient PAH1 are also involved in immune response. Myeloperoxidase (MPO) is an enzyme mainly released by activated neutrophils, characterized by powerful pro-oxidative and pro-inflammatory properties(165). Hypochlorous acid, generated by the MPO-H2-O2-chloride system, inactivates TIMP-1, promoting an imbalance between MMPs and tissue inhibitors of metalloproteinases (TIMPs) activities with an increase of proteolysis(166). Serum amyloid P component (SAP) is a short pentraxin produced in the liver in response to IL-6(167). The presence of this protein may possibly be explained by the higher levels of IL-6 in CHF patients. Interestingly, unique proteins from patient PAH2 seem to have no significant association with proteolysis (with

exception of cathepsin C), being mainly associated to immune response, particularly to antigen processing and presentation and macrophage activation. These findings appear to be in accordance with the lower proteolytic activity presented by patient PAH2; however, these data do not reflect the cachectic state.

Curiously, only WNK4 was identified in the urine of both PAH patients and it appears to be involved in the balance between kidney NaCl reabsorption and K^+ secretion to maintain integrated homeostasis(135). Mutations in WNK kinases were reported to cause human hypertension(168). WNK4 may also be involved in the pathogenesis of familiar PAH via interactions with Smad 2(136). To better validate the potential diagnosis value of this urinary protein, the search of urinary WNK4 was extended to samples from 20 subjects (diabetics with and without microvascular complications) analyzed under similar experimental conditions. No positive identification was achieved, emphasizing the potential diagnosis value of WNK4 for PAH.

Focusing on the 51 common proteins, label-free quantitative analysis based on the ratio between emPAI values of PAH patients and healthy individuals evidenced different relative excretion profiles. The presence of over-excreted proteins such as Ig kappa chain C region and Ig kappa chain V-II region is possibly a consequence of the chronic immune activation. Higher transferrin excretion levels in PAH patients, may be related to iron deficiency, a common feature of iPAH patients(169-171), being associated with poor outcomes. This deficiency may be caused by the inappropriately raised of hepcidin levels, which impair iron absorption by the gut. Inflammation can raise hepcidin through IL-6 induction(170). Although anemia and/or hypoxia suppress the expression of hepatic hepcidin, the inflammatory stimuli are strong enough to induce its release even in the setting of anemia(172). Thus, the chronic inflammation underlying PAH can be the cause of iron deficiency. Some of the proteins with lower excretion in PAH patients include ITIH4, osteopontin and glutaminyl-peptide cyclotransferase. Inter-alpha-trypsin inhibitor (ITI) proteins are serine proteases inhibitors which modulate endogenous protease activity(173). Therefore, the decreased ITIH4 excretion may be associated with the higher proteolytic activity noticed in some PAH patients. Osteopontin plasma levels are known to be increased in patients with iPAH and to be associated to a poor prognosis(174). However, the relationship with urinary excretion was not described. Osteopontin is broadly expressed and upregulated during inflammation, cancer, and various other conditions, but its exact role in the pathogenesis of iPAH is not completely understood(174). Decreased excretion of

glutaminyl-peptide cyclotransferase, an enzyme involved in cellular amino acid biosynthesis and protein modification, may be an indicator of the catabolic/anabolic imbalance.

VII. Conclusion

Considering the effect of PAH on urinary protein and proteolytic profiles, it was possible to conclude that:

(i) Urinary proteome is highly dynamic and reflects interindividual variations, emphasized by the presence of unique proteins in all individuals; however PAH seem to impact urinary protein and proteolytic profiles;

(ii) Gelatin zymography mainly highlight the presence of MMPs in the urine, with an increase in their activity in one of the PAH patients, suggesting that proteolytic profiles may differ according to the clinical classification of PAH;

(iii) Increased proteolytic activity observed in one PAH patient was related with the presence of unique urinary proteases and proteins involved in the immune response in PAH;

(iv) Data from label free quantitative analysis evidenced different protein relative excretion profiles that are, at least in part, in agreement with the catabolic/anabolic imbalance and the chronic inflammation state seen in PAH patients;

(v) WNK4 was only identified in the urine of PAH subjects, being a candidate biomarker for the diagnosis of PAH.

Taken together, data highlight the presence of high proteolytic activity in the urine of some PAH patients, emphasizing the disease-related inflammation and cachexia in these patients, and also allow suggesting WNK4 as a new potential biomarker for the diagnosis of PAH. Future work focused on a deeper analysis of urinary proteolysis in patients with distinct PAH clinical classifications will be important to better understand urine dynamics in response to disease pathogenesis. Moreover, the validation of WNK4 as a disease biomarker will ideally allow its application to clinics.

VIII. References

1. Dimopoulos S, Tzanis G, Manetos C, Tasoulis A, Mpouchla A, Tseliou E, Vasileiadis I, Diakos N, Terrovitis J, Nanas S. Peripheral muscle microcirculatory alterations in patients with pulmonary arterial hypertension: A pilot study. Respiratory Care. 2013 May 28, 2013.

2. Vonk Noordegraaf A, Galiè N. The role of the right ventricle in pulmonary arterial hypertension. European Respiratory Review. 2011 December 1, 2011;20(122):243-53.

3. Guazzi M, Galiè N. Pulmonary hypertension in left heart disease. European Respiratory Review. 2012;21(126):338-46.

4. Naeije R. Pulmonary hypertension and right heart failure in chronic obstructive pulmonary disease. Proceedings of the American Thoracic Society. 2005;2(1):20-2.

5. Anker SD, von Haehling S. Inflammatory mediators in chronic heart failure: an overview. Heart. 2004;90:464-70.

6. Jankowska EA, Ponikowski P, Piepoli MF, Banasiak W, Anker SD, Poole-Wilson PA. Autonomic imbalance and immune activation in chronic heart failure – Pathophysiological links. Cardiovascular Research. 2006 June 1, 2006;70(3):434-45.

7. Weber KT, Gerling IC, Kiani MF, Guntaka RV, Sun Y, Ahokas RA, Potlethwaite AE, Warrington KJ. Aldosteronism in Heart Failure: A Proinflammatory/Fibrogenic Cardiac Phenotype. Search for Biomarkers and Potential Drug Targets. Current Drug Targets. 2003;4:505-16.

8. Anker SD. Imbalance of catabolic and anabolic pathways in chronic heart failure: implications for the treatment of cardiac cachexia. Scandinavian Journal of Nutrition. 2002;46(1):3-10.

9. Sharma R, Anker SD. Immune and Neurohormonal Pathways in Chronic Heart Failure. Congestive Heart Failure. 2002;8(1):23-48.

10. Schulze PC, Späte U. Insulin-like growth factor-1 and muscle wasting in chronic heart failure. The International Journal of Biochemistry & Cell Biology. 2005;37(10):2023-35.

11. Yndestad A, Kristian Damås J, Øie E, Ueland T, Gullestad L, Aukrust P. Systemic inflammation in heart failure – The whys and wherefores. Heart Failure Reviews. 2006;11(1):83-92.

12. Strassburg S, Springer J, Anker SD. Muscle wasting in cardiac cachexia. The International Journal of Biochemistry & Cell Biology. 2005;37(10):1938-47.

13. Filippatos GS, Kanatselos C, Manolatos DD, Vougas B, Sideris A, Kardara D, Anker SD, Kardaras F, Uhal B. Studies on apoptosis and fibrosis in skeletal musculature: a comparison of heart failure patients with and without cardiac cachexia. International Journal of Cardiology. 2003;90(1):107-13.

14. Vachiéry J-L, Gaine S. Challenges in the diagnosis and treatment of pulmonary arterial hypertension. European Respiratory Review. 2012 December 1, 2012;21(126):313-20.

15. Rocchiccioli J, McMurray J, Dominiczak A. Biomarkers in heart failure: a clinical review. Heart Failure Reviews. 2010;15(4):251-73.

16. Lainscak M, Anker M, von Haehling S, Anker S. Biomarkers for Chronic Heart Failure: Diagnostic, Prognostic, and Therapeutic Challenges. Herz. 2009;34(8):589-93.

17. Lam L, Lind J, Semsarian C. Application of proteomics in cardiovascular medicine. International Journal of Cardiology. 2006;108(1):12-9.

18. Hu S, Loo JA, Wong DT. Human body fluid proteome analysis. Proteomics. 2006 Dec;6(23):6326-53.

19. Anker SD, Coats AJS. Cardiac Cachexia*A Syndrome With Impaired Survival and Immune and Neuroendocrine Activation. CHEST Journal. 1999;115(3):836-47.

20. Akashi Y, Springer J, Anker S. Cachexia in chronic heart failure: Prognostic implications and novel therapeutic approaches. Current Heart Failure Reports. 2005;2(4):198-203.

21. von Haehling S, Doehner W, Anker SD. Nutrition, metabolism, and the complex pathophysiology of cachexia in chronic heart failure. Cardiovascular Research. 2007 January 15, 2007;73(2):298-309.

22. von Haehling S, Lainscak M, Springer J, Anker SD. Cardiac cachexia: A systematic overview. Pharmacology & Therapeutics. 2009;121(3):227-52.

23. Anker SD, Sharma R. The syndrome of cardiac cachexia. International Journal of Cardiology. 2002;85(1):51-66.

24. Rydén M, Arner P. Fat loss in cachexia—is there a role for adipocyte lipolysis? Clinical Nutrition. 2007;26(1):1-6.

25. Anker SD, Ponikowski PP, Clark AL, Leyva F, Rauchhaus M, Kemp M, Teixeira MM, Hellewell PG, Hooper J, Poole-Wilson PA, Coats AJS. Cytokines and neurohormones relating to body composition alterations in the wasting syndrome of chronic heart failure. European Heart Journal. 1999 May 1, 1999;20(9):683-93.

26. Cavey J. Cardiac Cachexia. The Journal for Nurse Practitioners. 2011;7(7):578-81.

27. Levine B, Kalman J, Mayer L, Fillit HM, Packer M. Elevated Circulating Levels of Tumor Necrosis Factor in Severe Chronic Heart Failure. New England Journal of Medicine. 1990;323(4):236-41.

28. McMurray J, Abdullah I, Dargie HJ, Shapiro D. Increased concentrations of tumour necrosis factor in "cachectic" patients with severe chronic heart failure. British Heart Journal. 1991 November 1, 1991;66(5):356-8.

29. Testa M, Yeh M, Lee P, Berman JW, Lejemtel TH, Fanelli R, Loperfido F. Circulating Levels of Cytokines and Their Endogenous Modulators in Patients With Mild to Severe Congestive Heart Failure Due to Coronary Artery Disease or Hypertension. Journal of the American College of Cardiology. 1996;28(4):964-71.

30. Tsutamoto T, Hisanaga T, Wada A, Maeda K, Ohnishi M, Fukai D, Mabuchi N, Sawaki M, Kinoshita M. Interleukin-6 Spillover in the Peripheral Circulation Increases With the Severity of Heart Failure, and the High Plasma Level of Interleukin-6 Is an Important Prognostic Predictor in Patients With Congestive Heart Failure. Journal of the American College of Cardiology. 1998;31(2):391-8.

31. Torre-Amione G, Kapadia S, Benedict C, Oral H, Young JB, Mann DL. Proinflammatory cytokine levels in patients with depressed left ventricular ejection fraction: A report from the studies of left ventricular dysfunction (SOLVD). Journal of the American College of Cardiology. 1996;27(5):1201-6.

32. Aukrust P, Ueland T, Lien E, Bendtzen K, Müller F, Andreassen AK, Nordøy I, Aass H, Espevik T, Simonsen S, Frøland SS, Gullestad L. Cytokine network in congestive heart failure secondary to ischemic or idiopathic dilated cardiomyopathy. The American journal of cardiology. 1999;83(3):376-82.

33. Steinborn W, Anker SD. Cardiac Cachexia: Pathophysiology and Clinical Implications. Basic Applied Myology. 2003;13(4):191-201.

34. Torre-Amione G, Kapadia S, Lee J, Durand J-B, Bies RD, Young JB, Mann DL. Tumor Necrosis Factor-α and Tumor Necrosis Factor Receptors in the Failing Human Heart. Circulation. 1996 February 15, 1996;93(4):704-11.

35. Tsutamoto T, Wada A, Ohnishi M, Tsutsui T, Ishii C, Ohno K, Fujii M, Matsumoto T, Yamamoto T, Takayama T, Dohke T, Horie M. Transcardiac increase in tumor necrosis factor-α and left ventricular end-diastolic volume in patients with dilated cardiomyopathy. European Journal of Heart Failure. 2004 March 1, 2004;6(2):173-80.

36. Niebauer J, Volk H-D, Kemp M, Dominguez M, Schumann RR, Rauchhaus M, Poole-Wilson PA, Coats AJS, Anker SD. Endotoxin and immune activation in chronic heart failure: a prospective cohort study. The Lancet. 1999;353(9167):1838-42.

37. Skipworth RJE, Stewart GD, Ross JA, Guttridge DC, Fearon KCH. The molecular mechanisms of skeletal muscle wasting: Implications for therapy. The Surgeon. 2006;4(5):273-83.

38. Hasselgren P-O, Fischer JE. Muscle Cachexia: Current Concepts of Intracellular Mechanisms and Molecular Regulation. Annals of Surgery. 2001;233(1):9-17.

39. Glickman MH, Ciechanover A. The Ubiquitin-Proteasome Proteolytic Pathway: Destruction for the Sake of Construction. Physiological Reviews. 2002 April 1, 2002;82(2):373-428.

40. Varshavsky A. The N-end rule pathway of protein degradation. Genes to Cells. 1997;2(1):13-28.

41. Solomon V, Baracos V, Sarraf P, Goldberg AL. Rates of ubiquitin conjugation increase when muscles atrophy, largely through activation of the N-end rule pathway. Proceedings of the National Academy of Sciences. 1998 October 13, 1998;95(21):12602-7.

42. Saini A, Nasser A-S, Stewart CEH. Waste management—Cytokines, growth factors and cachexia. Cytokine & Growth Factor Reviews. 2006;17(6):475-86.

43. Loncar G, Fülster S, von Haehling S, Popovic V. Metabolism and the heart: An overview of muscle, fat, and bone metabolism in heart failure. International Journal of Cardiology. 2011 (0).

44. von Haehling S, Jankowska E, Anker S. Tumour necrosis factor-α and the failing heart: pathophysiology and therapeutic implications. Basic Research in Cardiology. 2004;99(1):18-28.

45. Dibbs Z, Thornby J, White BG, Mann DL. Natural variability of circulating levels of cytokines and cytokine receptors in patients with heart failure: implications for clinical trials. Journal of the American College of Cardiology. 1999;33(7):1935-42.

46. Francis SE, Holden H, Holt CM, Duff GW. Interleukin-1 in Myocardium and Coronary Arteries of Patients with Dilated Cardiomyopathy. Journal of Molecular and Cellular Cardiology. 1998;30(2):215-23.

47. Gulick T, Chung MK, Pieper SJ, Lange LG, Schreiner GF. Interleukin 1 and tumor necrosis factor inhibit cardiac myocyte ß-adrenergic responsiveness. Proc Natl Acad Sci USA. 1989;86(17):6754-7.

48. Grunfeld C, Zhao C, Fuller J, Pollock A, Moser A, Friedman J, Feingold KR. Endotoxin and cytokines induce expression of leptin, the ob gene product, in hamsters: a role for leptin in the anorexia of infection. The Journal of Clinical Investigations. 1996;97(9):2152-7.

49. Gayle D, Ilyin SE, Plata-Salamán CR. Central Nervous System IL-1β System and Neuropeptide Y mRNAs During IL-1β-induced Anorexia in Rats. Brain Research Bulletin. 1997;44(3):311-7.

50. Sharma R, Coats AJS, Anker SD. The role of inflammatory mediators in chronic heart failure: cytokines, nitric oxide, and endothelin-1. International Journal of Cardiology. 2000;72(2):175-86.

51. Packer M. The neurohormonal hypothesis: A theory to explain the mechanism of disease progression in heart failure. Journal of the American College of Cardiology. 1992;20(1):248-54.

52. Ferrara R, Mastrorilli F, Pasanisi G, Censi S, D'aiello N, Fucili A, Valgimigli M, Ferrari R. Neurohormonal modulation in chronic heart failure. European Heart Journal Supplements. 2002 April 1, 2002;4(suppl D):D3-D11.

53. Abassi Z, Karram T, Ellaham S, Winaver J, Hoffman A. Implications of the natriuretic peptide system in the pathogenesis of heart failure: diagnostic and therapeutic importance. Pharmacology & Therapeutics. 2004;102(3):223-41.

54. Brink M, Anwar A, Delafontaine P. Neurohormonal factors in the development of catabolic/anabolic imbalance and cachexia. International Journal of Cardiology. 2002;85(1):111-21.

55. Schakman O, Gilson H, Thissen JP. Mechanisms of glucocorticoid-induced myopathy. Journal of Endocrinology. 2008 April 1, 2008;197(1):1-10.

56. Gullestad L, Aukrust P, Ueland T, Espevik T, Yee G, Vagelos R, Frøland SS, Fowler M. Effect of high- versus low-dose angiotensin converting enzyme inhibition on cytokine levels in chronic heart failure. Journal of the American College of Cardiology. 1999;34(7):2061-7.

57. Packer M, Coats AJS, Fowler MB, Katus HA, Krum H, Mohacsi P, Rouleau JL, Tendera M, Castaigne A, Roecker EB, Schultz MK, Staiger C, Curtin EL, DeMets DL. Effect of Carvedilol on Survival in Severe Chronic Heart Failure. New England Journal of Medicine. 2001;344(22):1651-8.

58. So PP-S, Davies RA, Chandy G, Stewart D, Beanlands RSB, Haddad H, Pugliese C, Mielniczuk LM. Usefulness of Beta-Blocker Therapy and Outcomes in Patients With Pulmonary Arterial Hypertension. The American Journal of Cardiology. 2012 5/15/;109(10):1504-9.

59. Argilés JM, López-Soriano FJ, Busquets S. Novel approaches to the treatment of cachexia. Drug Discovery Today. 2008;13(1–2):73-8.

60. McCarthy HD, Crowder RE, Dryden S, Williams G. Megestrol acetate stimulates food and water intake in the rat: effects on regional hypothalamic neuropeptide Y concentrations. European Journal of Pharmacology. 1994;265(1–2):99-102.

61. Mantovani G, Macciò A, Massa E, Madeddu C. Managing cancer-related anorexia/cachexia. Drugs. 2001;61(4):499-514.

62. Costa AM, Spence KT, Plata-Salamán CR, ffrench-Mullen JM. Residual Ca2+ channel current modulation by megestrol acetate via a G-protein alpha s-subunit in rat hypothalamic neurones. The Journal of Physiology. 1995 September 1, 1995;487(Pt 2):291-303.

63. Srivastava MD, Srivastava BIS, Brouhard B. Δ9 Tetrahydrocannabinol and cannabidiol alter cytokine production by human immune cells. Immunopharmacology. 1998;40(3):179-85.

64. Watzl B, Scuderi P, Watson R. Marijuana components stimulate human peripheral blood mononuclear cell secretion of interferon-gamma and suppress interleukin-1 alpha in vitro. International Journal of Immunopharmacology. 1991;13(8):1091-7.

65. Sato Y, Fujiwara H, Takatsu Y. Biochemical markers in heart failure. Journal of cardiology. 2012;59(1):1-7.

66. Richards AM. New Biomarkers in Heart Failure: Applications in Diagnosis, Prognosis and Guidance of Therapy. Revista Española de Cardiología. 2010;63(06).

67. Members ATF, Dickstein K, Cohen-Solal A, Filippatos G, McMurray JJV, Ponikowski P, Poole-Wilson PA, Strömberg A, van Veldhuisen DJ, Atar D, Hoes AW, Keren A, Mebazaa A, Nieminen M, Priori SG, Swedberg K, Guidelines ECfP, Vahanian A, Camm J, De Caterina R, Dean V, Funck-Brentano C, Hellemans I, Kristensen SD, McGregor K, Sechtem U, Silber S, Tendera M, Widimsky P, Zamorano JL, Reviewers D, Auricchio A, Bax J, Böhm M, Corrà U, della Bella P, Elliott PM, Follath F, Gheorghiade M, Hasin Y, Hernborg A, Jaarsma T, Komajda M, Kornowski R, Piepoli M, Prendergast B, Tavazzi L, Vachiery J-L, Verheugt FWA, Zannad F. ESC Guidelines for the diagnosis and treatment of acute and chronic heart failure 2008: The Task Force for the Diagnosis and Treatment of Acute and Chronic Heart Failure 2008 of the European Society of Cardiology. Developed in collaboration with the Heart Failure Association of the ESC (HFA) and endorsed by the European Society of Intensive Care Medicine (ESICM). European Heart Journal. 2008 October 1, 2008;29(19):2388-442.

68. Emdin M, Vittorini S, Passino C, Clerico A. Old and new biomarkers of heart failure. European Journal of Heart Failure. 2009 April 1, 2009;11(4):331-5.

69. Palazzuoli A, Caputo M, Calabrò A, R N. Clinical impact of BNP and other emerging biomarkers in heart failure evaluation and management. Minerva Cardioangiologica. 2012;60(2):183-94.

70. Lainscak M, von Haehling S, Anker SD. Natriuretic peptides and other biomarkers in chronic heart failure: From BNP, NT-proBNP, and MR-proANP to routine biochemical markers. International Journal of Cardiology. 2009;132(3):303-11.

71. Lee D, Vasan RS. Novel markers for heart failure diagnosis and prognosis. Current Opinion in Cardiology. 2005;20(3):201-10.

72. Nagaya N, Uematsu M, Kojima M, Date Y, Nakazato M, Okumura H, Hosoda H, Shimizu W, Yamagishi M, Oya H, Koh H, Yutani C, Kangawa K. Elevated Circulating Level of Ghrelin in Cachexia Associated With Chronic Heart Failure. Circulation. 2001 October 23, 2001;104(17):2034-8.

73. Nishikimi T, Saito Y, Kitamura K, Ishimitsu T, Eto T, Kangawa K, Matsuo H, Omae T, Matsuoka H. Increased plasma levels of adrenomedullin in patients with heart failure. Journal of the American College of Cardiology. 1995;26(6):1424-31.

74. Moriyama Y, Yasue H, Yoshimura M, Mizuno Y, Nishiyama K, Tsunoda R, Kawano H, Kugiyama K, Ogawa H, Saito Y, Nakao K. The Plasma Levels of Dehydroepiandrosterone Sulfate Are Decreased in Patients with Chronic Heart Failure in Proportion to the Severity. Journal of Clinical Endocrinology & Metabolism. 2000 May 1, 2000;85(5):1834-40.

75. Kawano H, Nagayoshi Y, Soejima H, Tanaka Y, Yamabe H, Kinoshita Y, Ogawa H. Dehydroepiandrosterone levels vary according as heart failure condition in patients with idiopathic dilated cardiomyopathy. International Journal of Cardiology. 2008;125(2):277-9.

76. Pousset F, Isnard R, Lechat P, Kalotka H, Carayon A, Maistre G, Escolano S, Thomas D, Komajda M. Prognostic value of plasma endothelin-1 in patients with chronic heart failure. European Heart Journal. 1997 February 1, 1997;18(2):254-8.

77. Anker SD, Chua TP, Ponikowski P, Harrington D, Swan JW, Kox WJ, Poole-Wilson PA, Coats AJS. Hormonal Changes and Catabolic/Anabolic Imbalance in Chronic Heart Failure and Their Importance for Cardiac Cachexia. Circulation. 1997 July 15, 1997;96(2):526-34.

78. Roig E, Perez-Villa F, Morales M, Jiménez W, Orús J, Heras M, Sanz G. Clinical implications of increased plasma angiotensin II despite ACE inhibitor therapy in patients with congestive heart failure. European Heart Journal. 2000;21(1):53-7.

79. Güder G, Bauersachs J, Frantz S, Weismann D, Allolio B, Ertl G, Angermann CE, Störk S. Complementary and Incremental Mortality Risk Prediction by Cortisol and Aldosterone in Chronic Heart Failure. Circulation. 2007 April 3, 2007;115(13):1754-61.

80. Tsutamoto T, Hisanaga T, Fukai D, Wada A, Maeda Y, Maeda K, Kinoshita M. Prognostic value of plasma soluble intercellular adhesion molecule-1 and endothelin-1 concentration in patients with chronic congestive heart failure. The American journal of cardiology. 1995;76(11):803-8.

81. Anker SD, Volterrani M, Pflaum C-D, Strasburger CJ, Osterziel KJ, Doehner W, Ranke MB, Poole-Wilson PA, Giustina A, Dietz R, Coats AJS. Acquired growth hormone resistance in patients with chronic heart failure: implications for therapy with growth hormone. Journal of the American College of Cardiology. 2001;38(2):443-52.

82. Carlstedt F, Lind L, Lindahl B. Proinflammatory cytokines, measured in a mixed population on arrival in the emergency department, are related to mortality and severity of disease. Journal of Internal Medicine. 1997;242(5):361-5.

83. Keith M, Geranmayegan A, Sole MJ, Kurian R, Robinson A, Omran AS, Jeejeebhoy KN. Increased Oxidative Stress in Patients With Congestive Heart Failure 1. Journal of the American College of Cardiology. 1998;31(6):1352-6.

84. Haber HL, Leavy JA, Kessler PD, Kukin ML, Gottlieb SS, Packer M. The Erythrocyte Sedimentation Rate in Congestive Heart Failure. New England Journal of Medicine. 1991;324(6):353-8.

85. Sharma R, Rauchhaus M, Ponikowski PP, Varney S, Poole-Wilson PA, Mann DL, Coats AJS, Anker SD. The relationship of the erythrocyte sedimentation rate to inflammatory cytokines and survival in patients with chronic heart failure treated with angiotensin-converting enzyme inhibitors. Journal of the American College of Cardiology. 2000;36(2):523-8.

86. Anker SD, Doehner W, Rauchhaus M, Sharma R, Francis D, Knosalla C, Davos CH, Cicoira M, Shamim W, Kemp M, Segal R, Osterziel KJ, Leyva F, Hetzer R, Ponikowski P, Coats AJS. Uric Acid and Survival in Chronic Heart Failure. Circulation. 2003 April 22, 2003;107(15):1991-7.

87. Doehner W, Rauchhaus M, Florea VG, Sharma R, Bolger AP, Davos CH, Coats AJS, Anker SD. Uric acid in cachectic and noncachectic patients with chronic heart failure: Relationship to leg vascular resistance. American Heart Journal. 2001;141(5):792-9.

88. Gerszten RE, Wang TJ. The search for new cardiovascular biomarkers. Nature. 2008;451(7181):949-52.

89. Vasan RS. Biomarkers of Cardiovascular Disease - Molecular Basis and Practical Considerations. Circulation. 2006 May 16, 2006;113(19):2335-62.

90. Banks RE, Dunn MJ, Hochstrasser DF, Sanchez J-C, Blackstock W, Pappin DJ, Selby PJ. Proteomics: new perspectives, new biomedical opportunities. The Lancet. 2000;356(9243):1749-56.

91. Anderson L. Candidate-based proteomics in the search for biomarkers of cardiovascular disease. The Journal of Physiology. 2005 February 15, 2005;563(1):23-60.

92. Macri J, Rapundalo ST. Application of Proteomics to the Study of Cardiovascular Biology. Trends in Cardiovascular Medicine. 2001;11(2):66-75.

93. Arrell DK, Neverova I, Van Eyk JE. Cardiovascular Proteomics: Evolution and Potential. Circulation Research. 2001 April 27, 2001;88(8):763-73.

94. McGregor E, Dunn MJ. Proteomics of heart disease. Human Molecular Genetics. 2003 October 15, 2003;12(suppl 2):R135-R44.

95. Nair KS, Jaleel A, Asmann YW, Short KR, Raghavakaimal S. Proteomic research: potential opportunities for clinical and physiological investigators. American Journal of Physiology - Endocrinology And Metabolism. 2004 June 1, 2004;286(6):E863-E74.

96. Hanash S. Disease proteomics. Nature. 2003;422(6928):226-32.

97. Dohke T, Wada A, Isono T, Fujii M, Yamamoto T, Tsutamoto T, Horie M. Proteomic Analysis Reveals Significant Alternations of Cardiac Small Heat Shock Protein Expression in Congestive Heart Failure. Journal of Cardiac Failure. 2006;12(1):77-84.

98. Petrak J, Pospisilova J, Sedinova M, Jedelsky P, Lorkova L, Vit O, Kolar M, Strnad H, Benes J, Sedmera D, Cervenka L, Melenovsky V. Proteomic and transcriptomic analysis of heart failure due to volume overload in a rat aorto-caval fistula model provides support for new potential therapeutic targets - monoamine oxidase A and transglutaminase 2. Proteome Science. 2011;9(1):69. PubMed PMID: doi:10.1186/1477-5956-9-69.

99. Mazzola A, Cianti R, Bini L, Armini A, Eberini I, Pompella G, Capecchi PL, Natale M, Abbracchio MP, Laghi-Pasini F. Using peripheral blood mononuclear cells to determine proteome

profiles in human cardiac failure. European Journal of Heart Failure. 2008 August 1, 2008;10(8):749-57.

100. Baggerman G, Vierstraete E, De Loof A, Schoofs L. Gel-based versus gel-free proteomics: a review. Combinatorial Chemistry & High Throughput Screening. 2005;8(8):669-77.

101. Roepstorff P. Mass spectrometry based proteomics, background, status and future needs. Protein Cell. 2012 2012/09/01;3(9):641-7. English.

102. Abdallah C, Dumas-Gaudot E, Renaut J, Sergeant K. Gel-Based and Gel-Free Quantitative Proteomics Approaches at a Glance. International Journal of Plant Genomics. 2012;2012:17.

103. Fliser D, Novak J, Thongboonkerd V, Argilés À, Jankowski V, Girolami MA, Jankowski J, Mischak H. Advances in Urinary Proteome Analysis and Biomarker Discovery. Journal of the American Society of Nephrology. 2007 April 2007;18(4):1057-71.

104. Mann M, Hendrickson RC, Pandey A. ANALYSIS OF PROTEINS AND PROTEOMES BY MASS SPECTROMETRY. Annual Review of Biochemistry. 2001;70(1):437-73.

105. Washburn MP, Wolters D, Yates JR. Large-scale analysis of the yeast proteome by multidimensional protein identification technology. Nature Biotechnology. 2001;19(3):242-7.

106. Xu X, Veenstra TD. Analysis of biofluids for biomarker research. PROTEOMICS – Clinical Applications. 2008;2(10-11):1403-12.

107. Conrads TP, Hood BL, Veenstra TD. Sampling and analytical strategies for biomarker discovery using mass spectrometry. BioTechniques. 2006;40(6):799-805.

108. Zhou M, Conrads TP, Veenstra TD. Proteomics approaches to biomarker detection. Briefings in Functional Genomics & Proteomics. 2005 May 1, 2005;4(1):69-75.

109. Hawkridge AM, Heublein DM, Bergen HR, Cataliotti A, Burnett JC, Muddiman DC. Quantitative mass spectral evidence for the absence of circulating brain natriuretic peptide (BNP-32) in severe human heart failure. Proceedings of the National Academy of Sciences of the United States of America. 2005 November 29, 2005;102(48):17442-7.

110. Pinet F, Beseme O, Cieniewski-Bernard C, Drobecq H, Jourdain S, Lamblin N, Amouyel P, Bauters C. Predicting left ventricular remodeling after a first myocardial infarction by plasma proteome analysis. Proteomics. 2008;8(9):1798-808.

111. Zhang R, Barker L, Pinchev D, Marshall J, Rasamoelisolo M, Smith C, Kupchak P, Kireeva I, Ingratta L, Jackowski G. Mining biomarkers in human sera using proteomic tools. Proteomics. 2004;4(1):244-56.

112. Theodorescu D, Mischak H. Mass spectrometry based proteomics in urine biomarker discovery. World J Urol. 2007 2007/10/01;25(5):435-43.

113. Pisitkun T, Johnstone R, Knepper MA. Discovery of Urinary Biomarkers. Molecular & Cellular Proteomics. 2006 October 1, 2006;5(10):1760-71.

114. Hiemstra TF, Charles PD, Lilley KS. Uromodulin exclusion list improves urinary exosomal protein identification. Journal of Biomolecular Techniques. 2011;22(4):136-45.

115. Thongboonkerd V, McLeish KR, Arthur JM, Klein JB. Proteomic analysis of normal human urinary proteins isolated by acetone precipitation or ultracentrifugation. Kidney Int. 2002 10//print;62(4):1461-9.

116. Lu C-M, Wu Y-J, Chen C-C, Hsu J-L, Chen J-C, Chen J, Huang C-H, Ko Y-C. Identification of low-abundance proteins via fractionation of the urine proteome with weak anion exchange chromatography. Proteome Science. 2011;9(1):17.

117. Abdalla MA, Haj-Ahmad Y. Promising urinary protein biomarkers for the early detection of hepatocellular carcionoma among high-risk hepatitis C virus egyptian patients. Journal of Cancer. 2012;3:390-403.

118. Su L, Cao L, Zhou R, Jiang Z, Xiao K, Kong W, Wang H, Deng J, Wen B, Tan F, Zhang Y, Xie L. Identification of Novel Biomarkers for Sepsis Prognosis via Urinary Proteomic Analysis Using iTRAQ Labeling and 2D-LC-MS/MS. PLoS ONE. 2013;8(1):e54237.

119. Weissinger EM, Wittke S, Kaiser T, Haller H, Bartel S, Krebs R, Golovko I, Rupprecht HD, Haubitz M, Hecker H, Mischak H, Fliser D. Proteomic patterns established with capillary electrophoresis and mass spectrometry for diagnostic purposes. Kidney Int. 2004 06//print;65(6):2426-34.

120. Haubitz M, Wittke S, Weissinger EM, Walden M, Rupprecht HD, Floege J, Haller H, Mischak H. Urine protein patterns can serve as diagnostic tools in patients with IgA nephropathy. 2005 06//print;67(6):2313-20.

121. Rogers MA, Clarke P, Noble J, Munro NP, Paul A, Selby PJ, Banks RE. Proteomic Profiling of Urinary Proteins in Renal Cancer by Surface Enhanced Laser Desorption Ionization and Neural-Network Analysis: Identification of Key Issues Affecting Potential Clinical Utility. Cancer Research. 2003 October 15, 2003;63(20):6971-83.

122. Schaub S, Wilkins J, Weiler T, Sangster K, Rush D, Nickerson P. Urine protein profiling with surface-enhanced laser-desorption//ionization time-of-flight mass spectrometry. Kidney Int. 2004 01//print;65(1):323-32.

123. Schaub S, Rush D, Wilkins J, Gibson IW, Weiler T, Sangster K, Nicolle L, Karpinski M, Jeffery J, Nickerson P. Proteomic-Based Detection of Urine Proteins Associated with Acute Renal Allograft Rejection. Journal of the American Society of Nephrology. 2004 January 1, 2004;15(1):219-27.

124. Cadieux PA, Beiko DT, Watterson JD, Burton JP, Howard JC, Knudsen BE, Gan BS, McCormick JK, Chambers AF, Denstedt JD, Reid G. Surface-enhanced laser desorption/ionization-time of flight-mass spectrometry (SELDI-TOF-MS): A new proteomic urinary test for patients with urolithiasis. Journal of Clinical Laboratory Analysis. 2004;18(3):170-5.

125. Caseiro A, Ferreira R, Quintaneiro C, Pereira A, Marinheiro R, Vitorino R, Amado F. Protease profiling of different biofluids in type 1 diabetes mellitus. Clinical Biochemistry. 2012 12//;45(18):1613-9.

126. Snoek-van Beurden PAM, Von den Hoff JW. Zymographic techniques for the analysis of matrix metalloproteinases and theri inhibitors. BioTechniques. 2005;38(1):73-83.

127. Russell REK, Culpitt SV, DeMatos C, Donnelly L, Smith M, Wiggins J, Barnes PJ. Release and Activity of Matrix Metalloproteinase-9 and Tissue Inhibitor of Metalloproteinase-1 by Alveolar Macrophages from Patients with Chronic Obstructive Pulmonary Disease. American Journal of Respiratory Cell and Molecular Biology. 2002 2002/05/01;26(5):602-9.

128. Yan L, Borregaard N, Kjeldsen L, Moses MA. The High Molecular Weight Urinary Matrix Metalloproteinase (MMP) Activity Is a Complex of Gelatinase B/MMP-9 and Neutrophil Gelatinase-associated Lipocalin (NGAL): MODULATION OF MMP-9 ACTIVITY BY NGAL. Journal of Biological Chemistry. 2001 October 5, 2001;276(40):37258-65.

129. Gupta K, Shukla M, Cowland JB, Malemud CJ, Haqqi TM. Neutrophil gelatinase–associated lipocalin is expressed in osteoarthritis and forms a complex with matrix metalloproteinase 9. Arthritis & Rheumatism. 2007;56(10):3326-35.

130. Demestre M, Parkin-Smith G, Petzold A, Pullen AH. The pro and the active form of matrix metalloproteinase-9 is increased in serum of patients with amyotrophic lateral sclerosis. Journal of Neuroimmunology. 2005 2//;159(1–2):146-54.

131. McKittrick IB, Bogaert Y, Nadeau K, Snell-Bergeon J, Hull A, Jiang T, Wang X, Levi M, Moulton KS. Urinary matrix metalloproteinase activities: biomarkers for plaque angiogenesis and nephropathy in diabetes. American Journal of Physiology - Renal Physiology. 2011 December 1, 2011;301(6):F1326-F33.

132. Roy R, Louis G, Loughlin KR, Wiederschain D, Kilroy SM, Lamb CC, Zurakowski D, Moses MA. Tumor-specific urinary MMP fingerprinting: identification of high molecular weight urinary MMP species. Clinical Cancer Research. 2008;14(20):6610-7.

133. Subramanya AR, Liu J, Ellison DH, Wade JB, Welling PA. WNK4 diverts the thiazide-sensitive NaCl cotransporter to the lysosome and stimulates AP-3 interaction. The Journal of Biological Chemistry. 2009;284(27):18471-80.

134. Kahle KT, Wilson FH, Lifton RP. Regulation of diverse ion transport pathways by WNK4 kinase: a novel molecular switch. Trends in Endocrinology & Metabolism. 2005 4//;16(3):98-103.

135. Peng J-B, Warnock DG. WNK4-mediated regulation of renal ion transport proteins. American Journal of Physiology - Renal Physiology. 2007 October 1, 2007;293(4):F961-F73.

136. Lee B-H, Chen W, Stippec S, Cobb MH. Biological Cross-talk between WNK1 and the Transforming Growth Factor β-Smad Signaling Pathway. Journal of Biological Chemistry. 2007 June 22, 2007;282(25):17985-96.

137. Morrell NW. Pulmonary Hypertension Due to BMPR2 Mutation. Proceedings of the American Thoracic Society. 2006 2006/11/01;3(8):680-6.

138. Davies RJ, Holmes AM, Deighton J, Long L, Yang X, Barker L, Walker C, Budd DC, Upton PD, Morrell NW. BMP type II receptor deficiency confers resistance to growth inhibition by TGF-β in pulmonary artery smooth muscle cells: role of proinflammatory cytokines. American Journal of Physiology - Lung Cellular and Molecular Physiology. 2012 March 15, 2012;302(6):L604-L15.

139. Skipworth RJE, Stewart GD, Bhana M, Christie J, Sturgeon CM, Guttridge DC, Cronshaw AD, Fearon KCH, Ross JA. Mass spectrometric detection of candidate protein biomarkers of cancer cachexia in human urine. International Journal of Oncology. 2010;36(4):973-82.

140. Thongboonkerd V, Chutipongtanate S, Kanlaya R. Systematic Evaluation of Sample Preparation Methods for Gel-Based Human Urinary Proteomics: Quantity, Quality, and Variability. Journal of Proteome Research. 2005 2006/01/01;5(1):183-91.

141. Adachi J, Kumar C, Zhang Y, Olsen JV, Mann M. The human urinary proteome contains more than 1500 proteins, including a large proportion of membrane proteins. Genome Biology. 2006;7(9):R80.

142. Liu X, Shao C, Wei L, Duan J, Wu S, Li X, Li M, Sun W. An individual urinary proteome analysis in normal human beings to define the minimal sample number to represent the normal urinary proteome. Proteome Science. 2012;10(1):70.

143. González-Buitrago JM, Ferreira L. Use of urinary proteomics for the discovery of biomarkers of renal disease. European Renal Disease. 2007 (2):8-10.

144. Benisty JI, Folkman J, Zurakowski D, Louis G, Rich S, Langleben D, Moses MA. MAtrix metalloproteinases in the urine of patients with pulmonary arterial hypertension*. CHEST Journal. 2005;128(6_suppl):572S-S.

145. Wilkins MR. Pulmonary hypertension: the science behind the disease spectrum. European Respiratory Review. 2012 March 1, 2012;21(123):19-26.

146. Lepetit H, Eddahibi S, Fadel E, Frisdal E, Munaut C, Noel A, Humbert M, Adnot S, D'Ortho M-P, Lafuma C. Smooth muscle cell matrix metalloproteinases in idiopathic pulmonary arterial hypertension. European Respiratory Journal. 2005 May 1, 2005;25(5):834-42.

147. Mazzali M, Kipari T, Ophascharoensuk V, Wesson JA, Johnson R, Hughes J. Osteopontin—a molecule for all seasons. QJM. 2002 January 1, 2002;95(1):3-13.

148. Baker AH, Edwards DR, Murphy G. Metalloproteinase inhibitors: biological actions and therapeutic opportunities. Journal of Cell Science. 2002 October 1, 2002;115(19):3719-27.

149. Brömme D, Wilson S. Role of Cysteine Cathepsins in Extracellular Proteolysis. In: Parks WC, Mecham RP, editors. Extracellular Matrix Degradation. Biology of Extracellular Matrix. 2: Springer Berlin Heidelberg; 2011. p. 23-51.

150. Maciewicz RA, Wotton SF. Degradation of cartilage matrix components by the cysteine proteinases, cathepsins B and L. Biomedica biochimica acta. 1991;50(4-6):561-4.

151. Roughley PJ, Barrett AJ. The degradation of cartilage proteoglycans by tissue proteinases. Proteoglycan structure and its susceptibility to proteolysis. The Biochemical Journal. 1977;167(3):629-37.

152. Fosang AJ, Neame PJ, Last K, Hardingham TE, Murphy G, Hamilton JA. The interglobular domain of cartilage aggrecan is cleaved by PUMP, gelatinases, and cathepsin B. Journal of Biological Chemistry. 1992 September 25, 1992;267(27):19470-4.

153. Mort JS, Magny MC, Lee ER. Cathepsin B: an alternative protease for the generation of an aggrecan 'metalloproteinase' cleavage neoepitope. Biochem J. 1998 Nov 1, 1998;335(3):491-4.

154. Nguyen Q, Mort JS, Roughley PJ. Cartilage proteoglycan aggregate is degraded more exensively by cathepsin L than by cathepsin B. Biochemical Journal. 1990;266(2):569-73.

155. Maciewicz RA, Wotton SF, Etherington DJ, Duance VC. Susceptibility of the cartilage collagens types II, IX and XI to degradation by the cysteine proteinases, cathepsins B and L. FEBS Letters. 1990 8/20/;269(1):189-93.

156. Buck MR, Karustis DG, Day NA, Honn KV, Sloane BF. Degradation of extracellular-matrix proteins by human cathepsin B from normal and tumour tissues. The Biochemical Journal. 1992;282(Pt 1):273-8.

157. Sires UI, Schmid TM, Fliszar CJ, Wang ZQ, Gluck SL, Welgus HG. Complete degradation of type X collagen requires the combined action of interstitial collagenase and osteoclast-derived cathepsin-B. The Journal of Clinical Investigation. 1995;95(5):2089-95.

158. ISEMURA M, YOSIZAWA Z, TAKAHASHI K, KOSAKA H, KOJIMA N, ONO T. Characterization of Porcine Plasma Fibronectin and Its Fragmentation by Porcine Liver Cathepsin B. Journal of Biochemistry. 1981 July 1, 1981;90(1):1-9.

159. Baumgrass R, Williamson MK, Price PA. Identification of Peptide Fragments Generated by Digestion of Bovine and Human Osteocalcin with the Lysosomal Proteinases Cathepsin B, D, L, H, and S. Journal of Bone and Mineral Research. 1997;12(3):447-55.

160. Page AE, Hayman AR, Andersson LM, Chambers TJ, Warburton MJ. Degradation of bone matrix proteins by osteoclast cathepsins. The International Journal of Biochemistry & Cell Biology. 1993;25(4):545-50.

161. Tisdale MJ. Biology of Cachexia. Journal of the National Cancer Institute. 1997 December 3, 1997;89(23):1763-73.

162. Chen BB, Coon TA, Glasser JR, McVerry BJ, Zhao J, Zhao Y, Zou C, Ellis B, Sciurba FC, Zhang Y, Mallampalli RK. A combinatorial F box protein directed pathway controls TRAF adaptor stability to regulate inflammation. Nat Immunol. 2013 05//print;14(5):470-9.

163. Bordon Y. Signalling: Fine-tuning of inflammation by F-box proteins. Nat Rev Immunol. 2013 05//print;13(5):304-5.

164. Harris J, Schwinn N, Mahoney JA, Lin H-H, Shaw M, Howard CJ, Da Silva RP, Gordon S. A vitellogenic-like carboxypeptidase expressed by human macrophages is localized in endoplasmic reticulum and membrane ruffles. International Journal of Experimental Pathology. 2006;87(1):29-39.

165. Loria V, Dato I, Graziani F, Biasucci L. Myeloperoxidase: a new biomarker of inflammation in ischemic heart disease and acute coronary syndromes. Mediators of Inflammation. 2008;2008:1-4.

166. Wang Y, Rosen H, Madtes DK, Shao B, Martin TR, Heinecke JW, Fu X. Myeloperoxidase Inactivates TIMP-1 by Oxidizing Its N-terminal Cysteine Residue: AN OXIDATIVE MECHANISM FOR REGULATING PROTEOLYSIS DURING INFLAMMATION. Journal of Biological Chemistry. 2007 November 2, 2007;282(44):31826-34.

167. Deban L, Bottazzi B, Garlanda C, de la Torre YM, Mantovani A. Pentraxins: Multifunctional proteins at the interface of innate immunity and inflammation. BioFactors. 2009;35(2):138-45.

168. Wilson FH, Disse-Nicodème S, Choate KA, Ishikawa K, Nelson-Williams C, Desitter I, Gunel M, Milford DV, Lipkin GW, Achard J-M, Feely MP, Dussol B, Berland Y, Unwin RJ, Mayan H, Simon DB, Farfel Z, Jeunemaitre X, Lifton RP. Human hypertension caused by mutations in WNK kinases. Science. 2001;293:1107-12.

169. Ruiter G, Lankhorst S, Boonstra A, Postmus PE, Zweegman S, Westerhof N, van der Laarse WJ, Vonk-Noordegraaf A. Iron deficiency is common in idiopathic pulmonary arterial hypertension. European Respiratory Journal. 2011 June 1, 2011;37(6):1386-91.

170. Rhodes CJ, Howard LS, Busbridge M, Ashby D, Kondili E, Gibbs JSR, Wharton J, Wilkins MR. Iron Deficiency and Raised Hepcidin in Idiopathic Pulmonary Arterial Hypertension: Clinical Prevalence, Outcomes, and Mechanistic Insights. Journal of the American College of Cardiology. 2011 7/12/;58(3):300-9.

171. Decker I, Ghosh S, Comhair SA, Farha S, Wilson Tang WH, Park M, Wang S, Lichtin AE, Erzurum SC. High Levels of Zinc-Protoporphyrin Identify Iron Metabolic Abnormalities in Pulmonary Arterial Hypertension. Clinical and Translational Science. 2011;4(4):253-8.

172. Deicher R, Hörl WH. Hepcidin: a molecular link between inflammation and anaemia. Nephrology Dialysis Transplantation. 2004 March 1, 2004;19(3):521-4.

173. Singh K, Zhang LX, Bendelja K, Health R, Murphy S, Sharma S, Padbury JF, Lim Y-P. Inter-alpha inhibitor protein (IAIP) administration improves survival from neonatal sepsis in mice. Pediatric Research. 2010;68(3):242-7.

174. Lorenzen JM, Nickel N, Krämer R, Golpon H, Westerkamp V, Olsson KM, Haller H, Hoeper MM. OSteopontin in patients with idiopathic pulmonary hypertension. CHEST Journal. 2011;139(5):1010-7.

IX. Appendices

Appendix 1 – Total proteins identified by nanoLC-MS/MS.

Accession #	Protein ID	MW (DA)	pI
O95336	6PGL_HUMAN 6-phosphogluconolactonase OS=Homo sapiens GN=PGLS PE=1 SV=2	27530	5,7
P02763	A1AG1_HUMAN Alpha-1-acid glycoprotein 1 OS=Homo sapiens GN=ORM1 PE=1 SV=1	23497	4,93
P19652	A1AG2_HUMAN Alpha-1-acid glycoprotein 2 OS=Homo sapiens GN=ORM2 PE=1 SV=2	23588	5,03
P01009	A1AT_HUMAN Alpha-1-antitrypsin OS=Homo sapiens GN=SERPINA1 PE=1 SV=3	46707	5,37
P04217	A1BG_HUMAN Alpha-1B-glycoprotein OS=Homo sapiens GN=A1BG PE=1 SV=4	54220	5,56
P02750	A2GL_HUMAN Leucine-rich alpha-2-glycoprotein OS=Homo sapiens GN=LRG1 PE=1 SV=2	38154	6,45
P01023	A2MG_HUMAN Alpha-2-macroglobulin OS=Homo sapiens GN=A2M PE=1 SV=3	163188	6,03
P01011	AACT_HUMAN Alpha-1-antichymotrypsin OS=Homo sapiens GN=SERPINA3 PE=1 SV=2	47621	5,33
P60709	ACTB_HUMAN Actin, cytoplasmic 1 OS=Homo sapiens GN=ACTB PE=1 SV=1	41710	5,29
O00468	AGRIN_HUMAN Agrin OS=Homo sapiens GN=AGRN PE=1 SV=4	214706	6,02
Q96BJ3	AIDA_HUMAN Axin interactor, dorsalization-associated protein OS=Homo sapiens GN=AIDA PE=1 SV=1	35001	6,13
P02768	ALBU_HUMAN Serum albumin OS=Homo sapiens GN=ALB PE=1 SV=2	69321	5,92
P05062	ALDOB_HUMAN Fructose-bisphosphate aldolase B OS=Homo sapiens GN=ALDOB PE=1 SV=2	39448	8
Q9BT30	ALKB7_HUMAN Alpha-ketoglutarate-dependent dioxygenase alkB homolog 7 OS=Homo sapiens GN=ALKBH7 PE=2 SV=1	24501	6,61
P02760	AMBP_HUMAN Protein AMBP OS=Homo sapiens GN=AMBP PE=1 SV=1	38974	5,95
P15144	AMPN_HUMAN Aminopeptidase N OS=Homo sapiens GN=ANPEP PE=1 SV=4	109471	5,31
P04745	AMY1_HUMAN Alpha-amylase 1 OS=Homo sapiens GN=AMY1A PE=1 SV=2	57731	6,47
P04746	AMYP_HUMAN Pancreatic alpha-amylase OS=Homo sapiens GN=AMY2A PE=1 SV=2	57670	6,60

P54802	ANAG_HUMAN Alpha-N-acetylglucosaminidase OS=Homo sapiens GN=NAGLU PE=1 SV=2	82214	6,20
Q9UKU9	ANGL2_HUMAN Angiopoietin-related protein 2 OS=Homo sapiens GN=ANGPTL2 PE=2 SV=1	57068	7,23
P01019	ANGT_HUMAN Angiotensinogen OS=Homo sapiens GN=AGT PE=1 SV=1	53121	5,87
P01008	ANT3_HUMAN Antithrombin-III OS=Homo sapiens GN=SERPINC1 PE=1 SV=1	52569	6,32
Q9H6X2	ANTR1_HUMAN Anthrax toxin receptor 1 OS=Homo sapiens GN=ANTXR1 PE=1 SV=2	62749	7,53
P50995	ANX11_HUMAN Annexin A11 OS=Homo sapiens GN=ANXA11 PE=1 SV=1	54355	7,53
P04083	ANXA1_HUMAN Annexin A1 OS=Homo sapiens GN=ANXA1 PE=1 SV=2	38690	6,57
P07355	ANXA2_HUMAN Annexin A2 OS=Homo sapiens GN=ANXA2 PE=1 SV=2	38580	7,57
P09525	ANXA4_HUMAN Annexin A4 OS=Homo sapiens GN=ANXA4 PE=1 SV=4	35860	5,84
P05090	APOD_HUMAN Apolipoprotein D OS=Homo sapiens GN=APOD PE=1 SV=1	21262	5,06
P02649	APOE_HUMAN Apolipoprotein E OS=Homo sapiens GN=APOE PE=1 SV=1	36132	5,65
Q13510	ASAH1_HUMAN Acid ceramidase OS=Homo sapiens GN=ASAH1 PE=1 SV=5	44631	7,52
P61769	B2MG_HUMAN Beta-2-microglobulin OS=Homo sapiens GN=B2M PE=1 SV=1	13706	6,06
Q15582	BGH3_HUMAN Transforming growth factor-beta-induced protein ig-h3 OS=Homo sapiens GN=TGFBI PE=1 SV=1	74634	7,62
Q93088	BHMT1_HUMAN Betaine--homocysteine S-methyltransferase 1 OS=Homo sapiens GN=BHMT PE=1 SV=2	44970	6,58
Q13867	BLMH_HUMAN Bleomycin hydrolase OS=Homo sapiens GN=BLMH PE=1 SV=1	52528	5,87
Q9NZP8	C1RL_HUMAN Complement C1r subcomponent-like protein OS=Homo sapiens GN=C1RL PE=1 SV=2	53464	6,75
P55287	CAD11_HUMAN Cadherin-11 OS=Homo sapiens GN=CDH11 PE=1 SV=2	87911	4,75
P55290	CAD13_HUMAN Cadherin-13 OS=Homo sapiens GN=CDH13 PE=1 SV=1	78238	4,80
P12830	CADH1_HUMAN Cadherin-1 OS=Homo sapiens GN=CDH1 PE=1 SV=3	97396	4,58

Q8NFZ8	CADM4_HUMAN Cell adhesion molecule 4 OS=Homo sapiens GN=CADM4 PE=1 SV=1	42759	5,92
P62158	CALM_HUMAN Calmodulin OS=Homo sapiens GN=CALM1 PE=1 SV=2	16827	4,09
O75052	CAPON_HUMAN Carboxyl-terminal PDZ ligand of neuronal nitric oxide synthase protein OS=Homo sapiens GN=NOS1AP PE=1 SV=3	56115	5,89
P31944	CASPE_HUMAN Caspase-14 OS=Homo sapiens GN=CASP14 PE=1 SV=2	27662	5,44
P07858	CATB_HUMAN Cathepsin B OS=Homo sapiens GN=CTSB PE=1 SV=3	37797	5,88
P53634	CATC_HUMAN Dipeptidyl peptidase 1 OS=Homo sapiens GN=CTSC PE=1 SV=2	51820	6,54
P07339	CATD_HUMAN Cathepsin D OS=Homo sapiens GN=CTSD PE=1 SV=1	44524	6,10
P07711	CATL1_HUMAN Cathepsin L1 OS=Homo sapiens GN=CTSL1 PE=1 SV=2	37540	5,31
Q9UBR2	CATZ_HUMAN Cathepsin Z OS=Homo sapiens GN=CTSZ PE=1 SV=1	33846	6,70
Q96HB5	CC120_HUMAN Coiled-coil domain-containing protein 120 OS=Homo sapiens GN=CCDC120 PE=1 SV=1	67526	9,51
Q2M329	CCD96_HUMAN Coiled-coil domain-containing protein 96 OS=Homo sapiens GN=CCDC96 PE=2 SV=2	62673	4,92
P08571	CD14_HUMAN Monocyte differentiation antigen CD14 OS=Homo sapiens GN=CD14 PE=1 SV=2	40051	5,84
Q9HCU0	CD248_HUMAN Endosialin OS=Homo sapiens GN=CD248 PE=1 SV=1	80807	5,14
P16070	CD44_HUMAN CD44 antigen OS=Homo sapiens GN=CD44 PE=1 SV=3	81487	5,13
P13987	CD59_HUMAN CD59 glycoprotein OS=Homo sapiens GN=CD59 PE=1 SV=1	14168	6,02
P32320	CDD_HUMAN Cytidine deaminase OS=Homo sapiens GN=CDA PE=1 SV=2	16174	6,55
P31997	CEAM8_HUMAN Carcinoembryonic antigen-related cell adhesion molecule 8 OS=Homo sapiens GN=CEACAM8 PE=1 SV=2	38130	6,95
P00450	CERU_HUMAN Ceruloplasmin OS=Homo sapiens GN=CP PE=1 SV=1	122128	5,44
P05156	CFAI_HUMAN Complement factor I OS=Homo sapiens GN=CFI PE=1 SV=2	65707	7,72
Q7LBR1	CHM1B_HUMAN Charged multivesicular body protein 1b OS=Homo sapiens GN=CHMP1B PE=1 SV=1	22095	7,82

Q9H0W9	CK054_HUMAN Ester hydrolase C11orf54 OS=Homo sapiens GN=C11orf54 PE=1 SV=1	35095	6,23
Q6UXG3	CLM9_HUMAN CMRF35-like molecule 9 OS=Homo sapiens GN=CD300LG PE=1 SV=2	36037	5,68
Q9H6B4	CLMP_HUMAN CXADR-like membrane protein OS=Homo sapiens GN=CLMP PE=1 SV=1	41255	8,11
P10909	CLUS_HUMAN Clusterin OS=Homo sapiens GN=CLU PE=1 SV=1	52461	5,89
P10645	CMGA_HUMAN Chromogranin-A OS=Homo sapiens GN=CHGA PE=1 SV=7	50658	4,58
P0C0L4	CO4A_HUMAN Complement C4-A OS=Homo sapiens GN=C4A PE=1 SV=1	192650	6,65
P12109	CO6A1_HUMAN Collagen alpha-1(VI) chain OS=Homo sapiens GN=COL6A1 PE=1 SV=3	108462	5,26
Q02388	CO7A1_HUMAN Collagen alpha-1(VII) chain OS=Homo sapiens GN=COL7A1 PE=1 SV=2	295041	5,95
P39059	COFA1_HUMAN Collagen alpha-1(XV) chain OS=Homo sapiens GN=COL15A1 PE=1 SV=2	141632	4,89
Q6UX73	CP089_HUMAN UPF0764 protein C16orf89 OS=Homo sapiens GN=C16orf89 PE=1 SV=2	45362	5,82
P20813	CP2B6_HUMAN Cytochrome P450 2B6 OS=Homo sapiens GN=CYP2B6 PE=1 SV=1	56242	8,43
Q9H3G5	CPVL_HUMAN Probable serine carboxypeptidase CPVL OS=Homo sapiens GN=CPVL PE=1 SV=2	54129	5,39
P54108	CRIS3_HUMAN Cysteine-rich secretory protein 3 OS=Homo sapiens GN=CRISP3 PE=1 SV=1	27612	8,09
Q9UBG3	CRNN_HUMAN Cornulin OS=Homo sapiens GN=CRNN PE=1 SV=1	53502	5,73
P09603	CSF1_HUMAN Macrophage colony-stimulating factor 1 OS=Homo sapiens GN=CSF1 PE=1 SV=2	60142	5,16
O60494	CUBN_HUMAN Cubilin OS=Homo sapiens GN=CUBN PE=1 SV=5	398480	5,14
O60888	CUTA_HUMAN Protein CutA OS=Homo sapiens GN=CUTA PE=1 SV=2	19104	5,42
P01040	CYTA_HUMAN Cystatin-A OS=Homo sapiens GN=CSTA PE=1 SV=1	11000	5,38
P01034	CYTC_HUMAN Cystatin-C OS=Homo sapiens GN=CST3 PE=1 SV=1	15789	9
Q15828	CYTM_HUMAN Cystatin-M OS=Homo sapiens GN=CST6 PE=1 SV=1	16500	8,31

P08174	DAF_HUMAN Complement decay-accelerating factor OS=Homo sapiens GN=CD55 PE=1 SV=4	41374	7,79
P53355	DAPK1_HUMAN Death-associated protein kinase 1 OS=Homo sapiens GN=DAPK1 PE=1 SV=6	159945	6,37
Q07507	DERM_HUMAN Dermatopontin OS=Homo sapiens GN=DPT PE=2 SV=2	23989	4,70
Q01459	DIAC_HUMAN Di-N-acetylchitobiase OS=Homo sapiens GN=CTBS PE=1 SV=1	43732	6,19
Q9Y2E4	DIP2C_HUMAN Disco-interacting protein 2 homolog C OS=Homo sapiens GN=DIP2C PE=2 SV=2	170658	7,12
P24855	DNAS1_HUMAN Deoxyribonuclease-1 OS=Homo sapiens GN=DNASE1 PE=1 SV=1	31414	4,71
Q02487	DSC2_HUMAN Desmocollin-2 OS=Homo sapiens GN=DSC2 PE=1 SV=1	99899	5,19
P98172	EFNB1_HUMAN Ephrin-B1 OS=Homo sapiens GN=EFNB1 PE=1 SV=1	37982	9,10
P01133	EGF_HUMAN Pro-epidermal growth factor OS=Homo sapiens GN=EGF PE=1 SV=2	133906	5,53
O94919	ENDD1_HUMAN Endonuclease domain-containing 1 protein OS=Homo sapiens GN=ENDOD1 PE=1 SV=2	54981	5,55
P06733	ENOA_HUMAN Alpha-enolase OS=Homo sapiens GN=ENO1 PE=1 SV=2	47139	7,01
Q9UNN8	EPCR_HUMAN Endothelial protein C receptor OS=Homo sapiens GN=PROCR PE=1 SV=1	26655	6,70
Q96AP7	ESAM_HUMAN Endothelial cell-selective adhesion molecule OS=Homo sapiens GN=ESAM PE=1 SV=1	41151	9,42
P15311	EZRI_HUMAN Ezrin OS=Homo sapiens GN=EZR PE=1 SV=4	69370	5,94
Q9Y4F4	F179B_HUMAN Protein FAM179B OS=Homo sapiens GN=FAM179B PE=1 SV=4	189242	8,73
A4D161	F221A_HUMAN Protein FAM221A OS=Homo sapiens GN=FAM221A PE=2 SV=1	33061	6,33
Q01469	FABP5_HUMAN Fatty acid-binding protein, epidermal OS=Homo sapiens GN=FABP5 PE=1 SV=3	15155	6,60
Q9NYQ8	FAT2_HUMAN Protocadherin Fat 2 OS=Homo sapiens GN=FAT2 PE=1 SV=2	479018	5
Q12805	FBLN3_HUMAN EGF-containing fibulin-like extracellular matrix protein 1 OS=Homo sapiens GN=EFEMP1 PE=1 SV=2	54604	4,95
Q9UK99	FBX3_HUMAN F-box only protein 3 OS=Homo sapiens GN=FBXO3 PE=1 SV=3	54525	4,88

P08637	FCG3A_HUMAN Low affinity immunoglobulin gamma Fc region receptor III-A OS=Homo sapiens GN=FCGR3A PE=1 SV=2	29071	8,20
Q9Y6R7	FCGBP_HUMAN IgGFc-binding protein OS=Homo sapiens GN=FCGBP PE=1 SV=3	571639	5,14
P02765	FETUA_HUMAN Alpha-2-HS-glycoprotein OS=Homo sapiens GN=AHSG PE=1 SV=1	39300	5,43
P36980	FHR2_HUMAN Complement factor H-related protein 2 OS=Homo sapiens GN=CFHR2 PE=1 SV=1	30631	6
P02671	FIBA_HUMAN Fibrinogen alpha chain OS=Homo sapiens GN=FGA PE=1 SV=2	94914	5,70
P02679	FIBG_HUMAN Fibrinogen gamma chain OS=Homo sapiens GN=FGG PE=1 SV=3	51479	5,37
P20930	FILA_HUMAN Filaggrin OS=Homo sapiens GN=FLG PE=1 SV=3	434922	9,24
P02751	FINC_HUMAN Fibronectin OS=Homo sapiens GN=FN1 PE=1 SV=4	262460	5,46
P15328	FOLR1_HUMAN Folate receptor alpha OS=Homo sapiens GN=FOLR1 PE=1 SV=3	29799	8,3
Q9Y2I7	FYV1_HUMAN 1-phosphatidylinositol 3-phosphate 5-kinase OS=Homo sapiens GN=PIKFYVE PE=1 SV=3	236986	6,24
P04406	G3P_HUMAN Glyceraldehyde-3-phosphate dehydrogenase OS=Homo sapiens GN=GAPDH PE=1 SV=3	36030	8,57
Q8WWW8	GAB3_HUMAN GRB2-associated-binding protein 3 OS=Homo sapiens GN=GAB3 PE=2 SV=1	65548	6,8
P33402	GCYA2_HUMAN Guanylate cyclase soluble subunit alpha-2 OS=Homo sapiens GN=GUCY1A2 PE=1 SV=1	81698	7,77
P06396	GELS_HUMAN Gelsolin OS=Homo sapiens GN=GSN PE=1 SV=1	85644	5,90
P36268	GGT2_HUMAN Gamma-glutamyltranspeptidase 2 OS=Homo sapiens GN=GGT2 PE=1 SV=3	61732	7,22
Q16775	GLO2_HUMAN Hydroxyacylglutathione hydrolase, mitochondrial OS=Homo sapiens GN=HAGH PE=1 SV=2	33784	8,34
P15586	GNS_HUMAN N-acetylglucosamine-6-sulfatase OS=Homo sapiens GN=GNS PE=1 SV=3	62042	8,60
Q8NBJ4	GOLM1_HUMAN Golgi membrane protein 1 OS=Homo sapiens GN=GOLM1 PE=1 SV=1	45306	4,91
P55259	GP2_HUMAN Pancreatic secretory granule membrane major glycoprotein GP2 OS=Homo sapiens GN=GP2 PE=2 SV=3	59442	5,08
Q9NQ84	GPC5C_HUMAN G-protein coupled receptor family C group 5 member C OS=Homo sapiens GN=GPRC5C PE=1 SV=2	48162	8,72

Q9HCN6	GPVI_HUMAN Platelet glycoprotein VI OS=Homo sapiens GN=GP6 PE=1 SV=4	36843	9,35
Q8IUY3	GRAM2_HUMAN GRAM domain-containing protein 2 OS=Homo sapiens GN=GRAMD2 PE=2 SV=2	40223	8,73
P08263	GSTA1_HUMAN Glutathione S-transferase A1 OS=Homo sapiens GN=GSTA1 PE=1 SV=3	25615	8,91
Q02747	GUC2A_HUMAN Guanylin OS=Homo sapiens GN=GUCA2A PE=1 SV=2	12380	4,56
Q16661	GUC2B_HUMAN Guanylate cyclase activator 2B OS=Homo sapiens GN=GUCA2B PE=1 SV=1	12061	6,02
Q8TDG4	HELQ_HUMAN Helicase POLQ-like OS=Homo sapiens GN=HELQ PE=1 SV=2	124053	6,17
P02790	HEMO_HUMAN Hemopexin OS=Homo sapiens GN=HPX PE=1 SV=2	51643	6,55
Q86YZ3	HORN_HUMAN Hornerin OS=Homo sapiens GN=HRNR PE=1 SV=2	282228	10,05
P00738	HPT_HUMAN Haptoglobin OS=Homo sapiens GN=HP PE=1 SV=1	45177	6,13
P54652	HSP72_HUMAN Heat shock-related 70 kDa protein 2 OS=Homo sapiens GN=HSPA2 PE=1 SV=1	69978	5,56
P01765	HV304_HUMAN Ig heavy chain V-III region TIL OS=Homo sapiens PE=1 SV=1	12348	9,24
P01766	HV305_HUMAN Ig heavy chain V-III region BRO OS=Homo sapiens PE=1 SV=1	13218	6,45
Q2M3T9	HYAL4_HUMAN Hyaluronidase-4 OS=Homo sapiens GN=HYAL4 PE=1 SV=2	54214	8,68
Q16270	IBP7_HUMAN Insulin-like growth factor-binding protein 7 OS=Homo sapiens GN=IGFBP7 PE=1 SV=1	29111	8,25
P05155	IC1_HUMAN Plasma protease C1 inhibitor OS=Homo sapiens GN=SERPING1 PE=1 SV=2	55119	6,09
O75144	ICOSL_HUMAN ICOS ligand OS=Homo sapiens GN=ICOSLG PE=1 SV=2	33328	5,15
P01876	IGHA1_HUMAN Ig alpha-1 chain C region OS=Homo sapiens GN=IGHA1 PE=1 SV=2	37631	6,08
P01857	IGHG1_HUMAN Ig gamma-1 chain C region OS=Homo sapiens GN=IGHG1 PE=1 SV=1	36083	8,46
P01859	IGHG2_HUMAN Ig gamma-2 chain C region OS=Homo sapiens GN=IGHG2 PE=1 SV=2	35878	7,66
P01871	IGHM_HUMAN Ig mu chain C region OS=Homo sapiens GN=IGHM PE=1 SV=3	49276	6,35

P01591	IGJ_HUMAN Immunoglobulin J chain OS=Homo sapiens GN=IGJ PE=1 SV=4	18087	5,12
P01834	IGKC_HUMAN Ig kappa chain C region OS=Homo sapiens GN=IGKC PE=1 SV=1	11602	5,58
B9A064	IGLL5_HUMAN Immunoglobulin lambda-like polypeptide 5 OS=Homo sapiens GN=IGLL5 PE=2 SV=2	23049	9,08
Q969P0	IGSF8_HUMAN Immunoglobulin superfamily member 8 OS=Homo sapiens GN=IGSF8 PE=1 SV=1	64994	8,23
P30740	ILEU_HUMAN Leukocyte elastase inhibitor OS=Homo sapiens GN=SERPINB1 PE=1 SV=1	42715	5,90
P05154	IPSP_HUMAN Plasma serine protease inhibitor OS=Homo sapiens GN=SERPINA5 PE=1 SV=3	45646	9,30
P53990	IST1_HUMAN IST1 homolog OS=Homo sapiens GN=IST1 PE=1 SV=1	39725	5,22
Q14624	ITIH4_HUMAN Inter-alpha-trypsin inhibitor heavy chain H4 OS=Homo sapiens GN=ITIH4 PE=1 SV=4	103293	6,51
O60674	JAK2_HUMAN Tyrosine-protein kinase JAK2 OS=Homo sapiens GN=JAK2 PE=1 SV=2	130590	6,82
P13645	K1C10_HUMAN Keratin, type I cytoskeletal 10 OS=Homo sapiens GN=KRT10 PE=1 SV=6	58792	5,13
P35527	K1C9_HUMAN Keratin, type I cytoskeletal 9 OS=Homo sapiens GN=KRT9 PE=1 SV=3	62027	5,14
P35908	K22E_HUMAN Keratin, type II cytoskeletal 2 epidermal OS=Homo sapiens GN=KRT2 PE=1 SV=2	65393	8,07
P04264	K2C1_HUMAN Keratin, type II cytoskeletal 1 OS=Homo sapiens GN=KRT1 PE=1 SV=6	65999	8,15
P13647	K2C5_HUMAN Keratin, type II cytoskeletal 5 OS=Homo sapiens GN=KRT5 PE=1 SV=3	62340	7,59
Q14003	KCNC3_HUMAN Potassium voltage-gated channel subfamily C member 3 OS=Homo sapiens GN=KCNC3 PE=1 SV=3	80527	6,08
P06870	KLK1_HUMAN Kallikrein-1 OS=Homo sapiens GN=KLK1 PE=1 SV=2	28871	4,68
Q9UKR3	KLK13_HUMAN Kallikrein-13 OS=Homo sapiens GN=KLK13 PE=1 SV=1	30551	8,78
P01042	KNG1_HUMAN Kininogen-1 OS=Homo sapiens GN=KNG1 PE=1 SV=2	71912	6,34
P01593	KV101_HUMAN Ig kappa chain V-I region AG OS=Homo sapiens PE=1 SV=1	11985	5,67
P01614	KV201_HUMAN Ig kappa chain V-II region Cum OS=Homo sapiens PE=1 SV=1	12668	5,28

P01619	KV301_HUMAN Ig kappa chain V-III region B6 OS=Homo sapiens PE=1 SV=1	11628	9,34
P01621	KV303_HUMAN Ig kappa chain V-III region NG9 (Fragment) OS=Homo sapiens PE=1 SV=1	10722	6,29
P01623	KV305_HUMAN Ig kappa chain V-III region WOL OS=Homo sapiens PE=1 SV=1	11739	9,07
P04433	KV309_HUMAN Ig kappa chain V-III region VG (Fragment) OS=Homo sapiens PE=1 SV=1	12567	4,85
P04434	KV310_HUMAN Ig kappa chain V-III region VH (Fragment) OS=Homo sapiens PE=4 SV=1	12749	5,63
P18135	KV312_HUMAN Ig kappa chain V-III region HAH OS=Homo sapiens PE=2 SV=1	14064	7,74
P01625	KV402_HUMAN Ig kappa chain V-IV region Len OS=Homo sapiens PE=1 SV=2	12632	7,92
P0CG04	LAC1_HUMAN Ig lambda-1 chain C regions OS=Homo sapiens GN=IGLC1 PE=1 SV=1	23049	9,08
P0CG05	LAC2_HUMAN Ig lambda-2 chain C regions OS=Homo sapiens GN=IGLC2 PE=1 SV=1	11287	6,92
P0CF74	LAC6_HUMAN Ig lambda-6 chain C region OS=Homo sapiens GN=IGLC6 PE=4 SV=1	11270	6,92
Q6GTX8	LAIR1_HUMAN Leukocyte-associated immunoglobulin-like receptor 1 OS=Homo sapiens GN=LAIR1 PE=1 SV=1	31393	5,40
Q86UK5	LBN_HUMAN Limbin OS=Homo sapiens GN=EVC2 PE=1 SV=1	147856	6,53
P04180	LCAT_HUMAN Phosphatidylcholine-sterol acyltransferase OS=Homo sapiens GN=LCAT PE=1 SV=1	49546	5,71
P31025	LCN1_HUMAN Lipocalin-1 OS=Homo sapiens GN=LCN1 PE=1 SV=1	19238	5,39
Q08380	LG3BP_HUMAN Galectin-3-binding protein OS=Homo sapiens GN=LGALS3BP PE=1 SV=1	65289	5,13
Q5T7N2	LITD1_HUMAN LINE-1 type transposase domain-containing protein 1 OS=Homo sapiens GN=L1TD1 PE=1 SV=1	98789	4,87
Q12907	LMAN2_HUMAN Vesicular integral-membrane protein VIP36 OS=Homo sapiens GN=LMAN2 PE=1 SV=1	40203	6,46
Q8IYG6	LRC56_HUMAN Leucine-rich repeat-containing protein 56 OS=Homo sapiens GN=LRRC56 PE=2 SV=1	58697	8,05
P98164	LRP2_HUMAN Low-density lipoprotein receptor-related protein 2 OS=Homo sapiens GN=LRP2 PE=1 SV=3	521616	4,89
P01700	LV102_HUMAN Ig lambda chain V-I region HA OS=Homo sapiens PE=1 SV=1	11889	9,07

P01715	LV401_HUMAN Ig lambda chain V-IV region Bau OS=Homo sapiens PE=1 SV=1	11298	5,04
P01717	LV403_HUMAN Ig lambda chain V-IV region Hil OS=Homo sapiens PE=1 SV=1	11510	6,04
P10253	LYAG_HUMAN Lysosomal alpha-glucosidase OS=Homo sapiens GN=GAA PE=1 SV=4	105257	5,62
P61626	LYSC_HUMAN Lysozyme C OS=Homo sapiens GN=LYZ PE=1 SV=1	16526	9,38
P33908	MA1A1_HUMAN Mannosyl-oligosaccharide 1,2-alpha-mannosidase IA OS=Homo sapiens GN=MAN1A1 PE=1 SV=3	72922	6,04
Q9P0L2	MARK1_HUMAN Serine/threonine-protein kinase MARK1 OS=Homo sapiens GN=MARK1 PE=1 SV=2	88947	9,42
O00187	MASP2_HUMAN Mannan-binding lectin serine protease 2 OS=Homo sapiens GN=MASP2 PE=1 SV=4	75654	5,39
Q8IWD5	MFS6L_HUMAN Major facilitator superfamily domain-containing protein 6-like OS=Homo sapiens GN=MFSD6L PE=2 SV=2	63964	8,87
O43451	MGA_HUMAN Maltase-glucoamylase, intestinal OS=Homo sapiens GN=MGAM PE=1 SV=5	209720	5,27
Q13201	MMRN1_HUMAN Multimerin-1 OS=Homo sapiens GN=MMRN1 PE=1 SV=3	138023	8,15
P15941	MUC1_HUMAN Mucin-1 OS=Homo sapiens GN=MUC1 PE=1 SV=3	122029	6,96
P43121	MUC18_HUMAN Cell surface glycoprotein MUC18 OS=Homo sapiens GN=MCAM PE=1 SV=2	71563	5,58
P02144	MYG_HUMAN Myoglobin OS=Homo sapiens GN=MB PE=1 SV=2	17173	7,14
P17050	NAGAB_HUMAN Alpha-N-acetylgalactosaminidase OS=Homo sapiens GN=NAGA PE=1 SV=2	46534	4,98
O96009	NAPSA_HUMAN Napsin-A OS=Homo sapiens GN=NAPSA PE=1 SV=1	45358	6,15
P20929	NEBU_HUMAN Nebulin OS=Homo sapiens GN=NEB PE=1 SV=4	772441	9,11
P80188	NGAL_HUMAN Neutrophil gelatinase-associated lipocalin OS=Homo sapiens GN=LCN2 PE=1 SV=2	22574	9,02
P14543	NID1_HUMAN Nidogen-1 OS=Homo sapiens GN=NID1 PE=1 SV=3	136291	5,12
Q8TCU5	NMD3A_HUMAN Glutamate receptor ionotropic, NMDA 3A OS=Homo sapiens GN=GRIN3A PE=1 SV=2	125385	7,4
Q6UX06	OLFM4_HUMAN Olfactomedin-4 OS=Homo sapiens GN=OLFM4 PE=1 SV=1	57244	5,50

Q8IYS5	OSCAR_HUMAN Osteoclast-associated immunoglobulin-like receptor OS=Homo sapiens GN=OSCAR PE=2 SV=3	30462	6,09
P10451	OSTP_HUMAN Osteopontin OS=Homo sapiens GN=SPP1 PE=1 SV=1	35401	4,37
Q96FE7	P3IP1_HUMAN Phosphoinositide-3-kinase-interacting protein 1 OS=Homo sapiens GN=PIK3IP1 PE=1 SV=2	28230	4,92
Q504Q3	PAN2_HUMAN PAB-dependent poly(A)-specific ribonuclease subunit 2 OS=Homo sapiens GN=PAN2 PE=1 SV=3	135281	5,64
P42785	PCP_HUMAN Lysosomal Pro-X carboxypeptidase OS=Homo sapiens GN=PRCP PE=1 SV=1	55764	6,75
Q96RV3	PCX1_HUMAN Pecanex-like protein 1 OS=Homo sapiens GN=PCNX PE=2 SV=2	258514	6,8
P30086	PEBP1_HUMAN Phosphatidylethanolamine-binding protein 1 OS=Homo sapiens GN=PEBP1 PE=1 SV=3	21044	7,01
P0DJD8	PEPA3_HUMAN Pepsin A-3 OS=Homo sapiens GN=PGA3 PE=1 SV=1	41950	4,22
P05164	PERM_HUMAN Myeloperoxidase OS=Homo sapiens GN=MPO PE=1 SV=1	83815	9,19
P98160	PGBM_HUMAN Basement membrane-specific heparan sulfate proteoglycan core protein OS=Homo sapiens GN=HSPG2 PE=1 SV=4	468532	6,06
P16112	PGCA_HUMAN Aggrecan core protein OS=Homo sapiens GN=ACAN PE=1 SV=2	250040	4,1
O75594	PGRP1_HUMAN Peptidoglycan recognition protein 1 OS=Homo sapiens GN=PGLYRP1 PE=1 SV=1	21717	8,92
P01833	PIGR_HUMAN Polymeric immunoglobulin receptor OS=Homo sapiens GN=PIGR PE=1 SV=4	83232	5,58
Q9BZ72	PITM2_HUMAN Membrane-associated phosphatidylinositol transfer protein 2 OS=Homo sapiens GN=PITPNM2 PE=1 SV=1	148840	6,72
P00747	PLMN_HUMAN Plasminogen OS=Homo sapiens GN=PLG PE=1 SV=2	90510	7,04
Q96GD0	PLPP_HUMAN Pyridoxal phosphate phosphatase OS=Homo sapiens GN=PDXP PE=1 SV=2	31678	6,11
P11117	PPAL_HUMAN Lysosomal acid phosphatase OS=Homo sapiens GN=ACP2 PE=1 SV=3	48313	6,28
P15309	PPAP_HUMAN Prostatic acid phosphatase OS=Homo sapiens GN=ACPP PE=1 SV=3	44537	5,83
P22891	PROZ_HUMAN Vitamin K-dependent protein Z OS=Homo sapiens GN=PROZ PE=1 SV=2	44715	5,64
Q16651	PRSS8_HUMAN Prostasin OS=Homo sapiens GN=PRSS8 PE=1 SV=1	36408	5,51

P41222	PTGDS_HUMAN Prostaglandin-H2 D-isomerase OS=Homo sapiens GN=PTGDS PE=1 SV=1	21015	7,66
Q13332	PTPRS_HUMAN Receptor-type tyrosine-protein phosphatase S OS=Homo sapiens GN=PTPRS PE=1 SV=3	216905	6,06
P15151	PVR_HUMAN Poliovirus receptor OS=Homo sapiens GN=PVR PE=1 SV=2	45274	6,07
Q92692	PVRL2_HUMAN Poliovirus receptor-related protein 2 OS=Homo sapiens GN=PVRL2 PE=1 SV=1	57706	4,74
Q16769	QPCT_HUMAN Glutaminyl-peptide cyclotransferase OS=Homo sapiens GN=QPCT PE=1 SV=1	40851	6,12
Q86UN3	R4RL2_HUMAN Reticulon-4 receptor-like 2 OS=Homo sapiens GN=RTN4RL2 PE=1 SV=1	46077	7,58
Q86YV0	RASL3_HUMAN RAS protein activator like-3 OS=Homo sapiens GN=RASAL3 PE=1 SV=2	111829	9,03
P02753	RET4_HUMAN Retinol-binding protein 4 OS=Homo sapiens GN=RBP4 PE=1 SV=3	22995	5,76
P82980	RET5_HUMAN Retinol-binding protein 5 OS=Homo sapiens GN=RBP5 PE=1 SV=3	15921	6,09
P62987	RL40_HUMAN Ubiquitin-60S ribosomal protein L40 OS=Homo sapiens GN=UBA52 PE=1 SV=2	14719	9,87
P10153	RNAS2_HUMAN Non-secretory ribonuclease OS=Homo sapiens GN=RNASE2 PE=1 SV=2	18342	9,10
Q8WZ75	ROBO4_HUMAN Roundabout homolog 4 OS=Homo sapiens GN=ROBO4 PE=1 SV=1	107390	6,18
P62979	RS27A_HUMAN Ubiquitin-40S ribosomal protein S27a OS=Homo sapiens GN=RPS27A PE=1 SV=2	17953	9,68
P82663	RT25_HUMAN 28S ribosomal protein S25, mitochondrial OS=Homo sapiens GN=MRPS25 PE=1 SV=1	20103	8,99
P05109	S10A8_HUMAN Protein S100-A8 OS=Homo sapiens GN=S100A8 PE=1 SV=1	10828	6,51
P06702	S10A9_HUMAN Protein S100-A9 OS=Homo sapiens GN=S100A9 PE=1 SV=1	13234	5,71
Q96H78	S2544_HUMAN Solute carrier family 25 member 44 OS=Homo sapiens GN=SLC25A44 PE=2 SV=1	35370	9,64
P0C874	S31D3_HUMAN Putative spermatogenesis-associated protein 31D3 OS=Homo sapiens GN=SPATA31D3 PE=5 SV=1	102354	8,32
P02743	SAMP_HUMAN Serum amyloid P-component OS=Homo sapiens GN=APCS PE=1 SV=2	25371	6,10
P17900	SAP3_HUMAN Ganglioside GM2 activator OS=Homo sapiens GN=GM2A PE=1 SV=4	20825	5,17

Q8WVN6	SCTM1_HUMAN Secreted and transmembrane protein 1 OS=Homo sapiens GN=SECTM1 PE=1 SV=2	27022	7
P18827	SDC1_HUMAN Syndecan-1 OS=Homo sapiens GN=SDC1 PE=1 SV=3	32442	4,53
P04279	SEMG1_HUMAN Semenogelin-1 OS=Homo sapiens GN=SEMG1 PE=1 SV=2	52100	9,30
Q02383	SEMG2_HUMAN Semenogelin-2 OS=Homo sapiens GN=SEMG2 PE=1 SV=1	65405	9,08
Q9UPS6	SET1B_HUMAN Histone-lysine N-methyltransferase SETD1B OS=Homo sapiens GN=SETD1B PE=1 SV=2	208601	4,86
Q9H299	SH3L3_HUMAN SH3 domain-binding glutamic acid-rich-like protein 3 OS=Homo sapiens GN=SH3BGRL3 PE=1 SV=1	10431	4,82
Q8N114	SHSA5_HUMAN Protein shisa-5 OS=Homo sapiens GN=SHISA5 PE=1 SV=1	25564	6,26
Q9HAT2	SIAE_HUMAN Sialate O-acetylesterase OS=Homo sapiens GN=SIAE PE=1 SV=1	58277	6,93
O00241	SIRB1_HUMAN Signal-regulatory protein beta-1 OS=Homo sapiens GN=SIRPB1 PE=1 SV=5	43184	6,07
Q5TFQ8	SIRBL_HUMAN Signal-regulatory protein beta-1 isoform 3 OS=Homo sapiens GN=SIRPB1 PE=1 SV=1	43332	7,70
P08294	SODE_HUMAN Extracellular superoxide dismutase [Cu-Zn] OS=Homo sapiens GN=SOD3 PE=1 SV=2	25835	6,14
Q96P63	SPB12_HUMAN Serpin B12 OS=Homo sapiens GN=SERPINB12 PE=1 SV=1	46247	5,36
P29508	SPB3_HUMAN Serpin B3 OS=Homo sapiens GN=SERPINB3 PE=1 SV=2	44537	6,35
P48594	SPB4_HUMAN Serpin B4 OS=Homo sapiens GN=SERPINB4 PE=1 SV=2	44825	5,86
Q9UBC9	SPRR3_HUMAN Small proline-rich protein 3 OS=Homo sapiens GN=SPRR3 PE=1 SV=2	18142	8,86
Q8N3T6	T132C_HUMAN Transmembrane protein 132C OS=Homo sapiens GN=TMEM132C PE=2 SV=3	121711	5,95
Q8NBL3	T178A_HUMAN Transmembrane protein 178A OS=Homo sapiens GN=TMEM178A PE=2 SV=1	32997	8,83
Q8NAT2	TDRD5_HUMAN Tudor domain-containing protein 5 OS=Homo sapiens GN=TDRD5 PE=1 SV=3	109667	8,31
P05452	TETN_HUMAN Tetranectin OS=Homo sapiens GN=CLEC3B PE=1 SV=3	22522	5,52
Q9GZN2	TGIF2_HUMAN Homeobox protein TGIF2 OS=Homo sapiens GN=TGIF2 PE=1 SV=1	25863	7,77

P05543	THBG_HUMAN Thyroxine-binding globulin OS=Homo sapiens GN=SERPINA7 PE=1 SV=2	46295	5,87
O14773	TPP1_HUMAN Tripeptidyl-peptidase 1 OS=Homo sapiens GN=TPP1 PE=1 SV=2	61210	6,01
P02787	TRFE_HUMAN Serotransferrin OS=Homo sapiens GN=TF PE=1 SV=3	77014	6,81
P02788	TRFL_HUMAN Lactotransferrin OS=Homo sapiens GN=LTF PE=1 SV=6	78132	8,5
Q8N831	TSYL6_HUMAN Testis-specific Y-encoded-like protein 6 OS=Homo sapiens GN=TSPYL6 PE=2 SV=1	45845	5,45
P02766	TTHY_HUMAN Transthyretin OS=Homo sapiens GN=TTR PE=1 SV=1	15877	5,52
Q9GZX9	TWSG1_HUMAN Twisted gastrulation protein homolog 1 OS=Homo sapiens GN=TWSG1 PE=2 SV=1	24999	5,17
P30530	UFO_HUMAN Tyrosine-protein kinase receptor UFO OS=Homo sapiens GN=AXL PE=1 SV=3	98273	5,27
P07911	UROM_HUMAN Uromodulin OS=Homo sapiens GN=UMOD PE=1 SV=1	69714	5,05
Q6EMK4	VASN_HUMAN Vasorin OS=Homo sapiens GN=VASN PE=1 SV=1	71668	7,16
P19320	VCAM1_HUMAN Vascular cell adhesion protein 1 OS=Homo sapiens GN=VCAM1 PE=1 SV=1	81224	5,14
Q7Z5L0	VMO1_HUMAN Vitelline membrane outer layer protein 1 homolog OS=Homo sapiens GN=VMO1 PE=1 SV=1	21520	4,90
P04004	VTNC_HUMAN Vitronectin OS=Homo sapiens GN=VTN PE=1 SV=1	54271	5,55
Q96J92	WNK4_HUMAN Serine/threonine-protein kinase WNK4 OS=Homo sapiens GN=WNK4 PE=1 SV=1	134656	5,36
P25311	ZA2G_HUMAN Zinc-alpha-2-glycoprotein OS=Homo sapiens GN=AZGP1 PE=1 SV=2	34237	5,71
Q96C00	ZBTB9_HUMAN Zinc finger and BTB domain-containing protein 9 OS=Homo sapiens GN=ZBTB9 PE=1 SV=1	50570	6,29
Q96DA0	ZG16B_HUMAN Zymogen granule protein 16 homolog B OS=Homo sapiens GN=ZG16B PE=1 SV=3	22725	6,74
Q14584	ZN266_HUMAN Zinc finger protein 266 OS=Homo sapiens GN=ZNF266 PE=2 SV=2	62076	8,93
Q9H0M5	ZN700_HUMAN Zinc finger protein 700 OS=Homo sapiens GN=ZNF700 PE=2 SV=1	86176	9,15

Appendix 2 – Total proteins identified by nanoLC-MS/MS in healthy individuals.

Accession #	Protein ID	MW (Da)	pI
O95336	6PGL_HUMAN 6-phosphogluconolactonase OS=Homo sapiens GN=PGLS PE=1 SV=2	27530	5,7
P02763	A1AG1_HUMAN Alpha-1-acid glycoprotein 1 OS=Homo sapiens GN=ORM1 PE=1 SV=1	23497	4,93
P19652	A1AG2_HUMAN Alpha-1-acid glycoprotein 2 OS=Homo sapiens GN=ORM2 PE=1 SV=2	23588	5,03
P01009	A1AT_HUMAN Alpha-1-antitrypsin OS=Homo sapiens GN=SERPINA1 PE=1 SV=3	46707	5,37
P04217	A1BG_HUMAN Alpha-1B-glycoprotein OS=Homo sapiens GN=A1BG PE=1 SV=4	54220	5,56
P02750	A2GL_HUMAN Leucine-rich alpha-2-glycoprotein OS=Homo sapiens GN=LRG1 PE=1 SV=2	38154	6,45
P01011	AACT_HUMAN Alpha-1-antichymotrypsin OS=Homo sapiens GN=SERPINA3 PE=1 SV=2	47621	5,33
P60709	ACTB_HUMAN Actin, cytoplasmic 1 OS=Homo sapiens GN=ACTB PE=1 SV=1	41710	5,29
O00468	AGRIN_HUMAN Agrin OS=Homo sapiens GN=AGRN PE=1 SV=4	214706	6,02
P02768	ALBU_HUMAN Serum albumin OS=Homo sapiens GN=ALB PE=1 SV=2	69321	5,92
P05062	ALDOB_HUMAN Fructose-bisphosphate aldolase B OS=Homo sapiens GN=ALDOB PE=1 SV=2	39448	8
P02760	AMBP_HUMAN Protein AMBP OS=Homo sapiens GN=AMBP PE=1 SV=1	38974	5,95
P15144	AMPN_HUMAN Aminopeptidase N OS=Homo sapiens GN=ANPEP PE=1 SV=4	109471	5,31
P04745	AMY1_HUMAN Alpha-amylase 1 OS=Homo sapiens GN=AMY1A PE=1 SV=2	57731	6,47
P04746	AMYP_HUMAN Pancreatic alpha-amylase OS=Homo sapiens GN=AMY2A PE=1 SV=2	57670	6,6
P54802	ANAG_HUMAN Alpha-N-acetylglucosaminidase OS=Homo sapiens GN=NAGLU PE=1 SV=2	82214	6,2
Q9UKU9	ANGL2_HUMAN Angiopoietin-related protein 2 OS=Homo sapiens GN=ANGPTL2 PE=2 SV=1	57068	7,23
P01019	ANGT_HUMAN Angiotensinogen OS=Homo sapiens GN=AGT PE=1 SV=1	53121	5,87

P01008	ANT3_HUMAN Antithrombin-III OS=Homo sapiens GN=SERPINC1 PE=1 SV=1	52569	6,32
Q9H6X2	ANTR1_HUMAN Anthrax toxin receptor 1 OS=Homo sapiens GN=ANTXR1 PE=1 SV=2	62749	7,53
P50995	ANX11_HUMAN Annexin A11 OS=Homo sapiens GN=ANXA11 PE=1 SV=1	54355	7,53
P04083	ANXA1_HUMAN Annexin A1 OS=Homo sapiens GN=ANXA1 PE=1 SV=2	38690	6,57
P07355	ANXA2_HUMAN Annexin A2 OS=Homo sapiens GN=ANXA2 PE=1 SV=2	38580	7,57
P09525	ANXA4_HUMAN Annexin A4 OS=Homo sapiens GN=ANXA4 PE=1 SV=4	35860	5,84
P05090	APOD_HUMAN Apolipoprotein D OS=Homo sapiens GN=APOD PE=1 SV=1	21262	5,06
P02649	APOE_HUMAN Apolipoprotein E OS=Homo sapiens GN=APOE PE=1 SV=1	36132	5,65
P61769	B2MG_HUMAN Beta-2-microglobulin OS=Homo sapiens GN=B2M PE=1 SV=1	13706	6,06
Q15582	BGH3_HUMAN Transforming growth factor-beta-induced protein ig-h3 OS=Homo sapiens GN=TGFBI PE=1 SV=1	74634	7,62
Q93088	BHMT1_HUMAN Betaine--homocysteine S-methyltransferase 1 OS=Homo sapiens GN=BHMT PE=1 SV=2	44970	6,58
Q13867	BLMH_HUMAN Bleomycin hydrolase OS=Homo sapiens GN=BLMH PE=1 SV=1	52528	5,87
Q9NZP8	C1RL_HUMAN Complement C1r subcomponent-like protein OS=Homo sapiens GN=C1RL PE=1 SV=2	53464	6,75
P55287	CAD11_HUMAN Cadherin-11 OS=Homo sapiens GN=CDH11 PE=1 SV=2	87911	4,75
P55290	CAD13_HUMAN Cadherin-13 OS=Homo sapiens GN=CDH13 PE=1 SV=1	78238	4,8
P12830	CADH1_HUMAN Cadherin-1 OS=Homo sapiens GN=CDH1 PE=1 SV=3	97396	4,58
Q8NFZ8	CADM4_HUMAN Cell adhesion molecule 4 OS=Homo sapiens GN=CADM4 PE=1 SV=1	42759	5,92
P62158	CALM_HUMAN Calmodulin OS=Homo sapiens GN=CALM1 PE=1 SV=2	16827	4,09
P31944	CASPE_HUMAN Caspase-14 OS=Homo sapiens GN=CASP14 PE=1 SV=2	27662	5,44
P07339	CATD_HUMAN Cathepsin D OS=Homo sapiens GN=CTSD PE=1 SV=1	44524	6,1

P07711	CATL1_HUMAN Cathepsin L1 OS=Homo sapiens GN=CTSL1 PE=1 SV=2	37540	5,31
Q9UBR2	CATZ_HUMAN Cathepsin Z OS=Homo sapiens GN=CTSZ PE=1 SV=1	33846	6,7
P08571	CD14_HUMAN Monocyte differentiation antigen CD14 OS=Homo sapiens GN=CD14 PE=1 SV=2	40051	5,84
Q9HCU0	CD248_HUMAN Endosialin OS=Homo sapiens GN=CD248 PE=1 SV=1	80807	5,18
P16070	CD44_HUMAN CD44 antigen OS=Homo sapiens GN=CD44 PE=1 SV=3	81487	5,13
P13987	CD59_HUMAN CD59 glycoprotein OS=Homo sapiens GN=CD59 PE=1 SV=1	14168	6,02
P32320	CDD_HUMAN Cytidine deaminase OS=Homo sapiens GN=CDA PE=1 SV=2	16174	6,55
P31997	CEAM8_HUMAN Carcinoembryonic antigen-related cell adhesion molecule 8 OS=Homo sapiens GN=CEACAM8 PE=1 SV=2	38130	6,95
P00450	CERU_HUMAN Ceruloplasmin OS=Homo sapiens GN=CP PE=1 SV=1	122128	5,44
P05156	CFAI_HUMAN Complement factor I OS=Homo sapiens GN=CFI PE=1 SV=2	65707	7,72
Q7LBR1	CHM1B_HUMAN Charged multivesicular body protein 1b OS=Homo sapiens GN=CHMP1B PE=1 SV=1	22095	7,82
Q9H0W9	CK054_HUMAN Ester hydrolase C11orf54 OS=Homo sapiens GN=C11orf54 PE=1 SV=1	35095	6,23
Q6UXG3	CLM9_HUMAN CMRF35-like molecule 9 OS=Homo sapiens GN=CD300LG PE=1 SV=2	36037	5,68
P10909	CLUS_HUMAN Clusterin OS=Homo sapiens GN=CLU PE=1 SV=1	52461	5,89
P10645	CMGA_HUMAN Chromogranin-A OS=Homo sapiens GN=CHGA PE=1 SV=7	50658	4,58
P0C0L4	CO4A_HUMAN Complement C4-A OS=Homo sapiens GN=C4A PE=1 SV=1	192650	6,65
P12109	CO6A1_HUMAN Collagen alpha-1(VI) chain OS=Homo sapiens GN=COL6A1 PE=1 SV=3	108462	5,26
P39059	COFA1_HUMAN Collagen alpha-1(XV) chain OS=Homo sapiens GN=COL15A1 PE=1 SV=2	141632	4,89
Q6UX73	CP089_HUMAN UPF0764 protein C16orf89 OS=Homo sapiens GN=C16orf89 PE=1 SV=2	45362	5,82
P20813	CP2B6_HUMAN Cytochrome P450 2B6 OS=Homo sapiens GN=CYP2B6 PE=1 SV=1	56242	8,43

P54108	CRIS3_HUMAN Cysteine-rich secretory protein 3 OS=Homo sapiens GN=CRISP3 PE=1 SV=1	27612	8,09
Q9UBG3	CRNN_HUMAN Cornulin OS=Homo sapiens GN=CRNN PE=1 SV=1	53502	5,73
P09603	CSF1_HUMAN Macrophage colony-stimulating factor 1 OS=Homo sapiens GN=CSF1 PE=1 SV=2	60142	5,16
O60494	CUBN_HUMAN Cubilin OS=Homo sapiens GN=CUBN PE=1 SV=5	398480	5,14
O60888	CUTA_HUMAN Protein CutA OS=Homo sapiens GN=CUTA PE=1 SV=2	19104	5,42
P01040	CYTA_HUMAN Cystatin-A OS=Homo sapiens GN=CSTA PE=1 SV=1	11000	5,38
P01034	CYTC_HUMAN Cystatin-C OS=Homo sapiens GN=CST3 PE=1 SV=1	15789	9
Q15828	CYTM_HUMAN Cystatin-M OS=Homo sapiens GN=CST6 PE=1 SV=1	16500	8,31
P08174	DAF_HUMAN Complement decay-accelerating factor OS=Homo sapiens GN=CD55 PE=1 SV=4	41374	7,79
P53355	DAPK1_HUMAN Death-associated protein kinase 1 OS=Homo sapiens GN=DAPK1 PE=1 SV=6	159945	6,37
Q07507	DERM_HUMAN Dermatopontin OS=Homo sapiens GN=DPT PE=2 SV=2	23989	4,70
Q01459	DIAC_HUMAN Di-N-acetylchitobiase OS=Homo sapiens GN=CTBS PE=1 SV=1	43732	6,19
Q9Y2E4	DIP2C_HUMAN Disco-interacting protein 2 homolog C OS=Homo sapiens GN=DIP2C PE=2 SV=2	170658	7,12
P24855	DNAS1_HUMAN Deoxyribonuclease-1 OS=Homo sapiens GN=DNASE1 PE=1 SV=1	31414	4,71
Q02487	DSC2_HUMAN Desmocollin-2 OS=Homo sapiens GN=DSC2 PE=1 SV=1	99899	5,19
P98172	EFNB1_HUMAN Ephrin-B1 OS=Homo sapiens GN=EFNB1 PE=1 SV=1	37982	9,1
P01133	EGF_HUMAN Pro-epidermal growth factor OS=Homo sapiens GN=EGF PE=1 SV=2	133906	5,53
O94919	ENDD1_HUMAN Endonuclease domain-containing 1 protein OS=Homo sapiens GN=ENDOD1 PE=1 SV=2	54981	5,55
P06733	ENOA_HUMAN Alpha-enolase OS=Homo sapiens GN=ENO1 PE=1 SV=2	47139	7,01
Q9UNN8	EPCR_HUMAN Endothelial protein C receptor OS=Homo sapiens GN=PROCR PE=1 SV=1	26655	6,7

Q96AP7	ESAM_HUMAN Endothelial cell-selective adhesion molecule OS=Homo sapiens GN=ESAM PE=1 SV=1	41151	9,42
P15311	EZRI_HUMAN Ezrin OS=Homo sapiens GN=EZR PE=1 SV=4	69370	5,94
Q9Y4F4	F179B_HUMAN Protein FAM179B OS=Homo sapiens GN=FAM179B PE=1 SV=4	189242	8,73
A4D161	F221A_HUMAN Protein FAM221A OS=Homo sapiens GN=FAM221A PE=2 SV=1	33061	6,33
Q01469	FABP5_HUMAN Fatty acid-binding protein, epidermal OS=Homo sapiens GN=FABP5 PE=1 SV=3	15155	6,60
Q12805	FBLN3_HUMAN EGF-containing fibulin-like extracellular matrix protein 1 OS=Homo sapiens GN=EFEMP1 PE=1 SV=2	54604	4,95
P08637	FCG3A_HUMAN Low affinity immunoglobulin gamma Fc region receptor III-A OS=Homo sapiens GN=FCGR3A PE=1 SV=2	29071	8,20
Q9Y6R7	FCGBP_HUMAN IgGFc-binding protein OS=Homo sapiens GN=FCGBP PE=1 SV=3	571639	5,14
P02765	FETUA_HUMAN Alpha-2-HS-glycoprotein OS=Homo sapiens GN=AHSG PE=1 SV=1	39300	5,43
P36980	FHR2_HUMAN Complement factor H-related protein 2 OS=Homo sapiens GN=CFHR2 PE=1 SV=1	30631	6
P02671	FIBA_HUMAN Fibrinogen alpha chain OS=Homo sapiens GN=FGA PE=1 SV=2	94914	5,70
P20930	FILA_HUMAN Filaggrin OS=Homo sapiens GN=FLG PE=1 SV=3	434922	9,24
P02751	FINC_HUMAN Fibronectin OS=Homo sapiens GN=FN1 PE=1 SV=4	262460	5,46
P15328	FOLR1_HUMAN Folate receptor alpha OS=Homo sapiens GN=FOLR1 PE=1 SV=3	29799	8,3
P04406	G3P_HUMAN Glyceraldehyde-3-phosphate dehydrogenase OS=Homo sapiens GN=GAPDH PE=1 SV=3	36030	8,57
Q8WWW8	GAB3_HUMAN GRB2-associated-binding protein 3 OS=Homo sapiens GN=GAB3 PE=2 SV=1	65548	6,8
P33402	GCYA2_HUMAN Guanylate cyclase soluble subunit alpha-2 OS=Homo sapiens GN=GUCY1A2 PE=1 SV=1	81698	7,77
P06396	GELS_HUMAN Gelsolin OS=Homo sapiens GN=GSN PE=1 SV=1	85644	5,90
P36268	GGT2_HUMAN Gamma-glutamyltranspeptidase 2 OS=Homo sapiens GN=GGT2 PE=1 SV=3	61732	7,22
P15586	GNS_HUMAN N-acetylglucosamine-6-sulfatase OS=Homo sapiens GN=GNS PE=1 SV=3	62042	8,6

Q8NBJ4	GOLM1_HUMAN Golgi membrane protein 1 OS=Homo sapiens GN=GOLM1 PE=1 SV=1	45306	4,91
Q9NQ84	GPC5C_HUMAN G-protein coupled receptor family C group 5 member C OS=Homo sapiens GN=GPRC5C PE=1 SV=2	48162	8,72
Q9HCN6	GPVI_HUMAN Platelet glycoprotein VI OS=Homo sapiens GN=GP6 PE=1 SV=4	36843	9,35
Q8IUY3	GRAM2_HUMAN GRAM domain-containing protein 2 OS=Homo sapiens GN=GRAMD2 PE=2 SV=2	40223	8,73
P08263	GSTA1_HUMAN Glutathione S-transferase A1 OS=Homo sapiens GN=GSTA1 PE=1 SV=3	25615	8,91
Q02747	GUC2A_HUMAN Guanylin OS=Homo sapiens GN=GUCA2A PE=1 SV=2	12380	4,56
Q16661	GUC2B_HUMAN Guanylate cyclase activator 2B OS=Homo sapiens GN=GUCA2B PE=1 SV=1	12061	6,02
Q8TDG4	HELQ_HUMAN Helicase POLQ-like OS=Homo sapiens GN=HELQ PE=1 SV=2	124053	6,17
P02790	HEMO_HUMAN Hemopexin OS=Homo sapiens GN=HPX PE=1 SV=2	51643	6,55
Q86YZ3	HORN_HUMAN Hornerin OS=Homo sapiens GN=HRNR PE=1 SV=2	282228	10,05
P00738	HPT_HUMAN Haptoglobin OS=Homo sapiens GN=HP PE=1 SV=1	45177	6,13
P54652	HSP72_HUMAN Heat shock-related 70 kDa protein 2 OS=Homo sapiens GN=HSPA2 PE=1 SV=1	69978	5,56
P01765	HV304_HUMAN Ig heavy chain V-III region TIL OS=Homo sapiens PE=1 SV=1	12348	9,24
P01766	HV305_HUMAN Ig heavy chain V-III region BRO OS=Homo sapiens PE=1 SV=1	13218	6,45
Q2M3T9	HYAL4_HUMAN Hyaluronidase-4 OS=Homo sapiens GN=HYAL4 PE=1 SV=2	54214	8,68
Q16270	IBP7_HUMAN Insulin-like growth factor-binding protein 7 OS=Homo sapiens GN=IGFBP7 PE=1 SV=1	29111	8,25
P05155	IC1_HUMAN Plasma protease C1 inhibitor OS=Homo sapiens GN=SERPING1 PE=1 SV=2	55119	6,09
O75144	ICOSL_HUMAN ICOS ligand OS=Homo sapiens GN=ICOSLG PE=1 SV=2	33328	5,15
P01876	IGHA1_HUMAN Ig alpha-1 chain C region OS=Homo sapiens GN=IGHA1 PE=1 SV=2	37631	6,08
P01857	IGHG1_HUMAN Ig gamma-1 chain C region OS=Homo sapiens GN=IGHG1 PE=1 SV=1	36083	8,46

P01859	IGHG2_HUMAN Ig gamma-2 chain C region OS=Homo sapiens GN=IGHG2 PE=1 SV=2	35878	7,66
P01871	IGHM_HUMAN Ig mu chain C region OS=Homo sapiens GN=IGHM PE=1 SV=3	49276	6,35
P01591	IGJ_HUMAN Immunoglobulin J chain OS=Homo sapiens GN=IGJ PE=1 SV=4	18087	5,12
P01834	IGKC_HUMAN Ig kappa chain C region OS=Homo sapiens GN=IGKC PE=1 SV=1	11602	5,58
B9A064	IGLL5_HUMAN Immunoglobulin lambda-like polypeptide 5 OS=Homo sapiens GN=IGLL5 PE=2 SV=2	23049	9,08
Q969P0	IGSF8_HUMAN Immunoglobulin superfamily member 8 OS=Homo sapiens GN=IGSF8 PE=1 SV=1	64994	8,23
P30740	ILEU_HUMAN Leukocyte elastase inhibitor OS=Homo sapiens GN=SERPINB1 PE=1 SV=1	42715	5,9
P05154	IPSP_HUMAN Plasma serine protease inhibitor OS=Homo sapiens GN=SERPINA5 PE=1 SV=3	45646	9,3
P53990	IST1_HUMAN IST1 homolog OS=Homo sapiens GN=IST1 PE=1 SV=1	39725	5,22
Q14624	ITIH4_HUMAN Inter-alpha-trypsin inhibitor heavy chain H4 OS=Homo sapiens GN=ITIH4 PE=1 SV=4	103293	6,51
O60674	JAK2_HUMAN Tyrosine-protein kinase JAK2 OS=Homo sapiens GN=JAK2 PE=1 SV=2	130590	6,82
P13645	K1C10_HUMAN Keratin, type I cytoskeletal 10 OS=Homo sapiens GN=KRT10 PE=1 SV=6	58792	5,13
P35527	K1C9_HUMAN Keratin, type I cytoskeletal 9 OS=Homo sapiens GN=KRT9 PE=1 SV=3	62027	5,14
P35908	K22E_HUMAN Keratin, type II cytoskeletal 2 epidermal OS=Homo sapiens GN=KRT2 PE=1 SV=2	65393	8,07
P04264	K2C1_HUMAN Keratin, type II cytoskeletal 1 OS=Homo sapiens GN=KRT1 PE=1 SV=6	65999	8,15
P13647	K2C5_HUMAN Keratin, type II cytoskeletal 5 OS=Homo sapiens GN=KRT5 PE=1 SV=3	62340	7,59
Q14003	KCNC3_HUMAN Potassium voltage-gated channel subfamily C member 3 OS=Homo sapiens GN=KCNC3 PE=1 SV=3	80527	6,08
P06870	KLK1_HUMAN Kallikrein-1 OS=Homo sapiens GN=KLK1 PE=1 SV=2	28871	4,68
Q9UKR3	KLK13_HUMAN Kallikrein-13 OS=Homo sapiens GN=KLK13 PE=1 SV=1	30551	8,78
P01042	KNG1_HUMAN Kininogen-1 OS=Homo sapiens GN=KNG1 PE=1 SV=2	71912	6,34

P01614	KV201_HUMAN Ig kappa chain V-II region Cum OS=Homo sapiens PE=1 SV=1	12668	5,28
P01619	KV301_HUMAN Ig kappa chain V-III region B6 OS=Homo sapiens PE=1 SV=1	11628	9,34
P01621	KV303_HUMAN Ig kappa chain V-III region NG9 (Fragment) OS=Homo sapiens PE=1 SV=1	10722	6,29
P01623	KV305_HUMAN Ig kappa chain V-III region WOL OS=Homo sapiens PE=1 SV=1	11739	9,07
P04433	KV309_HUMAN Ig kappa chain V-III region VG (Fragment) OS=Homo sapiens PE=1 SV=1	12567	4,85
P04434	KV310_HUMAN Ig kappa chain V-III region VH (Fragment) OS=Homo sapiens PE=4 SV=1	12749	5,63
P18135	KV312_HUMAN Ig kappa chain V-III region HAH OS=Homo sapiens PE=2 SV=1	14064	7,74
P01625	KV402_HUMAN Ig kappa chain V-IV region Len OS=Homo sapiens PE=1 SV=2	12632	7,92
P0CG05	LAC2_HUMAN Ig lambda-2 chain C regions OS=Homo sapiens GN=IGLC2 PE=1 SV=1	11287	6,92
P0CF74	LAC6_HUMAN Ig lambda-6 chain C region OS=Homo sapiens GN=IGLC6 PE=4 SV=1	11270	6,92
Q6GTX8	LAIR1_HUMAN Leukocyte-associated immunoglobulin-like receptor 1 OS=Homo sapiens GN=LAIR1 PE=1 SV=1	31393	5,40
Q86UK5	LBN_HUMAN Limbin OS=Homo sapiens GN=EVC2 PE=1 SV=1	147856	6,53
P04180	LCAT_HUMAN Phosphatidylcholine-sterol acyltransferase OS=Homo sapiens GN=LCAT PE=1 SV=1	49546	5,71
P31025	LCN1_HUMAN Lipocalin-1 OS=Homo sapiens GN=LCN1 PE=1 SV=1	19238	5,39
Q08380	LG3BP_HUMAN Galectin-3-binding protein OS=Homo sapiens GN=LGALS3BP PE=1 SV=1	65289	5,13
Q5T7N2	LITD1_HUMAN LINE-1 type transposase domain-containing protein 1 OS=Homo sapiens GN=L1TD1 PE=1 SV=1	98789	4,87
Q12907	LMAN2_HUMAN Vesicular integral-membrane protein VIP36 OS=Homo sapiens GN=LMAN2 PE=1 SV=1	40203	6,46
P98164	LRP2_HUMAN Low-density lipoprotein receptor-related protein 2 OS=Homo sapiens GN=LRP2 PE=1 SV=3	521616	4,89
P01700	LV102_HUMAN Ig lambda chain V-I region HA OS=Homo sapiens PE=1 SV=1	11889	9,07
P01715	LV401_HUMAN Ig lambda chain V-IV region Bau OS=Homo sapiens PE=1 SV=1	11298	5,04

P01717	LV403_HUMAN Ig lambda chain V-IV region Hil OS=Homo sapiens PE=1 SV=1	11510	6,04
P10253	LYAG_HUMAN Lysosomal alpha-glucosidase OS=Homo sapiens GN=GAA PE=1 SV=4	105257	5,62
P61626	LYSC_HUMAN Lysozyme C OS=Homo sapiens GN=LYZ PE=1 SV=1	16526	9,38
P33908	MA1A1_HUMAN Mannosyl-oligosaccharide 1,2-alpha-mannosidase IA OS=Homo sapiens GN=MAN1A1 PE=1 SV=3	72922	6,04
O00187	MASP2_HUMAN Mannan-binding lectin serine protease 2 OS=Homo sapiens GN=MASP2 PE=1 SV=4	75654	5,39
Q8IWD5	MFS6L_HUMAN Major facilitator superfamily domain-containing protein 6-like OS=Homo sapiens GN=MFSD6L PE=2 SV=2	63964	8,87
O43451	MGA_HUMAN Maltase-glucoamylase, intestinal OS=Homo sapiens GN=MGAM PE=1 SV=5	209720	5,27
Q13201	MMRN1_HUMAN Multimerin-1 OS=Homo sapiens GN=MMRN1 PE=1 SV=3	138023	8,15
P15941	MUC1_HUMAN Mucin-1 OS=Homo sapiens GN=MUC1 PE=1 SV=3	122029	6,96
P43121	MUC18_HUMAN Cell surface glycoprotein MUC18 OS=Homo sapiens GN=MCAM PE=1 SV=2	71563	5,58
P02144	MYG_HUMAN Myoglobin OS=Homo sapiens GN=MB PE=1 SV=2	17173	7,14
O96009	NAPSA_HUMAN Napsin-A OS=Homo sapiens GN=NAPSA PE=1 SV=1	45358	6,15
P20929	NEBU_HUMAN Nebulin OS=Homo sapiens GN=NEB PE=1 SV=4	772441	9,11
P80188	NGAL_HUMAN Neutrophil gelatinase-associated lipocalin OS=Homo sapiens GN=LCN2 PE=1 SV=2	22574	9,02
P14543	NID1_HUMAN Nidogen-1 OS=Homo sapiens GN=NID1 PE=1 SV=3	136291	5,12
Q8TCU5	NMD3A_HUMAN Glutamate receptor ionotropic, NMDA 3A OS=Homo sapiens GN=GRIN3A PE=1 SV=2	125385	7,4
Q6UX06	OLFM4_HUMAN Olfactomedin-4 OS=Homo sapiens GN=OLFM4 PE=1 SV=1	57244	5,5
Q8IYS5	OSCAR_HUMAN Osteoclast-associated immunoglobulin-like receptor OS=Homo sapiens GN=OSCAR PE=2 SV=3	30462	6,09
P10451	OSTP_HUMAN Osteopontin OS=Homo sapiens GN=SPP1 PE=1 SV=1	35401	4,37
Q96FE7	P3IP1_HUMAN Phosphoinositide-3-kinase-interacting protein 1 OS=Homo sapiens GN=PIK3IP1 PE=1 SV=2	28230	4,92

Q504Q3	PAN2_HUMAN PAB-dependent poly(A)-specific ribonuclease subunit 2 OS=Homo sapiens GN=PAN2 PE=1 SV=3	135281	5,64
P42785	PCP_HUMAN Lysosomal Pro-X carboxypeptidase OS=Homo sapiens GN=PRCP PE=1 SV=1	55764	6,75
P30086	PEBP1_HUMAN Phosphatidylethanolamine-binding protein 1 OS=Homo sapiens GN=PEBP1 PE=1 SV=3	21044	7,01
P0DJD8	PEPA3_HUMAN Pepsin A-3 OS=Homo sapiens GN=PGA3 PE=1 SV=1	41950	4,22
P98160	PGBM_HUMAN Basement membrane-specific heparan sulfate proteoglycan core protein OS=Homo sapiens GN=HSPG2 PE=1 SV=4	468532	6,06
O75594	PGRP1_HUMAN Peptidoglycan recognition protein 1 OS=Homo sapiens GN=PGLYRP1 PE=1 SV=1	21717	8,92
P01833	PIGR_HUMAN Polymeric immunoglobulin receptor OS=Homo sapiens GN=PIGR PE=1 SV=4	83232	5,58
P00747	PLMN_HUMAN Plasminogen OS=Homo sapiens GN=PLG PE=1 SV=2	90510	7,04
Q96GD0	PLPP_HUMAN Pyridoxal phosphate phosphatase OS=Homo sapiens GN=PDXP PE=1 SV=2	31678	6,11
P15309	PPAP_HUMAN Prostatic acid phosphatase OS=Homo sapiens GN=ACPP PE=1 SV=3	44537	5,83
P22891	PROZ_HUMAN Vitamin K-dependent protein Z OS=Homo sapiens GN=PROZ PE=1 SV=2	44715	5,64
Q16651	PRSS8_HUMAN Prostasin OS=Homo sapiens GN=PRSS8 PE=1 SV=1	36408	5,51
P41222	PTGDS_HUMAN Prostaglandin-H2 D-isomerase OS=Homo sapiens GN=PTGDS PE=1 SV=1	21015	7,66
Q13332	PTPRS_HUMAN Receptor-type tyrosine-protein phosphatase S OS=Homo sapiens GN=PTPRS PE=1 SV=3	216905	6,06
Q92692	PVRL2_HUMAN Poliovirus receptor-related protein 2 OS=Homo sapiens GN=PVRL2 PE=1 SV=1	57706	4,74
Q16769	QPCT_HUMAN Glutaminyl-peptide cyclotransferase OS=Homo sapiens GN=QPCT PE=1 SV=1	40851	6,12
Q86UN3	R4RL2_HUMAN Reticulon-4 receptor-like 2 OS=Homo sapiens GN=RTN4RL2 PE=1 SV=1	46077	7,58
Q86YV0	RASL3_HUMAN RAS protein activator like-3 OS=Homo sapiens GN=RASAL3 PE=1 SV=2	111829	9,03
P02753	RET4_HUMAN Retinol-binding protein 4 OS=Homo sapiens GN=RBP4 PE=1 SV=3	22995	5,76
P82980	RET5_HUMAN Retinol-binding protein 5 OS=Homo sapiens GN=RBP5 PE=1 SV=3	15921	6,09

P10153	RNAS2_HUMAN Non-secretory ribonuclease OS=Homo sapiens GN=RNASE2 PE=1 SV=2	18342	9,1
Q8WZ75	ROBO4_HUMAN Roundabout homolog 4 OS=Homo sapiens GN=ROBO4 PE=1 SV=1	107390	6,18
P62979	RS27A_HUMAN Ubiquitin-40S ribosomal protein S27a OS=Homo sapiens GN=RPS27A PE=1 SV=2	17953	9,68
P82663	RT25_HUMAN 28S ribosomal protein S25, mitochondrial OS=Homo sapiens GN=MRPS25 PE=1 SV=1	20103	8,99
P05109	S10A8_HUMAN Protein S100-A8 OS=Homo sapiens GN=S100A8 PE=1 SV=1	10828	6,51
P06702	S10A9_HUMAN Protein S100-A9 OS=Homo sapiens GN=S100A9 PE=1 SV=1	13234	5,71
Q96H78	S2544_HUMAN Solute carrier family 25 member 44 OS=Homo sapiens GN=SLC25A44 PE=2 SV=1	35370	9,64
P0C874	S31D3_HUMAN Putative spermatogenesis-associated protein 31D3 OS=Homo sapiens GN=SPATA31D3 PE=5 SV=1	102354	8,32
Q8WVN6	SCTM1_HUMAN Secreted and transmembrane protein 1 OS=Homo sapiens GN=SECTM1 PE=1 SV=2	27022	7
Q02383	SEMG2_HUMAN Semenogelin-2 OS=Homo sapiens GN=SEMG2 PE=1 SV=1	65404	9,08
Q9UPS6	SET1B_HUMAN Histone-lysine N-methyltransferase SETD1B OS=Homo sapiens GN=SETD1B PE=1 SV=2	208601	4,86
Q9H299	SH3L3_HUMAN SH3 domain-binding glutamic acid-rich-like protein 3 OS=Homo sapiens GN=SH3BGRL3 PE=1 SV=1	10431	4,82
Q8N114	SHSA5_HUMAN Protein shisa-5 OS=Homo sapiens GN=SHISA5 PE=1 SV=1	25564	6,26
Q9HAT2	SIAE_HUMAN Sialate O-acetylesterase OS=Homo sapiens GN=SIAE PE=1 SV=1	58277	6,93
O00241	SIRB1_HUMAN Signal-regulatory protein beta-1 OS=Homo sapiens GN=SIRPB1 PE=1 SV=5	43184	6,07
Q5TFQ8	SIRBL_HUMAN Signal-regulatory protein beta-1 isoform 3 OS=Homo sapiens GN=SIRPB1 PE=1 SV=1	43332	7,7
P08294	SODE_HUMAN Extracellular superoxide dismutase [Cu-Zn] OS=Homo sapiens GN=SOD3 PE=1 SV=2	25835	6,14
Q96P63	SPB12_HUMAN Serpin B12 OS=Homo sapiens GN=SERPINB12 PE=1 SV=1	46247	5,36
P29508	SPB3_HUMAN Serpin B3 OS=Homo sapiens GN=SERPINB3 PE=1 SV=2	44537	6,35
P48594	SPB4_HUMAN Serpin B4 OS=Homo sapiens GN=SERPINB4 PE=1 SV=2	44825	5,86

Q9UBC9	SPRR3_HUMAN Small proline-rich protein 3 OS=Homo sapiens GN=SPRR3 PE=1 SV=2	18142	8,86
Q8N3T6	T132C_HUMAN Transmembrane protein 132C OS=Homo sapiens GN=TMEM132C PE=2 SV=3	121711	5,95
Q8NAT2	TDRD5_HUMAN Tudor domain-containing protein 5 OS=Homo sapiens GN=TDRD5 PE=1 SV=3	109667	8,31
P05452	TETN_HUMAN Tetranectin OS=Homo sapiens GN=CLEC3B PE=1 SV=3	22522	5,52
Q9GZN2	TGIF2_HUMAN Homeobox protein TGIF2 OS=Homo sapiens GN=TGIF2 PE=1 SV=1	25863	7,77
P05543	THBG_HUMAN Thyroxine-binding globulin OS=Homo sapiens GN=SERPINA7 PE=1 SV=2	46295	5,87
O14773	TPP1_HUMAN Tripeptidyl-peptidase 1 OS=Homo sapiens GN=TPP1 PE=1 SV=2	61210	6,01
P02787	TRFE_HUMAN Serotransferrin OS=Homo sapiens GN=TF PE=1 SV=3	77014	6,81
P02788	TRFL_HUMAN Lactotransferrin OS=Homo sapiens GN=LTF PE=1 SV=6	78132	8,5
Q8N831	TSYL6_HUMAN Testis-specific Y-encoded-like protein 6 OS=Homo sapiens GN=TSPYL6 PE=2 SV=1	45845	5,45
P02766	TTHY_HUMAN Transthyretin OS=Homo sapiens GN=TTR PE=1 SV=1	15877	5,52
Q9GZX9	TWSG1_HUMAN Twisted gastrulation protein homolog 1 OS=Homo sapiens GN=TWSG1 PE=2 SV=1	24999	5,17
P30530	UFO_HUMAN Tyrosine-protein kinase receptor UFO OS=Homo sapiens GN=AXL PE=1 SV=3	98273	5,27
P07911	UROM_HUMAN Uromodulin OS=Homo sapiens GN=UMOD PE=1 SV=1	69714	5,05
Q6EMK4	VASN_HUMAN Vasorin OS=Homo sapiens GN=VASN PE=1 SV=1	71668	7,16
P19320	VCAM1_HUMAN Vascular cell adhesion protein 1 OS=Homo sapiens GN=VCAM1 PE=1 SV=1	81224	5,14
Q7Z5L0	VMO1_HUMAN Vitelline membrane outer layer protein 1 homolog OS=Homo sapiens GN=VMO1 PE=1 SV=1	21520	4,9
P04004	VTNC_HUMAN Vitronectin OS=Homo sapiens GN=VTN PE=1 SV=1	54271	5,55
P25311	ZA2G_HUMAN Zinc-alpha-2-glycoprotein OS=Homo sapiens GN=AZGP1 PE=1 SV=2	34237	5,71
Q96C00	ZBTB9_HUMAN Zinc finger and BTB domain-containing protein 9 OS=Homo sapiens GN=ZBTB9 PE=1 SV=1	50570	6,29

Q96DA0	ZG16B_HUMAN Zymogen granule protein 16 homolog B OS=Homo sapiens GN=ZG16B PE=1 SV=3	22725	6,74
Q14584	ZN266_HUMAN Zinc finger protein 266 OS=Homo sapiens GN=ZNF266 PE=2 SV=2	62076	8,93
Q9H0M5	ZN700_HUMAN Zinc finger protein 700 OS=Homo sapiens GN=ZNF700 PE=2 SV=1	86176	9,15

Appendix 3 – Total proteins identified by nanoLC-MS/MS in PAH patients.

Accession #	Protein ID	MW (Da)	pI
P02763	A1AG1_HUMAN Alpha-1-acid glycoprotein 1 OS=Homo sapiens GN=ORM1 PE=1 SV=1	23497	4,93
P19652	A1AG2_HUMAN Alpha-1-acid glycoprotein 2 OS=Homo sapiens GN=ORM2 PE=1 SV=2	23588	5,03
P01009	A1AT_HUMAN Alpha-1-antitrypsin OS=Homo sapiens GN=SERPINA1 PE=1 SV=3	46707	5,37
P04217	A1BG_HUMAN Alpha-1B-glycoprotein OS=Homo sapiens GN=A1BG PE=1 SV=4	54220	5,56
P02750	A2GL_HUMAN Leucine-rich alpha-2-glycoprotein OS=Homo sapiens GN=LRG1 PE=1 SV=2	38154	6,45
P01023	A2MG_HUMAN Alpha-2-macroglobulin OS=Homo sapiens GN=A2M PE=1 SV=3	163188	6,03
P01011	AACT_HUMAN Alpha-1-antichymotrypsin OS=Homo sapiens GN=SERPINA3 PE=1 SV=2	47621	5,33
P60709	ACTB_HUMAN Actin, cytoplasmic 1 OS=Homo sapiens GN=ACTB PE=1 SV=1	41710	5,29
Q96BJ3	AIDA_HUMAN Axin interactor, dorsalization-associated protein OS=Homo sapiens GN=AIDA PE=1 SV=1	35001	6,13
P02768	ALBU_HUMAN Serum albumin OS=Homo sapiens GN=ALB PE=1 SV=2	69321	5,92
Q9BT30	ALKB7_HUMAN Alpha-ketoglutarate-dependent dioxygenase alkB homolog 7 OS=Homo sapiens GN=ALKBH7 PE=2 SV=1	24501	6,61
P02760	AMBP_HUMAN Protein AMBP OS=Homo sapiens GN=AMBP PE=1 SV=1	38974	5,95
P15144	AMPN_HUMAN Aminopeptidase N OS=Homo sapiens GN=ANPEP PE=1 SV=4	109471	5,31
P04746	AMYP_HUMAN Pancreatic alpha-amylase OS=Homo sapiens GN=AMY2A PE=1 SV=2	57670	6,6
P54802	ANAG_HUMAN Alpha-N-acetylglucosaminidase OS=Homo sapiens GN=NAGLU PE=1 SV=2	82214	6,2
P01008	ANT3_HUMAN Antithrombin-III OS=Homo sapiens GN=SERPINC1 PE=1 SV=1	52569	6,32
Q9H6X2	ANTR1_HUMAN Anthrax toxin receptor 1 OS=Homo sapiens GN=ANTXR1 PE=1 SV=2	62749	7,53
P05090	APOD_HUMAN Apolipoprotein D OS=Homo sapiens GN=APOD PE=1 SV=1	21262	5,06

Q13510	ASAH1_HUMAN Acid ceramidase OS=Homo sapiens GN=ASAH1 PE=1 SV=5	44631	7,52
Q9NZP8	C1RL_HUMAN Complement C1r subcomponent-like protein OS=Homo sapiens GN=C1RL PE=1 SV=2	53464	6,75
P12830	CADH1_HUMAN Cadherin-1 OS=Homo sapiens GN=CDH1 PE=1 SV=3	97396	4,58
Q8NFZ8	CADM4_HUMAN Cell adhesion molecule 4 OS=Homo sapiens GN=CADM4 PE=1 SV=1	42759	5,92
O75052	CAPON_HUMAN Carboxyl-terminal PDZ ligand of neuronal nitric oxide synthase protein OS=Homo sapiens GN=NOS1AP PE=1 SV=3	56115	5,89
P07858	CATB_HUMAN Cathepsin B OS=Homo sapiens GN=CTSB PE=1 SV=3	37797	5,88
P53634	CATC_HUMAN Dipeptidyl peptidase 1 OS=Homo sapiens GN=CTSC PE=1 SV=2	51820	6,54
P07339	CATD_HUMAN Cathepsin D OS=Homo sapiens GN=CTSD PE=1 SV=1	44524	6,1
P07711	CATL1_HUMAN Cathepsin L1 OS=Homo sapiens GN=CTSL1 PE=1 SV=2	37540	5,31
Q9UBR2	CATZ_HUMAN Cathepsin Z OS=Homo sapiens GN=CTSZ PE=1 SV=1	33846	6,7
Q96HB5	CC120_HUMAN Coiled-coil domain-containing protein 120 OS=Homo sapiens GN=CCDC120 PE=1 SV=1	67526	9,51
Q2M329	CCD96_HUMAN Coiled-coil domain-containing protein 96 OS=Homo sapiens GN=CCDC96 PE=2 SV=2	62672	4,92
P16070	CD44_HUMAN CD44 antigen OS=Homo sapiens GN=CD44 PE=1 SV=3	81487	5,13
P13987	CD59_HUMAN CD59 glycoprotein OS=Homo sapiens GN=CD59 PE=1 SV=1	14168	6,02
P31997	CEAM8_HUMAN Carcinoembryonic antigen-related cell adhesion molecule 8 OS=Homo sapiens GN=CEACAM8 PE=1 SV=2	38130	6,95
P00450	CERU_HUMAN Ceruloplasmin OS=Homo sapiens GN=CP PE=1 SV=1	122128	5,44
P05156	CFAI_HUMAN Complement factor I OS=Homo sapiens GN=CFI PE=1 SV=2	65707	7,72
P12109	CO6A1_HUMAN Collagen alpha-1(VI) chain OS=Homo sapiens GN=COL6A1 PE=1 SV=3	108462	5,2
Q02388	CO7A1_HUMAN Collagen alpha-1(VII) chain OS=Homo sapiens GN=COL7A1 PE=1 SV=2	295041	5,95
Q9H3G5	CPVL_HUMAN Probable serine carboxypeptidase CPVL OS=Homo sapiens GN=CPVL PE=1 SV=2	54129	5,39

O60494	CUBN_HUMAN Cubilin OS=Homo sapiens GN=CUBN PE=1 SV=5	398480	5,14
P01034	CYTC_HUMAN Cystatin-C OS=Homo sapiens GN=CST3 PE=1 SV=1	15789	9
Q01459	DIAC_HUMAN Di-N-acetylchitobiase OS=Homo sapiens GN=CTBS PE=1 SV=1	43732	6,19
P24855	DNAS1_HUMAN Deoxyribonuclease-1 OS=Homo sapiens GN=DNASE1 PE=1 SV=1	31414	4,71
P01133	EGF_HUMAN Pro-epidermal growth factor OS=Homo sapiens GN=EGF PE=1 SV=2	133906	5,53
O94919	ENDD1_HUMAN Endonuclease domain-containing 1 protein OS=Homo sapiens GN=ENDOD1 PE=1 SV=2	54981	5,55
Q9UNN8	EPCR_HUMAN Endothelial protein C receptor OS=Homo sapiens GN=PROCR PE=1 SV=1	26655	6,7
A4D161	F221A_HUMAN Protein FAM221A OS=Homo sapiens GN=FAM221A PE=2 SV=1	33061	6,33
Q9NYQ8	FAT2_HUMAN Protocadherin Fat 2 OS=Homo sapiens GN=FAT2 PE=1 SV=2	479018	5
Q12805	FBLN3_HUMAN EGF-containing fibulin-like extracellular matrix protein 1 OS=Homo sapiens GN=EFEMP1 PE=1 SV=2	54604	4,95
Q9UK99	FBX3_HUMAN F-box only protein 3 OS=Homo sapiens GN=FBXO3 PE=1 SV=3	54525	4,88
P02765	FETUA_HUMAN Alpha-2-HS-glycoprotein OS=Homo sapiens GN=AHSG PE=1 SV=1	39300	5,43
P02679	FIBG_HUMAN Fibrinogen gamma chain OS=Homo sapiens GN=FGG PE=1 SV=3	51479	5,37
P02751	FINC_HUMAN Fibronectin OS=Homo sapiens GN=FN1 PE=1 SV=4	262460	5,46
Q9Y2I7	FYV1_HUMAN 1-phosphatidylinositol 3-phosphate 5-kinase OS=Homo sapiens GN=PIKFYVE PE=1 SV=3	236986	6,24
Q16775	GLO2_HUMAN Hydroxyacylglutathione hydrolase, mitochondrial OS=Homo sapiens GN=HAGH PE=1 SV=2	33784	8,34
P15586	GNS_HUMAN N-acetylglucosamine-6-sulfatase OS=Homo sapiens GN=GNS PE=1 SV=3	62042	8,60
P55259	GP2_HUMAN Pancreatic secretory granule membrane major glycoprotein GP2 OS=Homo sapiens GN=GP2 PE=2 SV=3	59442	5,08
Q9HCN6	GPVI_HUMAN Platelet glycoprotein VI OS=Homo sapiens GN=GP6 PE=1 SV=4	36843	9,35
Q8TDG4	HELQ_HUMAN Helicase POLQ-like OS=Homo sapiens GN=HELQ PE=1 SV=2	124053	6,17

P02790	HEMO_HUMAN Hemopexin OS=Homo sapiens GN=HPX PE=1 SV=2	51643	6,55
Q86YZ3	HORN_HUMAN Hornerin OS=Homo sapiens GN=HRNR PE=1 SV=2	282228	10,05
P00738	HPT_HUMAN Haptoglobin OS=Homo sapiens GN=HP PE=1 SV=1	45177	6,13
Q16270	IBP7_HUMAN Insulin-like growth factor-binding protein 7 OS=Homo sapiens GN=IGFBP7 PE=1 SV=1	29111	8,25
P01876	IGHA1_HUMAN Ig alpha-1 chain C region OS=Homo sapiens GN=IGHA1 PE=1 SV=2	37631	6,08
P01857	IGHG1_HUMAN Ig gamma-1 chain C region OS=Homo sapiens GN=IGHG1 PE=1 SV=1	36083	8,46
P01859	IGHG2_HUMAN Ig gamma-2 chain C region OS=Homo sapiens GN=IGHG2 PE=1 SV=2	35878	7,66
P01591	IGJ_HUMAN Immunoglobulin J chain OS=Homo sapiens GN=IGJ PE=1 SV=4	18087	5,12
P01834	IGKC_HUMAN Ig kappa chain C region OS=Homo sapiens GN=IGKC PE=1 SV=1	11602	5,58
B9A064	IGLL5_HUMAN Immunoglobulin lambda-like polypeptide 5 OS=Homo sapiens GN=IGLL5 PE=2 SV=2	23049	9,08
P05154	IPSP_HUMAN Plasma serine protease inhibitor OS=Homo sapiens GN=SERPINA5 PE=1 SV=3	45646	9,30
Q14624	ITIH4_HUMAN Inter-alpha-trypsin inhibitor heavy chain H4 OS=Homo sapiens GN=ITIH4 PE=1 SV=4	103293	6,51
P13645	K1C10_HUMAN Keratin, type I cytoskeletal 10 OS=Homo sapiens GN=KRT10 PE=1 SV=6	58792	5,13
P35527	K1C9_HUMAN Keratin, type I cytoskeletal 9 OS=Homo sapiens GN=KRT9 PE=1 SV=3	62027	5,14
P35908	K22E_HUMAN Keratin, type II cytoskeletal 2 epidermal OS=Homo sapiens GN=KRT2 PE=1 SV=2	65393	8,07
P04264	K2C1_HUMAN Keratin, type II cytoskeletal 1 OS=Homo sapiens GN=KRT1 PE=1 SV=6	65999	8,15
P13647	K2C5_HUMAN Keratin, type II cytoskeletal 5 OS=Homo sapiens GN=KRT5 PE=1 SV=3	62340	7,59
Q14003	KCNC3_HUMAN Potassium voltage-gated channel subfamily C member 3 OS=Homo sapiens GN=KCNC3 PE=1 SV=3	80527	6,08
P01042	KNG1_HUMAN Kininogen-1 OS=Homo sapiens GN=KNG1 PE=1 SV=2	71912	6,34
P01593	KV101_HUMAN Ig kappa chain V-I region AG OS=Homo sapiens PE=1 SV=1	11985	5,67

P01614	KV201_HUMAN Ig kappa chain V-II region Cum OS=Homo sapiens PE=1 SV=1	12668	5,28
P01619	KV301_HUMAN Ig kappa chain V-III region B6 OS=Homo sapiens PE=1 SV=1	11628	9,34
P01621	KV303_HUMAN Ig kappa chain V-III region NG9 (Fragment) OS=Homo sapiens PE=1 SV=1	10722	6,29
P04433	KV309_HUMAN Ig kappa chain V-III region VG (Fragment) OS=Homo sapiens PE=1 SV=1	12567	4,85
P04434	KV310_HUMAN Ig kappa chain V-III region VH (Fragment) OS=Homo sapiens PE=4 SV=1	12749	5,63
P18135	KV312_HUMAN Ig kappa chain V-III region HAH OS=Homo sapiens PE=2 SV=1	14064	7,74
P01625	KV402_HUMAN Ig kappa chain V-IV region Len OS=Homo sapiens PE=1 SV=2	12632	7,92
P0CG04	LAC1_HUMAN Ig lambda-1 chain C regions OS=Homo sapiens GN=IGLC1 PE=1 SV=1	23049	9,08
P0CG05	LAC2_HUMAN Ig lambda-2 chain C regions OS=Homo sapiens GN=IGLC2 PE=1 SV=1	11287	6,92
Q6GTX8	LAIR1_HUMAN Leukocyte-associated immunoglobulin-like receptor 1 OS=Homo sapiens GN=LAIR1 PE=1 SV=1	31393	5,4
Q86UK5	LBN_HUMAN Limbin OS=Homo sapiens GN=EVC2 PE=1 SV=1	147856	6,53
P04180	LCAT_HUMAN Phosphatidylcholine-sterol acyltransferase OS=Homo sapiens GN=LCAT PE=1 SV=1	49546	5,71
Q08380	LG3BP_HUMAN Galectin-3-binding protein OS=Homo sapiens GN=LGALS3BP PE=1 SV=1	65289	5,13
Q8IYG6	LRC56_HUMAN Leucine-rich repeat-containing protein 56 OS=Homo sapiens GN=LRRC56 PE=2 SV=1	58697	8,05
P98164	LRP2_HUMAN Low-density lipoprotein receptor-related protein 2 OS=Homo sapiens GN=LRP2 PE=1 SV=3	521616	4,89
P01717	LV403_HUMAN Ig lambda chain V-IV region Hil OS=Homo sapiens PE=1 SV=1	11510	6,04
P10253	LYAG_HUMAN Lysosomal alpha-glucosidase OS=Homo sapiens GN=GAA PE=1 SV=4	105257	5,62
P61626	LYSC_HUMAN Lysozyme C OS=Homo sapiens GN=LYZ PE=1 SV=1	16526	9,38
Q9P0L2	MARK1_HUMAN Serine/threonine-protein kinase MARK1 OS=Homo sapiens GN=MARK1 PE=1 SV=2	88947	9,42
O00187	MASP2_HUMAN Mannan-binding lectin serine protease 2 OS=Homo sapiens GN=MASP2 PE=1 SV=4	75654	5,39

O43451	MGA_HUMAN Maltase-glucoamylase, intestinal OS=Homo sapiens GN=MGAM PE=1 SV=5	209720	5,27
P43121	MUC18_HUMAN Cell surface glycoprotein MUC18 OS=Homo sapiens GN=MCAM PE=1 SV=2	71563	5,58
P02144	MYG_HUMAN Myoglobin OS=Homo sapiens GN=MB PE=1 SV=2	17173	7,14
P17050	NAGAB_HUMAN Alpha-N-acetylgalactosaminidase OS=Homo sapiens GN=NAGA PE=1 SV=2	46534	4,98
O96009	NAPSA_HUMAN Napsin-A OS=Homo sapiens GN=NAPSA PE=1 SV=1	45358	6,15
P80188	NGAL_HUMAN Neutrophil gelatinase-associated lipocalin OS=Homo sapiens GN=LCN2 PE=1 SV=2	22574	9,02
Q8IYS5	OSCAR_HUMAN Osteoclast-associated immunoglobulin-like receptor OS=Homo sapiens GN=OSCAR PE=2 SV=3	30462	6,09
P10451	OSTP_HUMAN Osteopontin OS=Homo sapiens GN=SPP1 PE=1 SV=1	35401	4,37
Q96FE7	P3IP1_HUMAN Phosphoinositide-3-kinase-interacting protein 1 OS=Homo sapiens GN=PIK3IP1 PE=1 SV=2	28230	4,92
Q96RV3	PCX1_HUMAN Pecanex-like protein 1 OS=Homo sapiens GN=PCNX PE=2 SV=2	258514	6,8
P0DJD8	PEPA3_HUMAN Pepsin A-3 OS=Homo sapiens GN=PGA3 PE=1 SV=1	41950	4,22
P05164	PERM_HUMAN Myeloperoxidase OS=Homo sapiens GN=MPO PE=1 SV=1	83815	9,19
P98160	PGBM_HUMAN Basement membrane-specific heparan sulfate proteoglycan core protein OS=Homo sapiens GN=HSPG2 PE=1 SV=4	468532	6,06
P16112	PGCA_HUMAN Aggrecan core protein OS=Homo sapiens GN=ACAN PE=1 SV=2	250040	4,1
P01833	PIGR_HUMAN Polymeric immunoglobulin receptor OS=Homo sapiens GN=PIGR PE=1 SV=4	83232	5,58
Q9BZ72	PITM2_HUMAN Membrane-associated phosphatidylinositol transfer protein 2 OS=Homo sapiens GN=PITPNM2 PE=1 SV=1	148840	6,72
P00747	PLMN_HUMAN Plasminogen OS=Homo sapiens GN=PLG PE=1 SV=2	90510	7,04
Q96GD0	PLPP_HUMAN Pyridoxal phosphate phosphatase OS=Homo sapiens GN=PDXP PE=1 SV=2	31678	6,11
P11117	PPAL_HUMAN Lysosomal acid phosphatase OS=Homo sapiens GN=ACP2 PE=1 SV=3	48313	6,28
P41222	PTGDS_HUMAN Prostaglandin-H2 D-isomerase OS=Homo sapiens GN=PTGDS PE=1 SV=1	21015	7,66

P15151	PVR_HUMAN Poliovirus receptor OS=Homo sapiens GN=PVR PE=1 SV=2	45274	6,07
Q16769	QPCT_HUMAN Glutaminyl-peptide cyclotransferase OS=Homo sapiens GN=QPCT PE=1 SV=1	40851	6,12
P62987	RL40_HUMAN Ubiquitin-60S ribosomal protein L40 OS=Homo sapiens GN=UBA52 PE=1 SV=2	14719	9,87
P10153	RNAS2_HUMAN Non-secretory ribonuclease OS=Homo sapiens GN=RNASE2 PE=1 SV=2	18342	9,1
Q8WZ75	ROBO4_HUMAN Roundabout homolog 4 OS=Homo sapiens GN=ROBO4 PE=1 SV=1	107390	6,18
P62979	RS27A_HUMAN Ubiquitin-40S ribosomal protein S27a OS=Homo sapiens GN=RPS27A PE=1 SV=2	17953	9,68
P06702	S10A9_HUMAN Protein S100-A9 OS=Homo sapiens GN=S100A9 PE=1 SV=1	13234	5,71
Q96H78	S2544_HUMAN Solute carrier family 25 member 44 OS=Homo sapiens GN=SLC25A44 PE=2 SV=1	35370	9,64
P02743	SAMP_HUMAN Serum amyloid P-component OS=Homo sapiens GN=APCS PE=1 SV=2	25371	6,10
P17900	SAP3_HUMAN Ganglioside GM2 activator OS=Homo sapiens GN=GM2A PE=1 SV=4	20825	5,17
Q8WVN6	SCTM1_HUMAN Secreted and transmembrane protein 1 OS=Homo sapiens GN=SECTM1 PE=1 SV=2	27022	7
P18827	SDC1_HUMAN Syndecan-1 OS=Homo sapiens GN=SDC1 PE=1 SV=3	32442	4,53
P04279	SEMG1_HUMAN Semenogelin-1 OS=Homo sapiens GN=SEMG1 PE=1 SV=2	52100	9,3
Q02383	SEMG2_HUMAN Semenogelin-2 OS=Homo sapiens GN=SEMG2 PE=1 SV=1	65405	9,08
Q8N114	SHSA5_HUMAN Protein shisa-5 OS=Homo sapiens GN=SHISA5 PE=1 SV=1	25564	6,26
Q5TFQ8	SIRBL_HUMAN Signal-regulatory protein beta-1 isoform 3 OS=Homo sapiens GN=SIRPB1 PE=1 SV=1	43332	7,7
Q8NBL3	T178A_HUMAN Transmembrane protein 178A OS=Homo sapiens GN=TMEM178A PE=2 SV=1	32997	8,83
P05452	TETN_HUMAN Tetranectin OS=Homo sapiens GN=CLEC3B PE=1 SV=3	22522	5,52
O14773	TPP1_HUMAN Tripeptidyl-peptidase 1 OS=Homo sapiens GN=TPP1 PE=1 SV=2	61210	6,01
P02787	TRFE_HUMAN Serotransferrin OS=Homo sapiens GN=TF PE=1 SV=3	77014	6,81

P02788	TRFL_HUMAN Lactotransferrin OS=Homo sapiens GN=LTF PE=1 SV=6	78132	8,5
P30530	UFO_HUMAN Tyrosine-protein kinase receptor UFO OS=Homo sapiens GN=AXL PE=1 SV=3	98273	5,27
P07911	UROM_HUMAN Uromodulin OS=Homo sapiens GN=UMOD PE=1 SV=1	69714	5,05
Q6EMK4	VASN_HUMAN Vasorin OS=Homo sapiens GN=VASN PE=1 SV=1	71668	7,16
P19320	VCAM1_HUMAN Vascular cell adhesion protein 1 OS=Homo sapiens GN=VCAM1 PE=1 SV=1	81224	5,14
P04004	VTNC_HUMAN Vitronectin OS=Homo sapiens GN=VTN PE=1 SV=1	54271	5,55
Q96J92	WNK4_HUMAN Serine/threonine-protein kinase WNK4 OS=Homo sapiens GN=WNK4 PE=1 SV=1	134656	5,36
P25311	ZA2G_HUMAN Zinc-alpha-2-glycoprotein OS=Homo sapiens GN=AZGP1 PE=1 SV=2	34237	5,71

Appendix 4 – Proteins in common between all individuals.

Accession #	Protein ID	Relative Abundance (emPAI)				PAH/CONT Ratio
		PAH1	PAH2	CONT1	CONT2	
P02768	ALBU_HUMAN Serum albumin OS=Homo sapiens GN=ALB PE=1 SV=2	8	4,05	5,54	4,38	1,21
P04264	K2C1_HUMAN Keratin, type II cytoskeletal 1 OS=Homo sapiens GN=KRT1 PE=1 SV=6	2,07	0,72	1,97	1,11	0,91
P35908	K22E_HUMAN Keratin, type II cytoskeletal 2 epidermal OS=Homo sapiens GN=KRT2 PE=1 SV=2	1,38	0,73	1,28	0,62	1,11
P35527	K1C9_HUMAN Keratin, type I cytoskeletal 9 OS=Homo sapiens GN=KRT9 PE=1 SV=3	0,42	0,24	0,66	0,34	0,66
P13645	K1C10_HUMAN Keratin, type I cytoskeletal 10 OS=Homo sapiens GN=KRT10 PE=1 SV=6	1,09	0,84	1,31	0,46	1,09
P01834	IGKC_HUMAN Ig kappa chain C region OS=Homo sapiens GN=IGKC PE=1 SV=1	11,48	3,4	2,04	5,37	2,01
P02787	TRFE_HUMAN Serotransferrin OS=Homo sapiens GN=TF PE=1 SV=3	2,1	0,19	0,34	0,5	2,73
P10451	OSTP_HUMAN Osteopontin OS=Homo sapiens GN=SPP1 PE=1 SV=1	0,84	0,88	4,14	3,53	0,22
P02144	MYG_HUMAN Myoglobin OS=Homo sapiens GN=MB PE=1 SV=2	1,69	0,66	1,15	1,15	1,02
P98160	PGBM_HUMAN Basement membrane-specific heparan sulfate proteoglycan core protein OS=Homo sapiens GN=HSPG2 PE=1 SV=4	0,08	0,01	0,08	0,12	0,45
P41222	PTGDS_HUMAN Prostaglandin-H2 D-isomerase OS=Homo sapiens GN=PTGDS PE=1 SV=1	1,77	1,32	0,52	1,86	1,30
P02760	AMBP_HUMAN Protein AMBP OS=Homo sapiens GN=AMBP PE=1 SV=1	0,74	0,99	0,99	1,5	0,69
P07911	UROM_HUMAN Uromodulin OS=Homo sapiens GN=UMOD PE=1 SV=1	0,37	0,57	0,47	0,79	0,75
P01042	KNG1_HUMAN Kininogen-1 OS=Homo sapiens GN=KNG1 PE=1 SV=2	0,27	0,55	0,65	0,65	0,63
Q96FE7	P3IP1_HUMAN Phosphoinositide-3-kinase-interacting protein 1 OS=Homo sapiens GN=PIK3IP1 PE=1 SV=2	0,36	0,37	0,37	0,37	0,99
P01619	KV301_HUMAN Ig kappa chain V-III region B6 OS=Homo sapiens PE=1 SV=1	1,06	1,1	1,1	1,1	0,98
P15586	GNS_HUMAN N-acetylglucosamine-6-sulfatase OS=Homo sapiens GN=GNS PE=1 SV=3	0,15	0,24	0,16	0,24	0,98

P02790	HEMO_HUMAN Hemopexin OS=Homo sapiens GN=HPX PE=1 SV=2	0,29	0,09	0,09	0,3	0,97
P0DJD8	PEPA3_HUMAN Pepsin A-3 OS=Homo sapiens GN=PGA3 PE=1 SV=1	0,68	0,24	0,24	1,11	0,68
P01833	PIGR_HUMAN Polymeric immunoglobulin receptor OS=Homo sapiens GN=PIGR PE=1 SV=4	0,3	0,38	0,54	0,54	0,63
P10153	RNAS2_HUMAN Non-secretory ribonuclease OS=Homo sapiens GN=RNASE2 PE=1 SV=2	0,59	0,62	0,62	1,61	0,54
O14773	TPP1_HUMAN Tripeptidyl-peptidase 1 OS=Homo sapiens GN=TPP1 PE=1 SV=2	0,15	0,16	0,25	0,25	0,62
P05154	IPSP_HUMAN Plasma serine protease inhibitor OS=Homo sapiens GN=SERPINA5 PE=1 SV=3	0,46	0,34	0,63	0,63	0,63
Q14624	ITIH4_HUMAN Inter-alpha-trypsin inhibitor heavy chain H4 OS=Homo sapiens GN=ITIH4 PE=1 SV=4	0,09	0,04	0,36	0,55	0,14
O43451	MGA_HUMAN Maltase-glucoamylase, intestinal OS=Homo sapiens GN=MGAM PE=1 SV=5	0,04	0,02	0,04	0,02	1,00
P98164	LRP2_HUMAN Low-density lipoprotein receptor-related protein 2 OS=Homo sapiens GN=LRP2 PE=1 SV=3	0,02	0,03	0,04	0,02	0,83
P16070	CD44_HUMAN CD44 antigen OS=Homo sapiens GN=CD44 PE=1 SV=3	0,11	0,25	0,18	0,25	0,84
P05090	APOD_HUMAN Apolipoprotein D OS=Homo sapiens GN=APOD PE=1 SV=1	0,49	1,81	1,81	1,81	0,64
P04433	KV309_HUMAN Ig kappa chain V-III region VG (Fragment) OS=Homo sapiens PE=1 SV=1	0,4	0,41	0,41	0,41	0,99
P25311	ZA2G_HUMAN Zinc-alpha-2-glycoprotein OS=Homo sapiens GN=AZGP1 PE=1 SV=2	0,46	0,68	0,92	5,2	0,19
P30530	UFO_HUMAN Tyrosine-protein kinase receptor UFO OS=Homo sapiens GN=AXL PE=1 SV=3	0,09	0,1	0,1	0,2	0,63
P01876	IGHA1_HUMAN Ig alpha-1 chain C region OS=Homo sapiens GN=IGHA1 PE=1 SV=2	0,12	0,81	1,04	0,61	0,56
P00450	CERU_HUMAN Ceruloplasmin OS=Homo sapiens GN=CP PE=1 SV=1	0,11	0,16	0,04	0,2	1,13
P01614	KV201_HUMAN Ig kappa chain V-II region Cum OS=Homo sapiens PE=1 SV=1	0,95	0,98	0,41	0,41	2,35
O94919	ENDD1_HUMAN Endonuclease domain-containing 1 protein OS=Homo sapiens GN=ENDOD1 PE=1 SV=2	0,27	0,08	0,18	0,63	0,43
Q08380	LG3BP_HUMAN Galectin-3-binding protein OS=Homo sapiens GN=LGALS3BP PE=1 SV=1	0,14	0,41	0,32	0,51	0,66
P04434	KV310_HUMAN Ig kappa chain V-III region VH (Fragment) OS=Homo sapiens PE=4 SV=1	0,94	0,97	0,97	0,97	0,98

Q12805	FBLN3_HUMAN EGF-containing fibulin-like extracellular matrix protein 1 OS=Homo sapiens GN=EFEMP1 PE=1 SV=2	0,08	0,09	0,09	0,09	0,94
P01859	IGHG2_HUMAN Ig gamma-2 chain C region OS=Homo sapiens GN=IGHG2 PE=1 SV=2	0,27	0,28	0,28	0,64	0,60
Q9HCN6	GPVI_HUMAN Platelet glycoprotein VI OS=Homo sapiens GN=GP6 PE=1 SV=4	0,12	0,13	0,27	0,13	0,63
P01717	LV403_HUMAN Ig lambda chain V-IV region Hil OS=Homo sapiens PE=1 SV=1	0,44	0,45	0,45	0,45	0,99
Q6EMK4	VASN_HUMAN Vasorin OS=Homo sapiens GN=VASN PE=1 SV=1	0,06	0,46	0,37	0,46	0,63
P04004	VTNC_HUMAN Vitronectin OS=Homo sapiens GN=VTN PE=1 SV=1	0,08	0,09	0,18	0,09	0,63
Q6GTX8	LAIR1_HUMAN Leukocyte-associated immunoglobulin-like receptor 1 OS=Homo sapiens GN=LAIR1 PE=1 SV=1	0,15	0,15	0,33	0,15	0,63
Q8N114	SHSA5_HUMAN Protein shisa-5 OS=Homo sapiens GN=SHISA5 PE=1 SV=1	0,18	0,19	0,19	0,19	0,97
A4D161	F221A_HUMAN Protein FAM221A OS=Homo sapiens GN=FAM221A PE=2 SV=1	0,14	0,14	0,14	0,14	1,00
P31997	CEAM8_HUMAN Carcinoembryonic antigen-related cell adhesion molecule 8 OS=Homo sapiens GN=CEACAM8 PE=1 SV=2	0,12	0,12	0,12	0,26	0,63
Q8NFZ8	CADM4_HUMAN Cell adhesion molecule 4 OS=Homo sapiens GN=CADM4 PE=1 SV=1	0,11	0,11	0,23	0,23	0,48
Q16769	QPCT_HUMAN Glutaminyl-peptide cyclotransferase OS=Homo sapiens GN=QPCT PE=1 SV=1	0,11	0,12	0,24	0,55	0,29
P60709	ACTB_HUMAN Actin, cytoplasmic 1 OS=Homo sapiens GN=ACTB PE=1 SV=1	0,11	0,53	1,12	0,71	0,35
Q86UK5	LBN_HUMAN Limbin OS=Homo sapiens GN=EVC2 PE=1 SV=1	0,03	0,03	0,03	0,03	1,00